

HIGH VOLTAGE AC-DC LOAD FLOW IN ELECTRICAL POWER NETWORKS

by

Elssodani Abdelhadi Muhammed

Submitted in partial fulfilment of the requirements
for the degree of Master of Applied Science

at

Dalhousie University
Halifax, Nova Scotia
May 2014

© Copyright by Elssodani Abdelhadi Muhammed, 2014

Dedication

I dedicate this thesis to Professor Mo-El-Hawary and my family

Table of Contents

List of Tables	v
List of Figures	vii
Abstract	xi
List of Abbreviations and Symbols Used	xii
Acknowledgements	xiii
Chapter 1: Introduction	1
1.1 Overview	1
1.2 Thesis Objective	3
1.3 Significance of the Problem	3
1.4 Thesis Structure	3
Chapter 2: AC, and AC-DC Load Flow	5
2.1 A brief description of Load Flow Method	5
2.2 A Literature Review of AC Load Flow Methods	5
2.3 Formation of Nodal Admittance Matrix	8
2.3.1 Bus incidence matrix A	9
2.3.2 Branch Model	10
2.3.3 Shunt Elements	11
2.3.4 Transformer Model	12
2.3.5 Primitive Network Matrix	12
2.3.6 Nodal Admittance Matrix	14
2.4 Nodal Power Equations Using Nodal Admittances	14
2.5 Newton-Raphson Load flow	16
2.6 Newton-Raphson Solution Algorithm	20
2.7 Literature Review of AC-DC Load Flow	21
Chapter 3: HVDC Load Flow Solution Method	27
3.1 Introduction	27
3.2 Model of HVDC System	28
3.3 DC of Control Modelling Equations	32
3.4 AC-DC Load Flow Analysis Using the Newton-Raphson Method	33
3.4.1 Control Mode 1	37

3.4.2	Control Mode 2	37
3.4.3	Control Mode 3	37
3.4.4	Control Mode 4	38
3.4.5	Control Mode 5	38
3.4.6	Control Mode 6	39
3.4.7	Control Mode 7	39
3.5	Evaluation of Derivatives.....	39
Chapter 4:	Computational Results and Discussion.....	44
4.1	Introduction	44
4.2	Case Studies	44
4.2.1	IEEE 14-Busbar System:.....	45
4.2.2	IEEE 30-Busbar System:.....	45
4.3	Unified AC-DC Load Flow Method	45
4.4	Test Results	46
4.4.1:	14-Bus System with Two Terminal DC Converters	47
4.5	Analysis of Results for 14-Bus with Two DC Converter System.....	54
4.5.1:	14-Bus System with Three Terminal DC Converters	55
4.6	Analysis of Results for 14-Bus with Three DC Converter System.....	62
4.6.1:	30-Bus System with Two Terminal DC Converters	71
4.7	Analysis of Results for 30-Bus with Two DC Converter System.....	79
4.7.1:	30-Bus system with Three Terminal DC Converters	81
4.8	Analysis of Results for 30-Bus with Three DC Converter System.....	90
Chapter 5:	Conclusion and Future Work.....	100
5.1	Conclusion and Contributions.....	100
5.2	Suggestions for Future Work	102
References	104
Appendix A	109
A.1:	Derivation of Power Network Equations Using a Sample Network.....	109
A.2:	Generalization of Power Equations.....	110
Appendix B	Data for DC Converters.....	114

List of Tables

Table 1: Load Flow Solution of 14 Bus System for Mode 1 with Two Converters	47
Table 2: Load Flow Solution of 14 Bus System for Mode 2 with Two Converters	48
Table 3: Load Flow Solution of 14 Bus System for Mode 3 with Two Converters	49
Table 4: Load Flow Solution of 14 Bus System for Mode 4 with Two Converters	50
Table 5: Load Flow Solution of 14 Bus System for Mode 5 with Two Converters	51
Table 6: Load Flow solution of 14 Bus System for Mode 6 with Two Converters	52
Table 7: Load Flow Solution of 14 Bus System for Mode 7 with Two Converters	53
Table 8: Load Flow Solution of 14 Bus System for Mode 1 with Three Converters	55
Table 9: Load Flow Solution of 14 Bus System for Mode 2 with Three Converters	56
Table10:Load Flow Solution of 14 Bus System for Mode 3 with Three Converters	57
Table11:Load Flow Solution of 14 Bus System for Mode 4 with Three Converters	58
Table12:Load Flow Solution of 14 Bus System for Mode 5 with Three Converters	59
Table13:Load Flow Solution of 14 Bus System for Mode 6 with Three Converters	60
Table14:Load Flow Solution of 14 Bus System for Mode 7 with Three Converters	61
Table 15: Load Flow Solution of 30 Bus System for Mode 1 with Two Converters	71
Table 16: Load Flow Solution of 30 Bus System for Mode 2 with two Converters	72
Table17: Load Flow Solution of 30 Bus System for Mode 3 with Two Converters	73
Table 18: Load Flow Solution of 30 Bus System for Mode 4 with Two Converters	74
Table 19: Load Flow Solution of 30 Bus System for Mode 5 with Two converters	76
Table 20: Load Flow Solution of 30 Bus System for Mode 6 with Two Converters	77
Table 21: Load Flow Solution of 30 Bus System for Mode 7 with Two Converters	78

Table22:Load Flow Solution of 30 Bus System for Mode 1 with Three Converters	81
Table23:Load Flow Solution of 30 Bus System for Mode 2 with Three Converters	82
Table24:Load Flow Solution of 30 Bus System for Mode 3 with Three Converters	83
Table25:Load Flow Solution of 30 Bus System for Mode 4 with Three Converters	85
Table26:Load Flow Solution of 30 Bus System for Mode 5 with Three Converters	86
Table27:Load Flow Solution of 30 Bus System for Mode 6 with Three Converters	87
Table28:Load Flow Solution of 30 Bus System for Mode 7 with Three Converters	89
Table B.1: Data of Two Converters for 14-Bus system	114
Table B.2: Data of Three Converters for 14-Bus system	114
Table B.3: Data of Two Converters for 30-Bus system	114
Table B.4: Data of Three Converters for 30-Bus system	115

List of Figures

Figure 1: Comparison of Various Methods for Load Flow Solutions [Wood 1996][8]	7
Figure2: Illustration of the Structure of Bus Incidence Matrix by the Two Sub-Matrices	10
Figure 3: Equivalent pi-Model for a Transmission Line	11
Figure 4: Illustration of Shunt Conductance and Shunt Susceptance for an Instance Bus, k	11
Figure 5: One-Line Diagram of a Transmission Line with Transformer	12
Figure6: Equivalent pi-Model for a Transmission Line with Transformer Tap Parameter	12
Figure 7: The Vector of Diagonal Elements of $Y_{primitive}$	13
Figure 8: Flowchart for Implementation of Newton-Raphson AC Load Flow	20
Figure 9: Modelling of DC Converter Station k [Arnold 1990] [15]	28
Figure 10: A Single-Phase Equivalent Circuit for Basic Converters (Angles Referred to D.C. Reference) Arnold 1990] [15]	28
Figure 11: Flowchart of Unified AC-DC Load Flow	46
Figure 12: The Relation between the Voltage Magnitude V_4 and Modes Number of 14 Bus system	63
Figure 13: The Relation between the Voltage Magnitude V_5 and Modes Number of 14 Bus system	63
Figure 14: The Relation between the Voltage Magnitude V_7 and Modes Number of 14 Bus system	64
Figure 15: The Relation between the Voltage Magnitude V_9 and Modes Number of 14 Bus system	64

Figure 16: The Relation between the Voltage Magnitude _ V10 and Modes Number of 14	
Bus system	65
Figure 17: The Relation between the Voltage Magnitude _ V11 and Modes Number of 14	
Bus system	65
Figure 18: The Relation between the Voltage Magnitude _ V12 and Modes Number of 14	
Bus system	66
Figure 19: The Relation between the Voltage Magnitude _ V13 and Modes Number of 14	
Bus system	66
Figure 20: The Relation between the Voltage Magnitude _ V14 and Modes number of 14	
Bus system	67
Figure 21: The Relation between the Active Power P4 and Voltage Magnitude V4 of 14	
Bus system	67
Figure 22: The Relation between the Active Power P9 and Voltage Magnitude V9 of 14	
Bus system	68
Figure 23: The Relation between the Active Power P14 and Voltage Magnitude V14 of	
14 Bus system	68
Figure 24: The Relation between the Reactive Power Q4 and Voltage Magnitude V4 of	
14 Bus system	69
Figure 25: The Relation between the Reactive Power Q9 and Voltage Magnitude V9 of	
14 Bus system	69
Figure 26: The Relation between the Reactive Power Q14 and Voltage Magnitude V14 of	
14 Bus system	70

Figure 27: The Relation between the Voltage Magnitude _ V3 and Modes Number of 30	
Bus system	91
Figure 28: The Relation between the Voltage Magnitude _ V4 and Modes Number of 30	
Bus system	92
Figure 29: The Relation between the Voltage Magnitude _ V7 and Modes Number of 30	
Bus system	92
Figure 30: The Relation between the Voltage Magnitude _ V9 and Modes Number of 30	
Bus system	93
Figure 31: The Relation between the Voltage Magnitude _ V12 and Modes Number of 30	
Bus system	93
Figure 32: The Relation between the Voltage Magnitude _ V15 and Modes Number of 30	
Bus system	94
Figure 33: The Relation between the Voltage Magnitude _ V19 and Modes Number of 30	
Bus system	94
Figure 34: The Relation between the Voltage Magnitude _ V22 and Modes Number of 30	
Bus system	95
Figure 35: The Relation between the Voltage Magnitude _ V24 and Modes Number of 30	
Bus system	95
Figure 36: The Relation between the Voltage Magnitude _ V27 and Modes Number of 30	
Bus system	96
Figure 37: The Relation between the Voltage Magnitude _ V30 and Modes Number of 30	
Bus system	96

Figure 38: The Relation between the Active Power P_7 and Voltage Magnitude V_7 of 30 Bus system	97
Figure 39: The Relation between the Active Power P_{12} and Voltage Magnitude V_{12} of 30 Bus system	97
Figure 40: The Relation between the Active Power P_{21} and Voltage Magnitude V_{21} of 30 Bus system	98
Figure 41: The Relation between the Reactive Power Q_7 and Voltage Magnitude V_7 of 30 Bus system	98
Figure 42: The Relation between the Reactive Power Q_{12} and Voltage Magnitude V_{12} of 30 Bus system	99
Figure 43: The Relation between the Reactive Power Q_{21} and Voltage Magnitude V_{21} of 30 Bus system	99
Figure 44: Tree of the Connected Graph of a Sample Power Network	109
Figure 45: The Node 3 in the Sample Power Network Along with the all Branches Connected and the Illustration of Equivalent π Model for each Branch	109
Figure 46: Sample Network with Two Branches Connected to a Generator (Power Injector) Along with the Illustration of Equivalent π Model	110

Abstract

Power losses in the grid are important, and as the power losses decrease the efficiency increases. Not much research has been done recently on the Newton-Raphson Power Flow (NRPF) method in polar form for systems with High Voltage Direct Current (HVDC) subsystems. The point of departure for this thesis is based on decoupling the NR Power Flow method. Power flow problems are solved for many fundamental problems in the operation and planning of the power system. Although many methods are available to solve these problems, this thesis focuses on developing an enhanced HVDC power flow method with improved computational efficiency and convergence stability.

A comparison of the results with full Newton-Raphson Power Flow method is presented to evaluate the performance of the proposed method. Simulations were conducted on the 14-bus and 30-bus IEEE systems. Two and three converters are shown to improve the voltage magnitude, active and reactive power profile. The overall results indicate which mode is the best mode compared to others depending on the bus importance.

List of Abbreviations and Symbols Used

AC	Alternating current
AT	Autotransformer
CPU	Central Processing Unit
DC	Direct current
FACTS	Flexible AC Transmission Systems
FDCPFM	Fast Decoupled Power Flow Method
FDLF	Fast Decoupled Load Flow
FO	First Order
GS	Gauss-Seidel
HV	High Voltage
HVDC	High Voltage Direct Current
MTDC	Multiterminal Direct Current
KV	Kilovolt
LFC	Load Frequency Control
LP=PL	Load Flow or Power Flow
LV	Low Voltage
MV	Medium Voltage
MVA	Mega Volt-Ampere
MVAR	Mega Volt-Ampere Reactive
NR	Newton-Raphson
NRLF	Newton Raphson Load Flow
PF	Power Factor
PU	Per Unit
STATCOM	Static Synchronous Compensator
SVC	Static Var Compensator
TCR	Thyristor-controlled Reactor
VSI	Voltage Source Inverter
a=T	Transformer Tap Ratio

Acknowledgement

First of all I want to thank Allah for his help and mercy to complete this work. I would like to express my deepest gratitude to my advisor, Prof. Dr. El-Hawary, for his admirable guidance, encouragement, suggestions and untiring support throughout the research. He has been an advisor in the true sense, both academically and morally, throughout this thesis work.

I am truly indebted to my professors in the department of Electrical and Computer Engineering at Dalhousie University for their intellectual support through my studies.

Finally, special thanks also go to my family members, especially to my parents and friends whose endless love; inspiration and blessings helped me to complete my graduate work.

Chapter 1: Introduction

1.1 Overview

Electrical power systems are designed to serve the needs of real and reactive power, as demanded by various connected loads in the network. Load flow studies are necessary to determine the steady-state solution of a power system network at a given set of Busbar loads. In today's high technology age, the demand for electricity continues to increase. Due to the rapid growth in demand for electricity, electric power systems are becoming increasingly extensive and their control is becoming ever more complex. In addition, a guaranteed electricity supply is a necessity for industrial growth as well as in other areas of human activity.

To that end, power industry planners are demanding the provision of higher quality electrical power. This requires improving system security and its environmental impact, in tandem with the pursuit of greater efficiency. However, the criterion of perfection is never met because there are consistent differences between the model and reality. The power flow problem is solved by determining the values of steady-state complex voltages at all buses of the network, from which the active and reactive flows in every transmission line are calculated. Because the equations representing the power system are nonlinear, the well-established nodal properties of the power network and equipment are utilized in power flow solution methods. In its most basic form, these equations are derived by assuming that a perfect symmetry exists between the phases of the three-phase power system. Due to the nonlinear nature of the power flow equations, an iterative process obtains the numerical solution.

Recently, there have been considerable advances in High Voltage Direct Current (HVDC) technology, and engineers are now considering DC multi-terminal networks as a feasible option. Therefore, load flow analysis techniques have to be extended to deal with such mixed HVDC systems. Multiterminal DC networks integrated into an existing system can improve AC equipment, loading and stability, contribute to its load frequency control (LFC) and voltage regulation, increase interchange capacity, limit short circuit capacity, and contribute to the efficiency of electric power transmission. However, multi-terminal DC networks, as well as two-terminal DC links, require communication between converter terminals and control of DC system start-up and shut down. This communication is needed for the coordination of operating set points and for DC system structural changes, such as line or terminal outages. The integration of DC links or HVDC multi-terminal networks into AC systems is achievable and can be advantageous in certain applications such as bulk power transmission, AC network interconnections, and reinforcing AC networks.

1.2 Thesis Objective

This thesis is focused on the development of a computer program that solves the power flow method of large power systems with multi-terminal HVDC links. The program uses the Newton-Raphson Power Flow (NRPF) method to solve the non-linear set of equations in various electrical network systems. The Newton-Raphson method requires an enhanced HVDC power flow method devoid of its inherent limitations.

The main objectives of the thesis are:

- To utilize the NRPF method to solve the power flow problem of HVDC links and power system networks, and to study the characteristics of HVDC links and control active and reactive power flow.
- To develop a control strategy for converter stations that accounts for the interrelation between the reactive power requirements, DC bus voltages, DC current transformer taps, and converter control angles.

1.3 Significance of the Problem

The methodology presented in this thesis is based on a unified Newton-Raphson method that recognizes the interdependence of AC and DC equations and simultaneously solves the complete system. The Research on AC/DC load flow is rare and therefore in this thesis a method is proposed to solve a power flow problem with DC links.

1.4 Thesis Structure

This thesis is composed of five chapters, as follows. Chapter 1 introduces the problem of HVDC power flow, which is briefly reviewed and followed by an outline of the scope of

this thesis. In Chapter 2, the limitations of the three popular methods are described and a literature review of load flow solutions for the areas covered by this thesis is provided. In Chapter 3, the HVDC power flow problem solution and the related mathematical model – expanded using the Newton-Raphson method – are presented. Detailed simulation results are given in Chapter 4. Power flow and line flow solutions for this method is tested on IEEE 14-bus and 30-bus systems, power systems, and their power flow and HVDC power flow results are detailed in this chapter. Chapter 5 presents the conclusions of this research and offers suggestions and contribution for future work.

Chapter 2: AC, and AC-DC Load Flow

2.1 A brief description of Load Flow Method

In this chapter, a load flow method is described. Load flow analysis is the most important and fundamental tool applied to a power system to investigate problems in power system operations and planning. It analyzes the power systems in normal steady-state operation using simplified notation, such as a one-line diagram and per-unit system. The power flow problem consists of a given transmission network where all lines are represented by a Pi-equivalent circuit and transformers by an ideal voltage transformer in series with an impedance. Once the loads, active and reactive power injections and network parameters are defined, load flow analysis solves the bus voltages and phases, after which the branch power flow can be calculated. Generators and loads represent the boundary conditions of the solution. Mathematically, power flow requires a solution of a system of simultaneous nonlinear equations. However, with the continuous increase of power system scale, the dimension of load flow equations becomes very high, and for equations with such high dimensions, we cannot ensure that any mathematical method will arrive at the right solution. Hence, choosing a reliable method is essential [Wang 2009] [1], [Grainger 1994] [2].

2.2 A Literature Review of AC load flow methods

Early in the development of the first digital computers, the most widely used method was the Gauss-Seidel iterative method, which was based on the nodal admittance matrix of the power system (the impedance matrix that represents the topology and parameters of the power network) [Stagg 1968] [3]. Although the basis for this method is rather simple

and its memory requirement is relatively small, its convergence is nonetheless generally unsatisfactory.

To solve this problem, the sequential substitution method based on the nodal impedance matrix is used, which is also called the impedance method. The two main difficulties of the impedance method are [Brown 1963] [4]:

- High memory requirement, and
- Computing burden.

The first solution for overcoming the disadvantages of the impedance method is a piecewise solution of the impedance matrix load flow. It presents a method which involves splitting a power system into pieces to permit the use of the impedance matrix method on large systems. This method retains the same features and convergence characteristics of the impedance method [Andretich 1968] [5].

The other (and better) solution for overcoming the disadvantages of the impedance method is the Newton-Raphson method [Tinney 1967] [6], which is more widely in use. Its prominent features are:

- Better accuracy and reliability;
- Fewer iterations for convergence;
- Independently of the iteration number to the number of buses in the system; and
- Faster computations.

The Newton-Raphson power flow (NRPF) method is the most robust power flow algorithm in use today. Nevertheless, despite this method's popularity, load flow methods continue to be developed. Among these, the most successful are the fast-decoupled method [Stott 1974] [7].

Compared to the Newton method, the fast-decoupled method is faster, simpler, and more efficient algorithmically and requires less storage, but it may fail to converge when some of the basic assumptions do not hold. Convergence of iterative methods depends on the dominance of the diagonal elements of the bus admittance matrix. A comparison of the convergence of the Gauss-Seidel, Newton-Raphson and the fast-decoupled method power flow algorithms are shown in figure 1. [Wood 1996] [8].

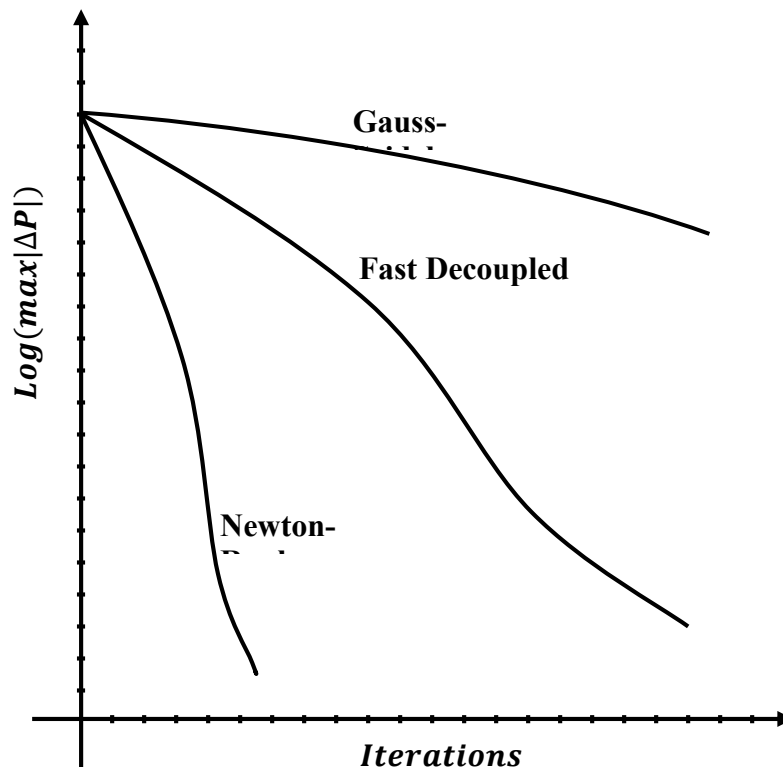


Figure 1: Comparison of Various Methods for Load Flow Solutions [Wood 1996] [8]

Because the Newton-Raphson method is a gradient method, it is quite complicated and therefore programming is also comparatively difficult and complicated. With this method, memory requirements are rather large, especially for large-size systems. Nonetheless, the method is versatile, reliable and accurate and best matched for load flow calculation of large-size systems [Murty 2011] [9].

Since the 1970s, research on load flow analysis has been very active. The artificial neural network algorithm [Nguyen 1995] [10] [Chan 2000] [11], the genetic algorithm [Wong 1999] [12] and Fuzzy-logic method [Lo 1999] [13] have also been the load flow analysis. However, these new models and new algorithms still cannot replace the Newton-Raphson or fast-decoupled methods.

According to the literature review, because of the applicability of the Newton-Raphson method to large-size systems and its stability for convergence, this thesis implements the Newton-Raphson method for the calculation of the actual state of power system based on network parameters, power injections, and loads.

2.3 Formation of Nodal Admittance Matrix

The formulation of an appropriate mathematical model is the first step in the analysis of an electrical network. The model must be able to describe the characteristics of individual network components and the relations that rule the interconnection of the components.

The network matrix equations provide a suitable mathematical model for digital processing. The elements of a network matrix depend on the selection of independent variables like currents or voltages (hence, the elements of network matrix will be impedances or admittances) [Stagg 1968] [3].

In the simulations presented in this thesis, the method of singular transformations is used for forming the bus admittance matrix. This method is chosen because, in practice, it performed faster simulations in a Matlab simulation environment compared to the methods described in [Zimmerman 2011] [14] and [Wang 2009] [1].

This section will explain the basic power network models, matrices, and works at the bus admittance matrix by singular transformations.

2.3.1 Bus incidence matrix A

The incidence of branches to buses in a connected power network is shown in the element-node incidence matrix A . However, it does not provide any information about the electrical characteristics of the power network parameters.

This matrix is rectangular, with a dimension of $N_{bus} \times N_{branch}$. The a_{ij} elements of A are 1 if the i^{th} branch is incident to and oriented *away from* the j^{th} bus, and the a_{ij} elements will be -1 if the i^{th} branch is incident to and oriented *toward* the j^{th} bus. The other elements are zero.

If the rows of A are arranged according to a particular tree, the matrix can be partitioned into two sub-matrices. The first part is the incidence of the links going from the buses to the zero reference bus that is equal to identity matrix I of the size N_{BUS} , and the last sub-matrix is the incidence of network branches, as shown in Figure 2.

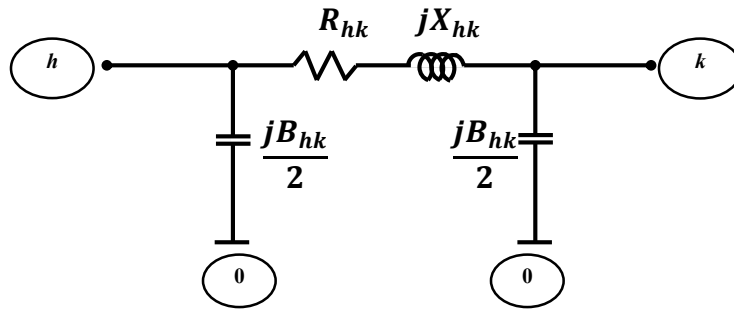


Figure 3: Equivalent pi-model for a transmission line

2.3.3 Shunt Elements

Shunt capacitors or reactors for voltage and/or reactive power control are represented by their per-phase susceptance at the corresponding bus. The sign of the susceptance value will determine the type of the shunt element (a positive sign shows a shunt capacitor and a negative sign shows a reactor). Figure 4 illustrates the shunt conductance and susceptance for an instance bus, k .

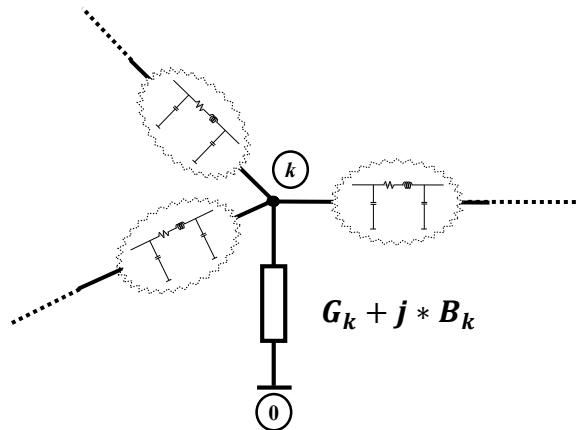


Figure 4: Illustration of shunt conductance and shunt susceptance for an instance bus, k

2.3.4 Transformer Model

Transmission lines with transformers can be modeled as series impedances in series with ideal transformers, as shown in figure 5. The two-transformer terminal buses h and k are named as the tap-side bus and the impedance-side bus, respectively.

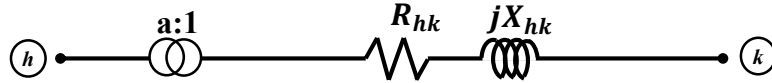


Figure 5: One-line diagram of a transmission line with transformer

In figure 6, the two-port pi-model of a transmission line is shown considering the effects of transformer tap value, a .

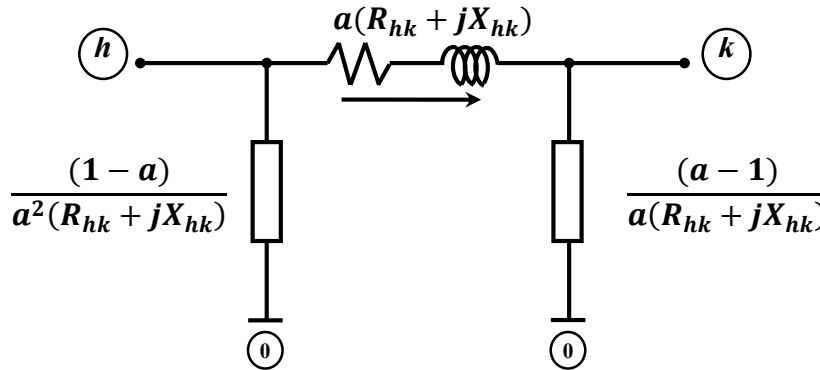


Figure 6: Equivalent pi-model for a transmission line with transformer tap parameter

2.3.5 Primitive Network Matrix

The electrical characteristics of the individual network components can be presented easily in the form of a primitive network matrix $\bar{Y}_{primitive}$. The primitive network matrix describes the characteristics of each component, but does not present anything about the network connections.

The diagonal elements of matrix $\bar{Y}_{primitive}$ are the self-admittances, and the off-diagonal elements are the mutual admittances. Assuming there is no mutual coupling between elements, the $\bar{Y}_{primitive}$ matrix will be a diagonal matrix. The diagonal elements of $\bar{Y}_{primitive}$ are like a vector that consists of two parts – first, the total bus admittances that are connected from buses to the reference bus (bus number 0), and next, the branch admittances, as depicted in figure 7.

$$\left[\begin{array}{c} \bar{Y}_{1,0} \\ \vdots \\ \bar{Y}_{N_{bus},0} \\ \bar{y}_1 \\ \vdots \\ \bar{y}_{N_{branch}} \end{array} \right] \begin{array}{l} \left. \vphantom{\begin{array}{c} \bar{Y}_{1,0} \\ \vdots \\ \bar{Y}_{N_{bus},0} \end{array}} \right\} \text{Total Bus Admittances} \\ \left. \vphantom{\begin{array}{c} \bar{y}_1 \\ \vdots \\ \bar{y}_{N_{branch}} \end{array}} \right\} \text{Branch Admittances} \end{array} \quad \left. \vphantom{\begin{array}{c} \bar{Y}_{1,0} \\ \vdots \\ \bar{Y}_{N_{bus},0} \\ \bar{y}_1 \\ \vdots \\ \bar{y}_{N_{branch}} \end{array}} \right]_{(N_{bus}+N_{branch}) \times 1}$$

Figure 7: The vector of diagonal elements of $\bar{Y}_{primitive}$

The bus admittance elements of this vector for tap-side buses are defined as:

$$\bar{Y}_{i,0} = \sum_{n=1}^{\text{all the branches connected to bus } i} \left(\frac{jB_n}{2} + \frac{(1-a)}{a^2(R_n+jX_n)} \right) + Y_{shunt} \quad (2-1)$$

Where R_n and X_n are, respectively, the resistance and reactance of the branches connected to bus i . Y_{shunt} is the shunt admittance connected to bus i .

The bus admittance elements for impedance-side buses are defined as:

$$\bar{Y}_{i,0} = \sum_{n=1}^{\text{all the branches connected to bus } i} \left(\frac{jB_n}{2} + \frac{(a-1)}{a(R_n+jX_n)} \right) + Y_{shunt} \quad (2-2)$$

The transformer taps value a , for a non-transformer branch, is considered 1. The branch admittance elements are defined as:

$$\bar{Y}_{1:N_{branch}} = \frac{1}{a(R_{hk} + jX_{hk})} \quad (2-3)$$

Where R_{hk} and X_{hk} are respectively, the resistance and reactance of an instance branch that connects bus h to k .

2.3.6 Nodal Admittance Matrix

It is necessary to convert the primitive network matrix into a network matrix that describes the performance of the interconnected network. This is done by using singular transformations of the bus primitive network matrix with the bus incidence matrix. Therefore, the bus admittance matrix \bar{Y}_{bus} can be extracted by using the bus incidence matrix \mathbf{A} to relate the primitive network's variables and parameters to the bus quantities of interconnected network [Stagg 1968] [3].

$$\mathbf{Y}_{bus} = \mathbf{A}^T \bar{\mathbf{Y}}_{primitive} \mathbf{A} \quad (2-4)$$

The bus incidence matrix is singular, so the $[\mathbf{A}^T \bar{\mathbf{Y}}_{primitive} \mathbf{A}]$ is a singular transformation of $\bar{\mathbf{Y}}_{primitive}$.

2.4 Nodal Power Equations Using Nodal Admittances

The power system load flow is considered a problem of finding the voltage and phase for each bus when all of the active and reactive power injections are specified. If complex power can be represented by equations of complex voltages, then a nonlinear equation solving method can be used to find a solution for the node voltage. In this section, the nodal power equations are deduced using nodal admittances [Wang 2009, p. 76] [1].

Complex node power equations have two representation forms: polar and rectangular, such that

$$\bar{S}_h = P_h + jQ_h = \bar{V}_h \sum_{k=1}^n \bar{Y}_{hk}^* \bar{V}_k^* \quad (2-5)$$

Where the index h is the bus number from 1 to N_{bus} . The node admittance matrix \bar{Y}_{hk} is a sparse matrix and, accordingly, there are a few terms in the summation. The elements of node admittance matrix can be written as:

$$\bar{Y}_{hk} = G_{hk} + jB_{hk} \quad (2-6)$$

Consequently, the complex node power can be expressed as:

$$P_h + jQ_h = \bar{V}_h \sum_{k=1}^{N_{bus}} (G_{hk} - jB_{hk}) \bar{V}_k^* \quad (2-7)$$

Furthermore, if we consider the voltages in polar form: $\bar{V}_h = |V_h|e^{j\theta_h}$,

$$P_h + jQ_h = |V_h|e^{j\theta_h} \sum_{k=1}^{N_{bus}} (G_{hk} - jB_{hk}) |V_k|e^{-j\theta_k} \quad (2-8)$$

$$P_h + jQ_h = |V_h| \sum_{k=1}^{N_{bus}} |V_k| (G_{hk} - jB_{hk}) e^{j(\theta_{hk})} \quad (2-9)$$

then $\theta_{hk} = \theta_h - \theta_k$ is the voltage phase difference between node h and k . By using the Euler rule, $e^{j\theta} = \cos \theta + j \sin \theta$, we can combine the exponential forms:

$$P_h + jQ_h = |V_h| \sum_{k=1}^{N_{bus}} |V_k| (G_{hk} - jB_{hk}) (\cos \theta_{hk} + j \sin \theta_{hk}) \quad (2-10)$$

$$P_h + jQ_h = |V_h| \sum_{k=1}^{N_{bus}} |V_k| (G_{hk} \cos \theta_{hk} + jG_{hk} \sin \theta_{hk} - jB_{hk} \cos \theta_{hk} + B_{hk} \sin \theta_{hk}) \quad (2-11)$$

Dividing the above equation into real and imaginary parts gives the active and reactive power injection at bus h in polar form:

$$P_h = |V_h| \sum_{k=1}^{N_{bus}} |V_k| (G_{hk} \cos \theta_{hk} + B_{hk} \sin \theta_{hk}) \quad (2-12)$$

$$Q_h = |V_h| \sum_{k=1}^{N_{bus}} |V_k| (G_{hk} \sin \theta_{hk} - B_{hk} \cos \theta_{hk}) \quad (2-13)$$

The last two equations are the polar form of the nodal active and reactive power equations, which are the main equations in the Newton-Raphson calculation procedure.

2.5 Newton-Raphson Load flow

Since the active and reactive powers are represented by equations of voltage magnitude and phases in the previous section, a non-linear equation-solving method can be applied to extract the voltage and phases for each bus.

The Newton-Raphson method is an efficient step-by-step procedure to solve nonlinear equations. Essentially, it transforms the procedure of solving nonlinear equations into the procedure of repeatedly solving linear equations. This chronological linearization process is the main part of the Newton-Raphson method [Wang 2009] [1].

To build mathematical models of the load flow problem, simultaneous nonlinear equations of node voltage phasors, which were derived in the previous section, are expressed in the following forms to define the power mismatches in polar coordinates:

$$\Delta P_h = P_{sp,h} - |V_h| \sum_{k=1}^{N_{bus}} |V_k| (G_{hk} \cos \theta_{hk} + B_{hk} \sin \theta_{hk}) = 0 \quad (2-14)$$

$$\Delta Q_h = Q_{sp,h} - |V_h| \sum_{k=1}^{N_{bus}} |V_k| (G_{hk} \sin \theta_{hk} - B_{hk} \cos \theta_{hk}) = 0 \quad (2-15)$$

- ΔP_h and ΔQ_h are the magnitudes of active and reactive power errors, respectively, and the index h is the bus number (from 1 to N_{bus}).
- $P_{sp,h}$ and $Q_{sp,h}$ are the specified active and reactive powers at bus h .

- G_{hk} and B_{hk} come from the definition of bus admittance matrix in the previous chapter, when it was divided into real and imaginary parts, as : $\bar{Y}_{hk} = G_{hk} + jB_{hk}$.

Keep in mind that the load flow analysis as well as the active and reactive powers at all the buses (except for the slack bus) in the power system network are explicitly specified.

Assuming that the slack bus is the first bus and the number of PV buses is N_{PV} , there will be $(N_{bus} - 1)$ equations for active power:

$$\left\{ \begin{array}{l} \Delta P_2 = P_{sp,2} - |V_2| \sum_{k=1}^{N_{bus}} |V_k| (G_{2k} \cos \theta_{2k} + B_{2k} \sin \theta_{2k}) = 0 \\ \vdots \\ \Delta P_{N_{bus}} = P_{sp,N_{bus}} - |V_{N_{bus}}| \sum_{k=1}^{N_{bus}} |V_k| (G_{N_{bus}k} \cos \theta_{N_{bus}k} + B_{N_{bus}k} \sin \theta_{N_{bus}k}) = 0 \end{array} \right. \quad (2-16)$$

and $(N_{bus} - N_{PV} - 1)$ equations for reactive power:

$$\left\{ \begin{array}{l} \Delta Q_2 = Q_{sp,2} - |V_2| \sum_{k=1}^{N_{bus}} |V_k| (G_{2k} \sin \theta_{2k} - B_{2k} \cos \theta_{2k}) = 0 \\ \vdots \\ \Delta Q_{N_{bus}} = Q_{sp,N_{bus}} - |V_{N_{bus}}| \sum_{k=1}^{N_{bus}} |V_k| (G_{N_{bus}k} \sin \theta_{N_{bus}k} - B_{N_{bus}k} \cos \theta_{N_{bus}k}) = 0 \end{array} \right. \quad (2-17)$$

Hence, the total number of the above equations will be $(2N_{bus} - N_{PV} - 2)$, which is equal to the number of unknowns, namely $(N_{bus} - N_{PV} - 1)$ voltage magnitudes and $(N_{bus} - 1)$ angles.

The load flow analysis considers the acceptable tolerance for ΔP_h and ΔQ_h and solves the bus voltages (on all buses except slack and PV buses) along with the bus angles (on all buses except slack bus).

By considering the first order of Taylor Series expansion and neglecting the higher order terms of the nonlinear equations for active and reactive power around the vector of unknowns that is composed of voltage magnitudes and angles of size $(2N_{bus} - N_{PV} - 2)$, we get:

$$\underbrace{\begin{bmatrix} \Delta P \\ \Delta Q \end{bmatrix}}_{\text{Mismatches}} = \underbrace{\begin{bmatrix} \mathbf{A} = \frac{\partial P}{\partial \theta} \\ \mathbf{C} = \frac{\partial Q}{\partial \theta} \end{bmatrix} \begin{bmatrix} \Delta \theta \\ \Delta V \end{bmatrix}}_{\text{Jacobians}} + \underbrace{\begin{bmatrix} \mathbf{B} = \frac{\partial P}{\partial V} \\ \mathbf{D} = \frac{\partial Q}{\partial V} \end{bmatrix} \begin{bmatrix} \Delta \theta \\ \Delta V \end{bmatrix}}_{\text{Corrections}} \quad (2-18)$$

$\Delta \theta$ and ΔV are the voltage angle correction values and voltage magnitude correction values, respectively. The last expression in extended form will be:

$$\begin{bmatrix} \Delta P_2 \\ \vdots \\ \Delta P_{N_{bus}} \\ \Delta Q_2 \\ \vdots \\ \Delta Q_{N_{bus}} \end{bmatrix} = \begin{bmatrix} \begin{bmatrix} A_{22} & \cdots & A_{2,N_{bus}} \\ \vdots & \ddots & \vdots \\ A_{N_{bus},2} & \cdots & A_{N_{bus},N_{bus}} \end{bmatrix} \\ \begin{bmatrix} C_{22} & \cdots & C_{2,N_{bus}} \\ \vdots & \ddots & \vdots \\ C_{N_{bus},2} & \cdots & C_{N_{bus},N_{bus}} \end{bmatrix} \end{bmatrix} \begin{bmatrix} \begin{bmatrix} B_{22} & \cdots & B_{2,N_{bus}} \\ \vdots & \ddots & \vdots \\ B_{N_{bus},2} & \cdots & B_{N_{bus},N_{bus}} \end{bmatrix} \\ \begin{bmatrix} D_{22} & \cdots & D_{2,N_{bus}} \\ \vdots & \ddots & \vdots \\ D_{N_{bus},2} & \cdots & D_{N_{bus},N_{bus}} \end{bmatrix} \end{bmatrix} \begin{bmatrix} \Delta \theta_2 \\ \vdots \\ \Delta \theta_{N_{bus}} \\ \Delta V_2 \\ \vdots \\ \Delta V_{N_{bus}} \end{bmatrix} \quad (2-19)$$

The matrices of \mathbf{A} , \mathbf{B} , \mathbf{C} and \mathbf{D} are the sub-blocks of the Jacobian matrix, where their elements can be calculated by differentiating the equations of active and reactive power with respect to voltage angles and magnitudes. Hence, the elements of the Jacobian matrix can be obtained using the following equations (for each sub-block, the first

equation is related to the off-diagonal elements and the second one is for diagonal elements):

$$\begin{cases} A_{ij} = \frac{\partial P_i}{\partial \theta_j} = -V_i V_j (G_{ij} \sin \theta_{ij} - B_{ij} \cos \theta_{ij}) & \text{for } i \neq j \\ A_{ii} = \frac{\partial P_i}{\partial \theta_i} = V_i \sum_{j \in N_{bus}}^{j \neq i} V_j (G_{ij} \sin \theta_{ij} - B_{ij} \cos \theta_{ij}) \end{cases} \quad (2-20)$$

$$\begin{cases} B_{ij} = \frac{\partial P_i}{\partial V_j} = -V_i (G_{ij} \cos \theta_{ij} + B_{ij} \sin \theta_{ij}) & \text{for } i \neq j \\ B_{ii} = \frac{\partial P_i}{\partial V_i} = \sum_{j \in N_{bus}}^{j \neq i} -V_j (G_{ij} \cos \theta_{ij} + B_{ij} \sin \theta_{ij}) - 2V_i G_{ii} \end{cases} \quad (2-21)$$

$$\begin{cases} C_{ij} = \frac{\partial Q_i}{\partial \theta_j} = V_i V_j (G_{ij} \cos \theta_{ij} + B_{ij} \sin \theta_{ij}) & \text{for } i \neq j \\ C_{ii} = \frac{\partial Q_i}{\partial \theta_i} = -V_i \sum_{j \in N_{bus}}^{j \neq i} V_j (G_{ij} \cos \theta_{ij} + B_{ij} \sin \theta_{ij}) \end{cases} \quad (2-22)$$

$$\begin{cases} D_{ij} = \frac{\partial Q_i}{\partial V_j} = -V_i (G_{ij} \sin \theta_{ij} - B_{ij} \cos \theta_{ij}) & \text{for } i \neq j \\ D_{ii} = \frac{\partial Q_i}{\partial V_i} = \sum_{j \in N_{bus}}^{j \neq i} -V_j (G_{ij} \sin \theta_{ij} - B_{ij} \cos \theta_{ij}) + 2V_i B_{ii} \end{cases} \quad (2-23)$$

A Jacobian matrix is a sparse matrix, and the place of zeros in this matrix is the same as the place of zeros in a bus admittance matrix. This is because, when considering the equations of a Jacobian matrix for off-diagonal elements, it can be seen that each of them is related to only one element of the bus admittance matrix. Therefore, if the element in the admittance matrix is zero, the corresponding element in the Jacobian matrix is also zero. However, the Jacobian matrix is not symmetrical. As the elements of a Jacobian matrix are a function of node voltage phasors, they vary with node voltages during the iterative process [Wang 2009] [1].

To save on computation time, voltage magnitudes in the correction vector can be changed to $\frac{\Delta V}{V}$, such as in the case of equations calculating sub-matrices for A and D $A_{ij} = D_{ij}$ and $B_{ij} = -C_{ij}$. If we consider this situation, the number of elements to be calculated for

the Jacobian matrix are only $2(N_{bus} - 1) + [2(N_{bus} - 1)]^2/2$ instead of $[2(N_{bus} - 1)]^2$ [Murty 2011] [9].

2.6 Newton-Raphson Solution Algorithm

The flowchart for the implementation of the Newton-Raphson Load Flow procedure in Polar Coordinates is depicted in Figure 8 below:

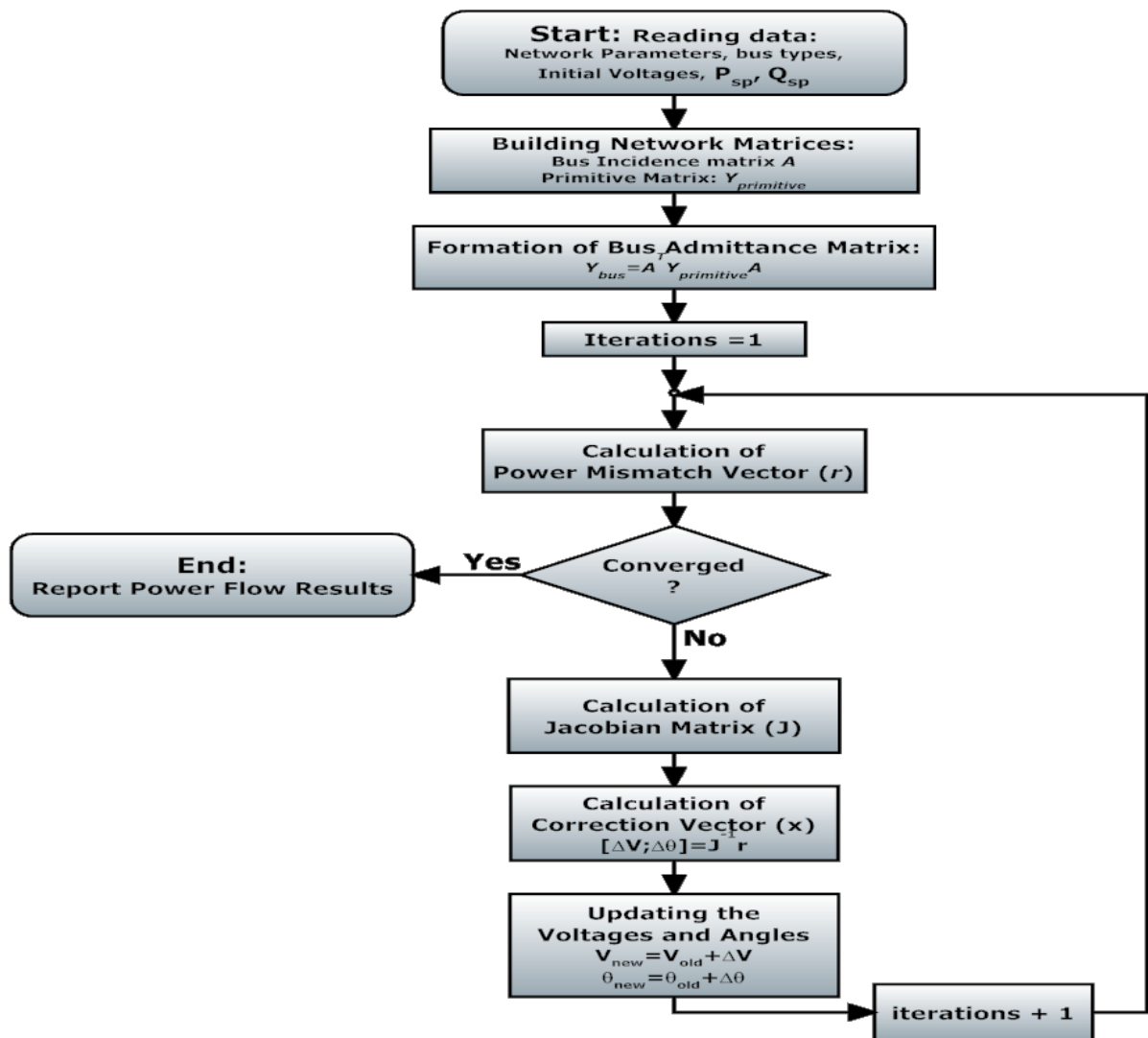


Figure 8: Flowchart for implementation of Newton-Raphson AC Load Flow

2.7 Literature Review of AC-DC Load Flow

In the literature, high voltage DC transmission is now an acceptable alternative to AC and is proving an economical solution not only for long distance transmission but also for underground and submarine transmission. It also serves as a means to interconnect systems of different frequencies or to deal with problems of stability or fault levels [Arnold1990] [15].

The growing number of schemes in existence and under consideration demands corresponding modelling facilities for planning and operational purposes. The basic load flow has to be substantially modified to be capable of modelling the operating state of the combined AC and DC systems under the specified conditions of load, generation, and DC system control strategies [Arnold1990] [15].

[Arrillaga 1978, 1980 and 1977][16] [17] [18] combine the converter equations along with the AC-DC power flow equations in order to solve the combined set simultaneously. On the other hand, [Reeves 1977 and 1973] [19] [20] solves the AC power flow equations first and then solve the DC system equations using the interface variables as computed from the AC load flow. The computed active and reactive power consumption at the converter terminals are then forced into the AC system as loads. This process continues until convergence is achieved. [El Marsafawy and Mathur 1980] [21] solve the DC system equations in a step-by-step manner and force the DC corrections in the solution of the AC system, with the process continuing until sufficient convergence is achieved.

[El-Hawary and Ibrahim 1995] [22] were responsible for the development of a computer program that solves a new approach for AC/DC load flow analysis. The program uses

Newton's method to solve the non-linear set of equations. Modifications to the alternative formulation of the AC/DC load flow problem combined with the results of this model raised doubts about the validity of neglecting the converter transformer reactance. This demonstrates that these reactance's may have adverse effects not only on the reactive power requirement of the converter station, but also on controlling DC voltages via phase or tap control. In any case, this model can only be applied to standard modes of control (i.e., constant power, current or voltage). The converter transformer reactance results in reduced accuracy and less confidence in the validity of the solution.

An alternative method for solving the AC/DC system with either DC-link or MTDC-mesh power flow calculations were offered by [Ding 1997] [23]. This involves a new approach to the load equivalent method, where the central idea is to treat the converters as voltage dependent loads. The method is more efficient and convenient than previous methods and is readily implemented in the AC power flow algorithm. Obtaining fast decoupled power flow for AC/MTDC systems is especially easy with this method.

[Mustafa and Abdul Kadir 2000] [24] presented a simplified and enhanced DC link model which integrated with an AC load flow with the minimum amount of modification. The load flow solution is based on the Fast Decoupled Method, which requires some iteration to obtain the results. The variables of the DC link chosen for the simulation are: the converter, terminal DC voltages, the converter transformer taps ratios, the firing angle of the rectifier, and the current in the HVDC link. This model resolves the HVDC link and develops and tests an algorithm power flow system.

The development of sequential AC-DC power flow algorithm with the AC/DC system consisting of balanced and unbalanced bipolar multi-terminal AC/DC models were

reviewed by [Arifoglu 2003] [25]. The algorithm for this method can also be implemented with current-, voltage- and power-controlled terminals without making any changes to the proposed method. In this situation, the dimensions of a Jacobian matrix will increase very rapidly. Using Newton's method, the storage requirements of a DC power flow technique are large and the solution time is extended.

The Decoupled AC/DC Load Flow Monte Carlo simulation method was developed by [Minassians & Gharehpetian 2004] [26]. It involved the analysis and resolution of 'DC traction systems modeling' with a type of AC/DC load flow to determine the electrical variables of AC and DC systems as a function of time and location. In this model, a minimum number of iterations are needed to avoid convergence problems. The Monte Carlo simulation method has since been implemented in the AC/DC load flow algorithm in order to determine the worst operating conditions of the systems.

[Panosyan et al. 2004] [27] developed a method that integrated HVDC links with the Newton-Raphson load flow algorithm in power systems. The method is modified to attain compatibility for AC/DC systems with integrated DC links in the AC network. Only elements of the residual vector and the Jacobian matrix that are associated with an AC/DC bus were modified in this method. Also, the modified Jacobian equation includes the DC real and reactive power at the AC/DC buses as well as their dependency on the AC system variables.

A model of a general purpose for AC/DC Load Flow utilizing the Newton-Raphson and Broyden Methods was proposed by [Osaloni & Radman 2005] [28]. In their model, the well-known Jacobian equation for the AC power flow is modified to achieve compatibility for systems with integrated DC links in the AC network. This model treats

the converters as voltage dependent PQ-Buses, and the DC variables are included in the power flow equations. The use of algorithms for both methods is more efficient and easier to implement when compared to other previously reported methods.

A detailed examination into the limitations of the transmitted power of an HVDC link system incorporated in the real AC power system was presented by [Lis 2007] [29], who demonstrated the impacts of the combined AC/DC system model, including the creation of an efficient and reliable AC/DC load flow method. This method has proven capable of accommodating different types of HVDC link system control modes. The effectiveness of the developed AC/DC load flow method and the influence of the system parameters on the capability of the HVDC transmission system are then investigated on a test system composed of two parallel HVDC/AC lines incorporated into AC power systems.

Through the utilization of the sequential AC/DC power flow, an effective method for solving AC networks containing VSC HVDC was presented in [Belmans 2010] [30]. A general solution was proposed which offers the ability to include an arbitrary DC system into existing AC networks. In VSC HVDC technology, the converter losses represent a significant proportion of the overall system losses. However, they are often neglected or simply inadequately accounted for in VSC HVDC power flows. Moreover, the power set-points are defined with respect to the system voltage, which necessitates an additional iterative procedure for the DC slack bus converter. The DC system modelling method is claimed to be devoid of any restriction on the HVDC grid topology.

A method designed to enhance DC models with a correction term, based on historical data while preserving its computational efficiency and linear formulation, was presented in [Kumar 2010] [31]. Here, the precision of the DC method is fully dependent on

configuration and operating conditions of individual power systems, and thus it is crucial to carefully implement DC models. The DC model is 60 times faster than the AC model. Due to the fast solution time, the DC power flow model has become a commonly used analysis technique in power systems and market applications. The improved DC method can be very suitable when a large number of power flow system calculations are needed under different generation/loading conditions.

The development of power flow algorithms for combining an accurate AC model with a DC model is discussed by [Overbye and Kim 2011] [32]. This approach formulates both nonlinear and linear algebraic equations and deals with trade-off issues between the accuracy of the AC model and the faster solution of the DC model. It shows that the hybrid model can be used for applications requiring greater accuracy than the DC model allows.

[Haileselassie & Allen 2011] [33] discuss a numerical iteration method based upon the Newton Raphson approximation for analyzing power flow in multi-terminal HVDC networks. In this method, the power flow of a terminal HVDC grid is tested and analyzed. It was observed that even with unsatisfactory initial estimates of the unknown variables, the solution set was seen to converge quite rapidly. The proposed method can be used to analyze power flows in complex DC network systems.

Other work resolved [Ayan & Arifoglu 2011] [34] the load flow analysis of AC power systems by utilizing both the numerical analysis methods and the heuristic methods. This involved implementing the load flow of integrated AC/DC power systems by using the available numerical methods. The literature presents many methods of implementing load flow analysis of integrated AC/DC power systems. In this particular method, the

sequential load flow analysis of AC/DC system is implemented by using Genetic Algorithm (which is one of the heuristic methods) and applying it to the load flow problem of integrated AC/DC power systems.

More recently [Zhijun 2012] [35], other researchers have proposed a robust non-divergent power flow calculation algorithm based on nonlinear programming. The Interior Point Method (IPM) is used to solve this model, which is also applicable for large-scale AC/DC power grids. The special structure of the proposed model requires the size of coefficient of correction equations in the IPM to be reduced to the same size as the Jacobian in the conventional Newton method. Further, the coefficients are symmetrical positive-definite with a diagonal perturbation, which leads to a better convergence than Newton direction. The algorithm has the following features: (1) the size of the correction equations is the same as that in the conventional NR method; (2) the number of total non-zeros in the coefficient of correction equations are almost the same as Jacobian power flow equations; and (3) the coefficient of correction equations is symmetrical positive-definite. The algorithm can be accomplished with three or four times less CPU time as the conventional Newton-Raphson algorithm for large-scale power flow analysis.

Chapter 3: HVDC Load Flow Solution Method

3.1 Introduction

High Voltage Direct Current (HVDC) transmission is important for long distance, underground, and submarine transmission. Due to the increasing strains on existing systems, it is necessary to develop a better method for performing the load flow analysis of an integrated HVDC power system. However, the power flow has to be substantially enhanced to be capable of modeling the operating state of the combined AC and DC systems, and this must be done fast and efficiently under the specified conditions of load generation and DC system control strategies.

The development of an enhanced HVDC-load flow system based on the Newton - Raphson method is the focus of this chapter. The variation of the DC link chosen for the problem formulation are: (1) the converter, terminal DC voltage; (2) the real and imaginary components of the transformer secondary current; (3) converting transformer tap ratios; (4) the firing angle of the rectifier; and (5) the current in the DC link. The equations relating these five variables and their solution strategy are discussed. As the model developed is independent of a particular control mode of the DC link, the AC and DC link equations are solved separately and thus the integration into a standard load flow program is possible without significant modifications of the AC load flow algorithm. In the AC system iterations, each converter is designed as a complex power load at the AC terminal bus bar, and the DC link equations are solved using the most recent value of the AC bus bar voltage. The AC and DC system equations are solved simultaneously, taking

into account the inter-connectedness of both equations [Arrillaga and Arnold1990] [15] [Osaloni & Radman 2005] [28].

3.2 Model of HVDC System

HVDC converters included in the load flow analysis of power systems have been modeled in the polar coordinate form. An HVDC converter connected to an AC bus bar 'i' and a DC bus bar 'k' is shown in Figure 9:

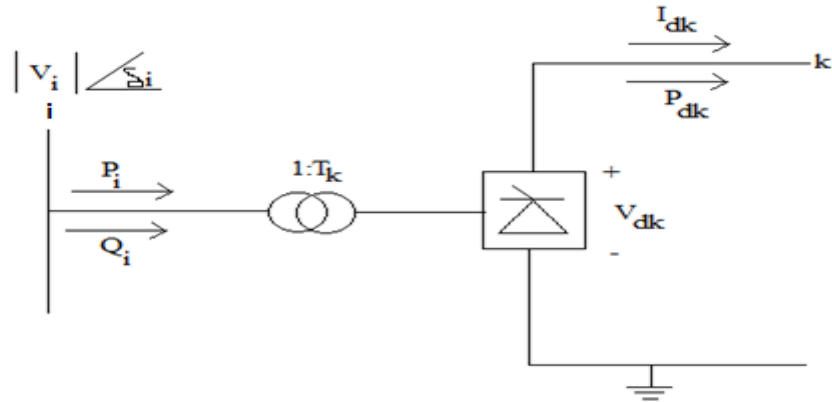


Figure 9: Modelling of DC Converter Station k [Arnold1990] [15]

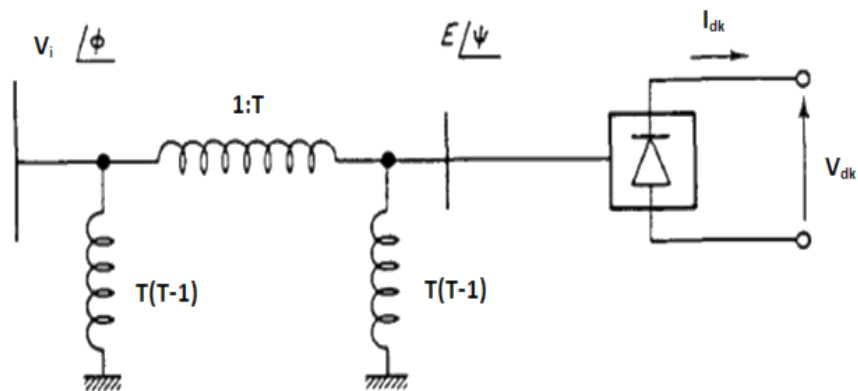


Figure 10: A Single-Phase Equivalent Circuit for Basic Converters (Angles Referred to DC. Reference) Arnold1990] [15]

All model equations are given by [Arrillaga and Arnold1990] [15]; [J. Crainger and D. Stevenson1994] [2]; [Q. F. Ding et.al 1997] [23]:-

The DC voltage at converter station k is:

$$V_{dk} = (K_1 T_k |V_i| \cos \Theta_k - \frac{3}{\pi} X_{ck} I_{dk}) (sgn)_k \quad (3-1)$$

Where

$|V_i|$ = AC terminal Voltage

T_k = Converter transformer taps ratio

X_{ck} = Commutating reactance

I_{dk} = DC current

$$K_1 = \frac{3\sqrt{2}}{\pi}$$

$(sgn)_k = 1$ if the converter at the AC bus bar 'i' is a rectifier.

$= -1$ if the converter at the AC bus bar 'i' is an inverter.

Θ_k = Converter control angle.

$\Theta_k = \alpha_k$; For rectifier operation.

$\Theta_k = \gamma_k$; For inverter operation.

$\Phi_k = \emptyset_k$; for rectifying mode.

$\Phi_k = (\pi - \emptyset_k)$; for inverting mode.

G is a conductance matrix of MTDC system.

All the angles are calculated by degree.

For the AC line current of the inverter transformers with converter station k, we can write the relation as

$$I_i = T_i \frac{3\sqrt{2}}{\pi} I_{dk} \quad (3-2)$$

If the AC current is $\frac{1}{\sqrt{3}}$ times the DC current, we have

$$I_{ac} = \frac{1}{\sqrt{3}} I_{dc} \quad (3-3)$$

The DC network equations are obtained as:

$$I_{dk} = [G]V_{dk} \quad (3-4)$$

The variables $P_i(dc)$ and $Q_i(dc)$ are calculated by:

$$P_i(dc) = P_{dk} \quad (3-5)$$

$$P_i(dc) = (sgn)_k K_1 |V_i| I_{dk} \cos \Phi_k \quad (3-6)$$

$$Q_i(dc) = (sgn)_k K_1 |V_i| I_{dk} \sin \Phi_k \quad (3-7)$$

$$P_{dk} = V_{dk} I_{dk} \quad (3-8)$$

$$Q_{dk} = 0 \quad (3-9)$$

The active and reactive power flow from the bus i to all converter stations connected to it k is

$$P_i(dc) = K_1 |V_i| \sum_{k=1}^n (sgn)_k T_k I_{dk} \cos \Phi_k \quad (3-10)$$

$$Q_i(dc) = K_1 |V_i| \sum_{k=1}^n T_k I_{dk} \sin \Phi_k \quad (3-11)$$

These equations, with new injected power $-P_d$ and $-Q_d$ can be written as

$$P_{sch} - P_{cal}(AC) - P_{cal}(DC) = 0 \quad (3-12)$$

$$Q_{sch} - Q_{cal}(AC) - Q_{cal}(DC) = 0 \quad (3-13)$$

Where:

P_{sch} : is the AC system load on the bus bar.

$P_{cal}(AC)$: is the injected power at the terminal busbar as a function of the AC system variables.

$P_{sch}(DC)$: is the injected power at the terminal Busbar as a function of the DC system variables.

And similarly, Q_{sch} , $Q_{cal}(AC)$ and $Q_{sch}(DC)$.

The injected powers $P_{sch}(DC)$, and $Q_{sch}(DC)$ are the functions of the converter, AC terminal Busbar voltage and of the DC system variables. So, we have

$$P_{sch}(DC) = R(V, U_{dc}) \quad (3-14)$$

$$Q_{sch}(DC) = R(V, U_{dc}) \quad (3-15)$$

The equations derived from the specified AC system conditions may therefore be summarized as

$$\begin{bmatrix} \Delta P(V, \delta) \\ \Delta Q(V, \delta) \\ \Delta P(V, \delta, U_{dc}) \\ \Delta Q(V, \delta, U_{dc}) \end{bmatrix} = 0 \quad (3-16)$$

Where the mismatches at the converter buses are indicated separately. These can be written as

$$\Delta R(V, U_{dc})_k = 0 \quad (3-17)$$

K=1 means the number of converters present.

The normal AC power flow equations are valid, except that mismatches power flow equations at the converter station AC buses are modified. Therefore, the mismatches power flow equations may be summarized as follows:

$$\begin{bmatrix} \Delta P(V, \delta) \\ \Delta Q(V, \delta) \\ \Delta P(V, \delta, U_{dc}) \\ \Delta Q(V, \delta, U_{dc}) \\ \Delta R(V, U_{dc}) \end{bmatrix} = 0 \quad (3-18)$$

For the combined AC/DC system model, the operating state can be defined by the following vector

$$U = [V, \delta, U_{dc}]^T \quad (3-19)$$

Where V is the vector of the voltage magnitudes at all AC system buses and δ is vector of the voltage angles at all AC system buses, except that a once slack bus, which is assumed to be equal to zero.

In the power flow equations R of AC-MTDC system, the only modification required to the usual real and reactive mismatches equations occurs for those equations, which relate to the converter terminal AC buses.

3.3 DC of Control Modelling Equations

There are a number of different modes in which a converter station can be operated, including, but not limited to, constant current or constant power.

Converting controls, which are normally specified, are:

1. Control converter equation for the DC current:

$$I_{dk} - I_{dk}^{sp} = 0 \quad (3-20)$$

2. Control converter equation for the DC voltage:

$$V_{dk} - V_{dk}^{sp} = 0 \quad (3-21)$$

3. Control converter equation for the DC power:

$$V_{dk}I_{dk} - P_{dk}^{sp} = 0 \quad (3-22)$$

4. Control converter equation transformer taps:

$$T_k - T_k^{sp} = 0 \quad (3-23)$$

5. Control converter equation for the control angle:

$$\cos \theta_k - \cos \theta_k^{sp} = 0 \quad (3-24)$$

These control converter equations easily include in the solution algorithms. Nonstandard modes such as specified AC terminal voltage may also be included with the usual control modes as converter equations.

3.4 AC-DC Load Flow Analysis Using the Newton-Raphson Method

This section describes how the DC equations are integrated into the Newton-Raphson-based AC power flow analysis.

- The unknown variables of the AC system are $|V|, \delta$.
- The unknown variables of the DC system $V_d, I_d, T, \cos \Theta$ and Φ .

These variables need to be updated during the iteration process. To begin with, the active and reactive power mismatches at converter i are defined by:

$$\begin{aligned} \Delta P_i(|V|, \delta, U_{dc}) &= P_{i,sch} - P_{i,cal}(|V|, \delta) - P_{i,cal}(|V|, U_{dc}) \\ &= (P_{Gi} - P_{Di}) - P_{i,cal}(|V|, \delta) - P_{i,cal}(|V|, U_{dc}) \end{aligned} \quad (3-25)$$

$$\begin{aligned} \Delta Q_i(|V|, \delta, U_{dc}) &= Q_{i,sch} - Q_{i,cal}(|V|, \delta) - Q_{i,cal}(|V|, U_{dc}) \\ &= (Q_{Gi} - Q_{Di}) - Q_{i,cal}(|V|, \delta) - Q_{i,cal}(|V|, U_{dc}) \end{aligned} \quad (3-26)$$

The variables of active and reactive power mismatches are calculated by

- For an AC system

$$P_{i,cal}(|V|, \delta) = |V_i|^2 G_{ii} + \sum_{n \neq i}^N |Y_{in} V_n V_i| \cos(\theta_{in} + \delta_n - \delta_i) \quad (3-27)$$

$$Q_{i,cal}(|V|, \delta) = -|V_i|^2 B_{ii} - \sum_{n \neq i}^N |Y_{in} V_n V_i| \sin(\theta_{in} + \delta_n - \delta_i) \quad (3-28)$$

- For a DC system

$$P_{i,cal}(|V|, U_{dc}) = K_1 |V_i| \sum_{k=1}^n (\text{sgn})_k T_k I_{dk} \cos \Phi_k \quad (3-29)$$

$$Q_{i,cal}(|V|, U_{dc}) = K_1 |V_i| \sum_{k=1}^n T_k I_{dk} \sin \Phi_k \quad (3-30)$$

The power balance equations at a bus that has converters connected to it can be mathematically written as:

$$\begin{aligned}\Delta P_i(|V|, \delta, U_{dc}) &= P_{i,sch} - P_{i,cal}(|V|, \delta) - P_{i,cal}(|V|, U_{dc}) = 0 \\ &= (P_{Gi} - P_{Di}) - |V_i|^2 G_{ii} - \sum_{\substack{n=1 \\ n \neq i}}^N |Y_{in} V_n V_i| \cos(\theta_{in} + \delta_n - \delta_i) \\ &\quad - K_1 |V_i| \sum_{k=1}^n (sgn)_k T_k I_{dk} \cos \Phi_k = 0\end{aligned}\quad (3-31)$$

$$\begin{aligned}\Delta Q_i(|V|, \delta, U_{dc}) &= Q_{i,sch} - Q_{i,cal}(|V|, \delta) - Q_{i,cal}(|V|, U_{dc}) = 0 \\ &= (Q_{Gi} - Q_{Di}) + |V_i|^2 B_{ii} + \sum_{\substack{n=1 \\ n \neq i}}^N |Y_{in} V_n V_i| \sin(\theta_{in} + \delta_n - \delta_i) \\ &\quad - K_1 |V_i| \sum_{k=1}^n T_k I_{dk} \sin \Phi_k = 0\end{aligned}\quad (3-32)$$

$$U_{dc} = [V_d, I_d, T, \cos \Theta \text{ and } \Phi]^T \quad (3-33)$$

Where: U_{dc} is the a vector variable of the DC system.

The active and reactive power mismatches are a function of the changes in DC variables.

Thus, in order to account for DC equations in an AC Jacobian matrix, the mismatched equations for the DC system need to be defined:

$$R_l(|V_i|, U_{dc})_k = 0, \quad l = \{1, 2, 3, 4, 5\}$$

$$\text{➤ } R_1(|V_i|, U_{dc})_k = V_{dk} - (sgn)_k k_1 T_k |V_i| \cos \Phi_k \quad (3-34)$$

$$\text{➤ } R_2(|V_i|, U_{dc})_k = V_{dk} - (k_1 T_k |V_i| \cos \Theta_k - \frac{3}{\pi} I_{dk} X_{ck}) (sgn)_k \quad (3-35)$$

$$\text{➤ } R_3(|V_i|, U_{dc})_k = (V_{dk}, I_{dk}), \text{ DC equation at the DC bus which is connected to converter station } k. \quad (3-36)$$

$$\text{➤ } R_4(|V_i|, U_{dc})_k = \text{Control equation of converter station } k. \quad (3-37)$$

$$\text{➤ } R_5(|V_i|, U_{dc})_k = \text{Control equation of converter station } k. \quad (3-38)$$

Where: l = the number of DC variables, k = the number of Bus

The Newton-Raphson equations for AC/DC power flow analysis can be written in matrix form as [T Smed et.al. 1991] [36]:

$$\begin{bmatrix} \Delta P_i(|V|, \delta) \\ \Delta P_j(|V|, \delta, U_{dc}) \\ \text{-----} \\ \Delta Q_i(|V|, \delta) \\ \Delta Q_j(|V|, \delta, U_{dc}) \\ \text{-----} \\ \Delta R(|V|, U_{dc}) \end{bmatrix} = J \begin{bmatrix} \Delta \delta_i \\ \Delta \delta_j \\ \text{-----} \\ \Delta |V_i| / |V_i| \\ \Delta |V_j| / |V_j| \\ \text{-----} \\ \Delta U_{dc} \end{bmatrix} \quad (3-39)$$

$$\begin{bmatrix} \Delta P_i(|V|, \delta) \\ \Delta P_j(|V|, \delta, U_{dc}) \\ \text{-----} \\ \Delta Q_i(|V|, \delta) \\ \Delta Q_j(|V|, \delta, U_{dc}) \\ \text{-----} \\ \Delta R(|V|, U_{dc}) \end{bmatrix} = \begin{bmatrix} J_1 & J_2 & 0 \\ J_3 & J_4 & A \\ 0 & 0 & 0 \\ & & C \\ & & D \\ & & E \end{bmatrix} \begin{bmatrix} \Delta \delta_i \\ \Delta \delta_j \\ \text{-----} \\ \Delta |V_i| / |V_i| \\ \Delta |V_j| / |V_j| \\ \text{-----} \\ \Delta U_{dc} \end{bmatrix} \quad (3-40)$$

Where:

$$\begin{bmatrix} \Delta P_i(|V|, \delta) \\ \Delta P_j(|V|, \delta, U_{dc}) \\ \text{-----} \\ \Delta Q_i(|V|, \delta) \\ \Delta Q_j(|V|, \delta, U_{dc}) \\ \text{-----} \\ \Delta R(|V|, U_{dc}) \end{bmatrix} = \text{Mismatch vector}$$

$$\begin{bmatrix} J_1 & J_2 & 0 \\ J_3 & J_4 & A \\ 0 & 0 & 0 \\ & & C \\ & & D \\ & & E \end{bmatrix} = \text{AC-DC Jacobian matrix}$$

$$\begin{bmatrix} \Delta\delta_i \\ \Delta\delta_j \\ \text{---} \\ \Delta|V_i|/|V_i| \\ \Delta|V_j|/|V_j| \\ \text{---} \\ \Delta U_{dc} \end{bmatrix} = \text{Correction vector} \begin{bmatrix} \Delta P_i(|V|, \delta) \\ \Delta P_j(|V|, \delta, U_{dc}) \\ \text{---} \\ \Delta Q_i(|V|, \delta) \\ \Delta Q_j(|V|, \delta, U_{dc}) \\ \text{---} \\ \Delta R(|V|, U_{dc}) \end{bmatrix} =$$

$$\begin{bmatrix} \frac{\partial P_i}{\partial \delta_i} & \frac{\partial P_i}{\partial \delta_j} & |V_i| \frac{\partial P_i}{\partial |V_i|} & |V_j| \frac{\partial P_i}{\partial |V_j|} & 0 \\ \frac{\partial P_j}{\partial \delta_i} & \frac{\partial P_j}{\partial \delta_j} & |V_i| \frac{\partial P_j}{\partial |V_i|} & |V_j| \frac{\partial P_j}{\partial |V_j|} & \frac{\partial P_i}{\partial U_{dc}} \\ \text{---} & \text{---} & \text{---} & \text{---} & \text{---} \\ \frac{\partial Q_i}{\partial \delta_i} & \frac{\partial Q_i}{\partial \delta_j} & |V_i| \frac{\partial Q_i}{\partial |V_i|} & |V_j| \frac{\partial Q_i}{\partial |V_j|} & 0 \\ \frac{\partial Q_j}{\partial \delta_i} & \frac{\partial Q_j}{\partial \delta_j} & |V_i| \frac{\partial Q_j}{\partial |V_i|} & |V_j| \frac{\partial Q_j}{\partial |V_j|} & \frac{\partial Q_i}{\partial U_{dc}} \\ \text{---} & \text{---} & \text{---} & \text{---} & \text{---} \\ 0 & 0 & |V_i| \frac{\partial R}{\partial |V_i|} & |V_j| \frac{\partial R}{\partial |V_j|} & \frac{\partial R}{\partial U_{dc}} \end{bmatrix} \begin{bmatrix} \Delta\delta_i \\ \Delta\delta_j \\ \text{---} \\ \Delta|V_i|/|V_i| \\ \Delta|V_j|/|V_j| \\ \text{---} \\ \Delta U_{dc} \end{bmatrix} \quad (3-41)$$

The state variables In the correction vector are updated by:

$$\delta_i^{(n+1)} = \delta_i^{(n)} + \Delta\delta_i^{(n)} \quad (3-42)$$

$$|V_i|^{(n+1)} = |V_i|^{(n)} \left(1 + \frac{\Delta|V_i|^{(n)}}{|V_i|^{(n)}}\right) \quad (3-43)$$

$$U_{dc}^{(n+1)} = U_{dc}^{(n)} + \Delta U_{dc}^{(n)} \quad (3-44)$$

Where n is the iteration count.

For each converter station, R_1 , R_2 and R_3 are always used, whereas the control equations for R_4 and R_5 are further divided into three possible modes of operation. In each mode, some of the variables are specified. Then, The partial derivatives of R_4 and R_5 for the converter DC with respect to each of the variables in U_{dc} can be divided into seven modes, as follows:

3.4.1 Control Mode 1

This mode specifies P_{dk} and T_k and hence Eq. (3-22) and Eq. (3-23) are applied.

$$\frac{\partial R_{4,k}}{\partial V_{dk}} = I_{dk}$$

$$\frac{\partial R_{4,k}}{\partial I_{dk}} = V_{dk}$$

$$\frac{\partial R_{4,k}}{\partial T_k} = \frac{\partial R_{4,k}}{\partial \cos \Theta_k} = \frac{\partial R_{4,k}}{\partial \Phi_k} = 0$$

$$\frac{\partial R_{5,k}}{\partial T_k} = 1$$

$$\frac{\partial R_{5,k}}{\partial V_{dk}} = \frac{\partial R_{5,k}}{\partial I_{dk}} = \frac{\partial R_{5,k}}{\partial \cos \Theta_k} = \frac{\partial R_{5,k}}{\partial \Phi_k} = 0$$

3.4.2 Control Mode 2

This mode specifies P_{dk} and Θ_k , and hence Eq.(3-22) and Eq.(3-24) are applied.

$$\frac{\partial R_{4,k}}{\partial V_{dk}} = I_{dk}$$

$$\frac{\partial R_{4,k}}{\partial I_{dk}} = V_{dk}$$

$$\frac{\partial R_{4,k}}{\partial T_k} = \frac{\partial R_{4,k}}{\partial \cos \Theta_k} = \frac{\partial R_{4,k}}{\partial \Phi_k} = 0$$

$$\frac{\partial R_{5,k}}{\partial \cos \Theta_k} = 1$$

$$\frac{\partial R_{5,k}}{\partial V_{dk}} = \frac{\partial R_{5,k}}{\partial I_{dk}} = \frac{\partial R_{5,k}}{\partial T_k} = \frac{\partial R_{5,k}}{\partial \Phi_k} = 0$$

3.4.3 Control Mode 3

This mode specifies I_{dk} and T_k and hence Eq. (3-20) and Eq. (3-23) are applied.

$$\frac{\partial R_{4,k}}{\partial I_{dk}} = 1$$

$$\frac{\partial R_{4,k}}{\partial V_{dk}} = \frac{\partial R_{4,k}}{\partial T_k} = \frac{\partial R_{4,k}}{\partial \cos \Theta_k} = \frac{\partial R_{4,k}}{\partial \Phi_k} = 0$$

$$\frac{\partial R_{5,k}}{\partial T_k} = 1$$

$$\frac{\partial R_{5,k}}{\partial V_{dk}} = \frac{\partial R_{5,k}}{\partial I_{dk}} = \frac{\partial R_{5,k}}{\partial \cos \Theta_k} = \frac{\partial R_{5,k}}{\partial \Phi_k} = 0$$

3.4.4 Control Mode 4

This mode specifies I_{dk} and Θ_k and hence Eq.(3-20) and Eq. (3-24) are applied.

$$\frac{\partial R_{4,k}}{\partial I_{dk}} = 1$$

$$\frac{\partial R_{4,k}}{\partial V_{dk}} = \frac{\partial R_{4,k}}{\partial T_k} = \frac{\partial R_{4,k}}{\partial \cos \Theta_k} = \frac{\partial R_{4,k}}{\partial \Phi_k} = 0$$

$$\frac{\partial R_{5,k}}{\partial \cos \Theta_k} = 1$$

$$\frac{\partial R_{5,k}}{\partial V_{dk}} = \frac{\partial R_{5,k}}{\partial I_{dk}} = \frac{\partial R_{5,k}}{\partial T_k} = \frac{\partial R_{5,k}}{\partial \Phi_k} = 0$$

3.4.5 Control Mode 5

This mode specifies T_k and Θ_k and hence Eq. (3-23) and Eq. (3-24) are applied.

$$\frac{\partial R_{4,k}}{\partial T_k} = 1$$

$$\frac{\partial R_{4,k}}{\partial V_{dk}} = \frac{\partial R_{4,k}}{\partial I_{dk}} = \frac{\partial R_{4,k}}{\partial \cos \Theta_k} = \frac{\partial R_{4,k}}{\partial \Phi_k} = 0$$

$$\frac{\partial R_{5,k}}{\partial \cos \Theta_k} = 1$$

$$\frac{\partial R_{5,k}}{\partial V_{dk}} = \frac{\partial R_{5,k}}{\partial I_{dk}} = \frac{\partial R_{5,k}}{\partial T_k} = \frac{\partial R_{5,k}}{\partial \Phi_k} = 0$$

3.4.6 Control Mode 6

This mode specifies V_{dk} and T_k and hence Eq. (3-21) and Eq. (3-23) are applied.

$$\frac{\partial R_{4,k}}{\partial V_{dk}} = 1$$

$$\frac{\partial R_{4,k}}{\partial I_{dk}} = \frac{\partial R_{4,k}}{\partial T_{dk}} = \frac{\partial R_{4,k}}{\partial \cos \Theta_k} = \frac{\partial R_{4,k}}{\partial \Phi_k} = 0$$

$$\frac{\partial R_{5,k}}{\partial T_k} = 1$$

$$\frac{\partial R_{5,k}}{\partial V_{dk}} = \frac{\partial R_{5,k}}{\partial I_{dk}} = \frac{\partial R_{5,k}}{\partial \cos \Theta_k} = \frac{\partial R_{5,k}}{\partial \Phi_k} = 0$$

3.4.7 Control Mode 7

This mode specifies V_{dk} and Θ_k , and hence Eq. (3-21) and Eq. (3-24) are applied.

$$\frac{\partial R_{4,k}}{\partial V_{dk}} = 1$$

$$\frac{\partial R_{4,k}}{\partial I_{dk}} = \frac{\partial R_{4,k}}{\partial T_{dk}} = \frac{\partial R_{4,k}}{\partial \cos \Theta_k} = \frac{\partial R_{4,k}}{\partial \Phi_k} = 0$$

$$\frac{\partial R_{5,k}}{\partial \cos \Theta_k} = 1$$

$$\frac{\partial R_{5,k}}{\partial V_{dk}} = \frac{\partial R_{5,k}}{\partial I_{dk}} = \frac{\partial R_{5,k}}{\partial T_k} = \frac{\partial R_{5,k}}{\partial \Phi_k} = 0$$

3.5 Evaluation of Derivatives

The diagonal and off-diagonal elements for each of the sub-matrices in the Jacobian matrix are given below:

A-Sub-matrix $J_1 = \frac{\partial P}{\partial \delta}$

$$\frac{\partial P_i}{\partial \delta_i} = -Q_{i,cal}(|V|, \delta) - B_{ii}|V_i|^2$$

$$\frac{\partial P_i}{\partial \delta_j} = -|V_j V_i Y_{ij}| \sin(\theta_{ij} + \delta_j - \delta_i)$$

B-Sub-matrix $J_4 = |V| \frac{\partial P}{\partial |V|}$

- For a voltage controlled bus i or a load bus i

$$|V_i| \frac{\partial Q_i}{\partial |V_i|} = -\frac{\partial P_i}{\partial \delta_i} - 2B_{ii}|V_i|^2$$

$$|V_j| \frac{\partial Q_i}{\partial |V_j|} = +\frac{\partial P_i}{\partial \delta_j}$$

- For a converter DC link k connected to the bus i

$$|V_i| \frac{\partial Q_i}{\partial |V_i|} = -\frac{\partial P_i}{\partial \delta_j} - 2B_{ii}|V_i|^2 + Q_{i,cal}(|V|, U_{dc})$$

$$|V_j| \frac{\partial Q_i}{\partial |V_j|} = +\frac{\partial P_i}{\partial \delta_j}$$

C-Sub-matrix $J_3 = \frac{\partial Q}{\partial \delta}$

$$\frac{\partial Q_i}{\partial \delta_i} = P_{i,cal}(|V|, \delta) - G_{ii}|V_i|^2$$

$$\frac{\partial Q_i}{\partial \delta_j} = -|V_j V_i Y_{ij}| \cos(\theta_{ij} + \delta_j - \delta_i)$$

D-Sub-matrix $J_2 = |V| \frac{\partial P}{\partial |V|}$

- For a voltage controlled bus i or a load bus i

$$|V_i| \frac{\partial P_i}{\partial |V_i|} = \frac{\partial Q_i}{\partial \delta_i} + 2G_{ii}|V_i|^2$$

$$|V_j| \frac{\partial P_i}{\partial |V_j|} = |V_j V_i Y_{ij}| \cos(\theta_{ij} + \delta_j - \delta_i) = -\frac{\partial Q_i}{\partial \delta_i}$$

➤ For a converter DC link k connected to the bus i

$$|V_i| \frac{\partial P_i}{\partial |V_i|} = \frac{\partial Q_i}{\partial \delta_i} + 2G_{ii}|V_i|^2 + P_{i,cal}(|V|, U_{dc})$$

$$|V_j| \frac{\partial P_i}{\partial |V_j|} = |V_j V_i Y_{ij}| \cos(\theta_{ij} + \delta_j - \delta_i) = -\frac{\partial Q_i}{\partial \delta_i}$$

Sub-matrix A, C, D, E from equations following

$$\text{E-Sub-matrix A} = \frac{\partial P(|V|, \delta, U_{dc})}{\partial U_{dc}}$$

For converter DC link k connected to AC bus i

$$\frac{\partial P_i}{\partial I_{dk}} = (\text{sgn})_k K_1 T_k |V_i| \cos \Phi_k$$

$$\frac{\partial P_i}{\partial T_k} = (\text{sgn})_k K_1 I_{dk} |V_i| \cos \Phi_k$$

$$\frac{\partial P_i}{\partial \Phi_k} = -(\text{sgn})_k K_1 T_k I_{dk} |V_i| \sin \Phi_k$$

$$\frac{\partial P_i}{\partial V_{dk}} = \frac{\partial P_i}{\partial \cos \Theta_k} = 0$$

$$\text{F-Sub-matrix C} = \frac{\partial Q(|V|, \delta, U_{dc})}{\partial U_{dc}}$$

For converter DC link k connected to AC bus i

$$\frac{\partial Q_i}{\partial I_{dk}} = K_1 T_k |V_i| \sin \Phi_k$$

$$\frac{\partial Q_i}{\partial T_k} = K_1 I_{dk} |V_i| \sin \Phi_k$$

$$\frac{\partial Q_i}{\partial \Phi_k} = K_1 T_k I_{dk} |V_i| \cos \Phi_k$$

$$\frac{\partial Q_i}{\partial V_{dk}} = \frac{\partial Q_i}{\partial \cos \Theta_k} = 0$$

G-Sub-matrix $D = |V| \frac{\partial R}{\partial |V|}$

The partial derivatives of $R(|V|, U_{dc})$ for the converter DC link with respect to the voltage at bus i are:

$$|V_i| \frac{\partial R_{1,k}}{\partial |V_i|} = -(sgn)_k K_1 T_k |V_i| \cos \Phi_k$$

$$|V_i| \frac{\partial R_{2,k}}{\partial |V_i|} = -(sgn)_k T_k |V_i| \cos \Theta_k$$

$$|V_i| \frac{\partial R_{3,k}}{\partial |V_i|} = |V_i| \frac{\partial R_{4,k}}{\partial |V_i|} = |V_i| \frac{\partial R_{5,k}}{\partial |V_i|} = 0$$

H-Sub-matrix $E = \frac{\partial R}{\partial U_{dc}}$

The partial derivatives of R_1 and R_2 for the converter DC link 'k' with respect to each of the variables in U_{dc} are

1. The partial derivatives for R_1 :

$$\frac{\partial R_{1,k}}{\partial V_{dk}} = 1$$

$$\frac{\partial R_{1,k}}{\partial T_k} = -(sgn)_k K_1 |V_i| \cos \Phi_k$$

$$\frac{\partial R_{1,k}}{\partial \Phi_k} = (sgn)_k K_1 T_k |V_i| \sin \Phi_k$$

$$\frac{\partial R_{1,k}}{\partial I_{dk}} = \frac{\partial R_{1,k}}{\partial \cos \Theta_k} = 0$$

2. The partial derivatives for R_2 :

$$\frac{\partial R_{2,k}}{\partial V_{dk}} = 1$$

$$\frac{\partial R_{2,k}}{\partial I_{dk}} = (sgn)_k \frac{3}{\pi} X_{ck}$$

$$\frac{\partial R_{2,k}}{\partial T_k} = -(sgn)_k K_1 |V_i| \cos \Theta_k$$

$$\frac{\partial R_{2,k}}{\partial \cos \Theta_k} = (sgn)_k K_1 T_k |V_i|$$

$$\frac{\partial R_{2,k}}{\partial \Phi_k} = 0$$

3. The DC network equations which are connected to the $R_{3,k}$ for converter station in the system can be calculated as follows:

$$R_{3,k} = (sgn)_k I_{dk} - \sum_{j=1}^{N_{dc}} (sgn)_k Gdc_{kj} V_{dj}$$

Where: – N_{dc} Is the number of converters

The partial derivatives of R_3 for converter station k with respect to each of the variables in the U_{dc} are:

$$\frac{\partial R_{3,k}}{\partial V_{dk}} = -Gdc_{kj}$$

$$\frac{\partial R_{3,k}}{\partial I_{dk}} = (sgn)_k$$

$$\frac{\partial R_{3,k}}{\partial T_k} = \frac{\partial R_{3,k}}{\partial \cos \Theta_k} = \frac{\partial R_{3,k}}{\partial \Phi_k} = 0$$

Chapter 4: Computational Results and Discussion

4.1 Introduction

This chapter summarizes the results of extensive computational testing of the proposed algorithms, as outlined in the previous chapter. As a result of the unavailability of standard HVDC test systems, the proposed models were tested on an existing AC system, modified to include DC links. In each system, one and three AC lines are replaced by one and two DC lines, respectively. The power controls on these lines are taken as power flowing in the replaced AC lines.

Additionally, in this chapter, a detailed simulation of IEEE 14 – and 30-bus systems are conducted. The standard bus system has been modified into two and three -terminal DC link systems in order to solve the AC, DC and HVDC systems independently. In terms of accuracy and computational speed, this enhanced method is superior to any conventional Newton-Raphson (NR) load flow and performs effectively under various types of network conditions where other methods cannot give satisfactory results. Simulation studies have also been conducted under different control specifications. It is not possible to compare results of various research papers because each one uses a different test system.

4.2 Case Studies

The test systems are based on the Institute of Electrical and Electronics Engineers' (IEEE) 14- and 30-bus system case studies for power system networks. The system base MVA and the base voltage are 100 MVA and 100 KV, respectively. The tolerance for convergence checking is 0.00001, the details of which are provided here:

4.2.1 IEEE 14-Busbar System:

Case I: The AC line between bus bars 4 and 5 is replaced by two DC links.

Case II: The AC lines between bus bars 2-4, 2-5, and 4-5 are replaced by a DC link; a three-terminal DC link is obtained between bus bars 2, 4 and 5.

4.2.2 IEEE 30-Busbar System:

Case I: AC line between bus bars 2 and 5 is replaced by two DC links.

Case II: A three-terminal DC link is formed between bus bars 2 and 7 by placing an AC line connecting bus bars 2 and 5 by a two-terminal DC link and introducing a two-terminal DC link between bus bars 2 and 7 and bus bars 5 and 7.

4.3 Unified AC-DC Load Flow Method

In the figure 11, the flowchart of AC/DC power flow implemented in this chapter is shown.

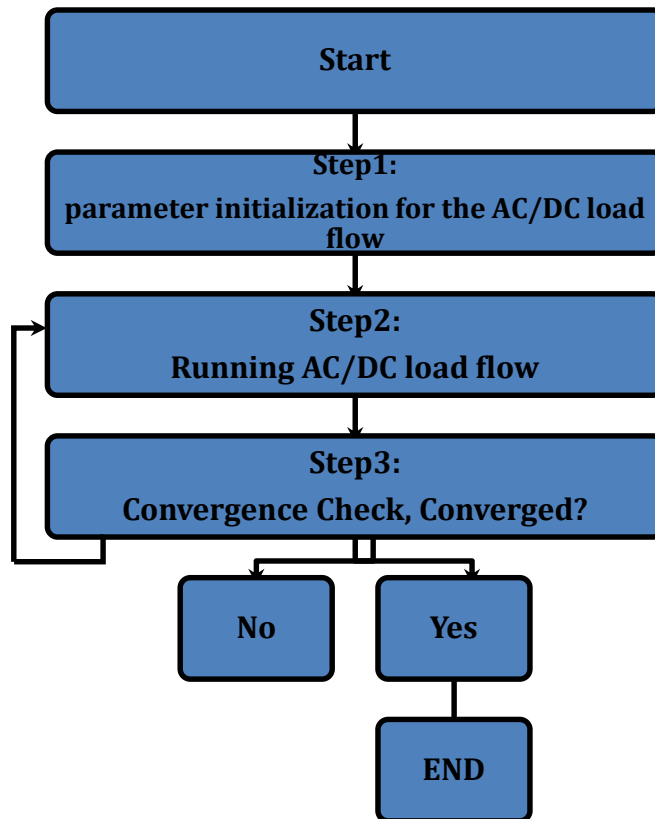


Figure 11: Flowchart of Unified AC-DC Load Flow

4.4 Test Results

The test results of the method are compared with those corresponding to the Newton-Raphson power flow method. A number of sample systems are studied through the proposed method and its HVDC power flow performance. In order to investigate the feasibility of the proposed technique, a large number of power systems of varying sizes have been modified under different system conditions in two- and three-terminal DC link configurations in order to solve HVDC power flow problems. Several case studies ref.

[36] and the control models for power flow analyses were performed and are provided in Appendix B. Other test results are presented in the following tables.

4.4.1 : 14-Bus system with two terminal DC converters

Table 1: Load Flow solution of 14 Bus system for mode 1 with two converters

I- Voltage magnitude, angle, active, and reactive powers

Load Flow solution				
Bus	V	Ang	P(pu)	Q(pu)
1	1.0600	0.0000	0.0000	0.0000
2	1.0450	-9.7872	0.2724	0.1803
3	1.0100	-20.8167	0.9901	0.2567
4	0.9791	-20.9028	0.5057	0.0850
5	0.9800	-18.9441	0.1381	0.0571
6	1.0700	-24.8154	0.2048	0.1190
7	1.0374	-23.8475	0.0520	0.0305
8	1.0900	-23.8475	0.0360	0.0421
9	1.0311	-25.4315	0.3591	0.2635
10	1.0224	-25.6149	0.1422	0.1001
11	1.0436	-25.3287	0.0810	0.0662
12	1.0556	-25.7292	0.1068	0.0423
13	1.0477	-25.7671	0.2169	0.1272
14	1.0142	-26.6614	0.1902	0.0910

II- Results of the DC converters output

Converters No.	Variables				
	V_d	I_d	T	$\cos\theta$	Φ
1	0.941	0.101	1.000	0.854	19.372
2	0.926	0.136	1.000	0.998	24.356

Table 2: Load Flow solution of 14-Bus system for mode 2 with two converters

I- Voltage magnitude, angle, active, and reactive powers

Load flow Solution				
Bus	V	Ang	P(pu)	Q(pu)
1	1.0600	0.0000	0.0000	0.0000
2	1.0450	-9.7872	0.2993	0.1583
3	1.0100	-20.8167	1.1140	0.2797
4	0.9889	-20.9028	0.4912	0.0496
5	0.9926	-18.9441	0.1097	0.0321
6	1.0700	-24.8154	0.1912	0.1096
7	1.0420	-23.8475	0.0130	0.0171
8	1.0900	-23.8475	0.0082	0.0230
9	1.0284	-25.4315	0.3054	0.2187
10	1.0260	-25.6149	0.1637	0.0985
11	1.0455	-25.3287	0.0497	0.0457
12	1.0559	-25.7292	0.1278	0.0350
13	1.0483	-25.7671	0.2045	0.0814
14	1.0169	-26.6614	0.2138	0.0682

II- Results of the DC converters output

Converters No.	Variables				
	V_d	I_d	T	$\cos\theta$	Φ
1	0.865	0.097	0.812	0.882	46.466
2	1.070	-0.642	1.500	0.771	21.159

Table 3: Load Flow solution of 14-Bus system for mode 3 with two converters

I- Voltage magnitude, angle, active, and reactive powers

Load flow Solution				
Bus	V	Ang	P(pu)	Q(pu)
1	1.0600	0.0000	0.0000	0.0000
2	1.0350	-7.0180	0.2317	0.2234
3	1.0100	-16.1181	0.9611	0.3234
4	1.0061	-14.9323	0.5314	0.1072
5	1.0333	-12.8106	0.0846	0.0681
6	1.0700	-18.5825	0.1198	0.2073
7	1.0509	-17.7965	0.0247	0.0415
8	1.0800	-17.7965	0.0090	0.0110
9	1.0339	-19.3107	0.3842	0.1761
10	1.0326	-19.4634	0.1900	0.1580
11	1.0474	-19.1425	0.1143	0.0245
12	1.0536	-19.4540	0.0840	0.0773
13	1.0471	-19.5159	0.2615	0.1684
14	1.0214	-20.4230	0.1589	0.1360

II- Results of the DC converters output

Converters No.	Variables				
	V_d	I_d	T	$\cos\theta$	Φ
1	0.921	0.068	1.000	0.943	17.778
2	1.445	-1.000	1.180	0.625	8.990

Table 4: Load Flow solution of 14-Bus system for mode 4 with two converters

I- Voltage magnitude, angle, active, and reactive powers

Load flow Solution				
Bus	V	Ang	P(pu)	Q(pu)
1	1.0600	0.0000	0.0000	0.0000
2	1.0450	-10.0631	0.4021	0.1393
3	1.0100	-21.2192	1.1412	0.2870
4	0.9917	-21.6967	0.6015	0.0421
5	0.9951	-19.9557	0.0920	0.1038
6	1.0700	-25.7145	0.3534	0.1092
7	1.0431	-24.6993	0.0391	0.0344
8	1.0900	-24.6993	0.0107	0.0265
9	1.0165	-26.3145	0.4015	0.2341
10	1.0269	-26.5036	0.2000	0.1280
11	1.0460	-26.2251	0.0559	0.0609
12	1.0560	-26.6239	0.0775	0.0490
13	1.0485	-26.6662	0.1683	0.1211
14	1.0176	-27.5525	0.1789	0.0843

II- Results of the DC converters output

Converters No.	Variables				
	V_d	I_d	T	$\cos\theta$	Φ
1	1.023	0.045	1.016	0.784	43.250
2	1.110	-1.000	0.931	0.952	28.367

Table 5: Load Flow solution of 14-Bus system for mode 5 with two converters

I- Voltage magnitude, angle, active, and reactive powers

Load flow Solution				
Bus	V	Ang	P(pu)	Q(pu)
1	1.0600	0.0000	0.0000	0.0000
2	1.0450	5.9622	0.2522	0.3018
3	1.0100	8.5001	0.9568	0.3725
4	1.0451	13.5722	0.5550	0.1203
5	1.0534	2.8641	0.0866	0.0900
6	1.0700	2.2454	0.2843	0.3775
7	1.0153	7.8015	0.0000	0.0000
8	1.0900	7.8015	0.0143	0.0122
9	1.0947	4.6974	0.3161	0.2800
10	1.0673	3.8775	0.1499	0.1580
11	1.0211	2.8589	0.1061	0.0912
12	1.0686	1.6395	0.1773	0.0287
13	1.0747	1.6475	0.2182	0.1680
14	1.0242	2.2510	0.2588	0.1410

II- Results of the DC converters output

Converters No.	Variables				
	V_d	I_d	T	$\cos\theta$	Φ
1	1.097	0.842	1.000	0.920	38.635
2	1.600	-0.513	1.016	0.661	7.510

Table 6: Load Flow solution of 14-Bus system for mode 6 with two converters

I- Voltage magnitude, angle, active, and reactive powers

Load flow Solution				
Bus	V	Ang	P(pu)	Q(pu)
1	1.0600	0.0000	0.0000	0.0000
2	1.0450	-4.7302	0.3820	0.2241
3	1.0100	-11.1646	0.9712	0.3437
4	1.1027	-9.7196	0.5210	0.0601
5	1.0777	-12.7604	0.1623	0.0458
6	1.0700	-16.6018	0.1319	0.1120
7	1.1025	-13.7614	0.0288	0.0319
8	1.0900	-13.7614	0.0154	0.0126
9	1.0848	-15.9355	0.3951	0.2011
10	1.0756	-16.3805	0.1300	0.0687
11	1.0721	-16.6378	0.0728	0.0580
12	1.0603	-17.3923	0.1510	0.0361
13	1.0576	-17.4022	0.1450	0.1079
14	1.0520	-17.6705	0.1699	0.1529

II- Results of the DC converters output

Converters No.	Variables				
	V_d	I_d	T	$\cos\theta$	Φ
1	1.250	1.173	1.103	0.679	52.229
2	0.980	-0.096	1.082	0.445	33.068

Table 7: Load Flow solution of 14-Bus system for mode 7 with two converters

I- Voltage magnitude, angle, active, and reactive powers

Load flow Solution				
Bus	V	Ang	P(pu)	Q(pu)
1	1.0600	0.0000	0.0000	0.0000
2	1.0450	-4.7322	0.3060	0.1994
3	1.0100	-11.1525	1.1143	0.2225
4	1.1042	-9.9518	0.5621	0.1100
5	1.0940	-13.0746	0.0979	0.0893
6	1.0700	-16.8456	0.3910	0.0950
7	1.1079	-14.0272	0.0367	0.0138
8	1.0900	-14.0272	0.0400	0.0621
9	1.0580	-16.2194	0.4120	0.2402
10	1.0799	-16.6598	0.1496	0.0985
11	1.0743	-16.9017	0.0697	0.0778
12	1.0607	-17.6356	0.0978	0.0335
13	1.0584	-17.6536	0.1495	0.1384
14	1.0578	-17.9414	0.2337	0.1182

II- Results of the DC converters output

Converters No.	Variables				
	V_d	I_d	T	$\cos\theta$	Φ
1	1.287	1.035	1.084	0.903	13.214
2	0.840	-1.019	0.974	0.715	18.688

4.5 Analysis of Results for 14-Bus with two DC converter system

For 14 bus systems with two converters we concluded that the overall active power is improved after using the converters as well as the overall reactive power for mode 1. For mode 2 to mode 7 the active and reactive power is improved for some buses but became worse for others. For example the active power at bus 4 without using the converters was 47.8 MW and became 50.57 MW after using the converters for mode 1 but it is changed to be 49.12 MW for mode 2, 53.14 MW for mode 3, 60.15 MW for mode 4, 55.50 MW for mode 5, 52.10 MW for mode 6, and 56.21 MW for mode 7. Also the reactive power at bus 4 without using the converters was 3.9 MVAR and became 8.50 MVAR for mode 1 but it is changed to be 4.96 MVAR for mode 2, 10.72 MVAR for mode 3, 4.21 MVAR for mode 4, 12.03 MVAR for mode 5, 6.01 MVAR for mode 6, 11.00 MVAR for mode 7.

For bus 12 without using the converters was 6.1 MW and became 10.68 MW after using the converters for mode 1 but it is changed to be 12.78 MW for mode 2, 8.40 MW for mode 3, 7.75 MW for mode 4, 17.73 MW for mode 5, 15.10 MW for mode 6, and 9.78 MW for mode 7. Also the reactive power at bus 12 without using the converters was 1.6 MVAR and became 4.23 MVAR for mode 1 but it is changed to be 3.50 MVAR for mode 2, 7.73 MVAR for mode 3, 4.90 MVAR for mode 4, 2.87 MVAR for mode 5, 3.61 MVAR for mode 6, 3.35 MVAR for mode 7.

4.5.1: 14-Bus system with three terminal DC converters

Table 8: Load Flow solution of 14-Bus system for mode 1 with three converters

I- Voltage magnitude, angle, active, and reactive powers

Load flow Solution				
Bus	V	Ang	P(pu)	Q(pu)
1	1.0600	0.0000	0.0000	0.0000
2	1.0450	-2.8397	0.3180	0.0594
3	1.0100	-9.4914	0.9992	0.2761
4	0.9585	-0.3098	0.5159	0.0659
5	0.9771	0.0441	0.0910	0.0818
6	1.0700	-5.4062	0.1251	0.1525
7	0.9756	3.3505	0.0405	0.0239
8	1.0900	3.3505	0.0120	0.0750
9	0.8276	0.2675	0.3358	0.2241
10	0.8625	-0.9402	0.1199	0.0900
11	0.9596	-3.2158	0.0465	0.0283
12	1.0393	-6.0271	0.0893	0.0678
13	1.0188	-5.4156	0.1927	0.0939
14	0.8927	-3.2500	0.1601	0.0661

II- Results of the DC converters output

Converters No.	Variables				
	V_d	I_d	T	$\cos\theta$	Φ
1	1.095	0.318	1.000	0.942	25.600
2	1.120	-0.956	0.950	0.877	32.593
3	1.043	1.019	1.030	0.935	15.471

Table 9: Load Flow solution of 14-Bus system for mode 2 with three converters

I- Voltage magnitude, angle, active, and reactive powers

Load flow Solution				
Bus	V	Ang	P(pu)	Q(pu)
1	1.0600	0.0000	0.0000	0.0000
2	1.0450	-2.1422	0.2291	0.1394
3	1.0100	-8.1140	0.9524	0.2001
4	0.9648	-2.8925	0.5274	0.0947
5	0.9730	-2.0002	0.1626	0.0552
6	1.0700	-6.3372	0.1469	0.0816
7	1.0152	-1.2113	0.0255	0.0492
8	1.0900	-1.2113	0.0179	0.0106
9	1.0091	-4.2296	0.3601	0.2730
10	1.0129	-4.8933	0.1236	0.1178
11	1.0390	-5.7312	0.0729	0.0801
12	1.0541	-7.0799	0.0992	0.0200
13	1.0462	-6.9092	0.1611	0.1234
14	1.0069	-6.4771	0.1981	0.1097

II- Results of the DC converters output

Converters No.	Variables				
	V_d	I_d	T	$\cos\theta$	Φ
1	0.997	0.433	0.981	0.894	63.466
2	1.051	-0.783	1.118	0.920	61.138
3	1.003	0.439	1.103	0.411	42.261

Table 10: Load Flow solution of 14-Bus system for mode 3 with three converters

I- Voltage magnitude, angle, active, and reactive powers

Load flow Solution				
Bus	V	Ang	P(pu)	Q(pu)
1	1.0600	0.0000	0.0000	0.0000
2	1.0350	-17.8224	0.2595	0.1482
3	1.0100	-30.6656	0.9889	0.2494
4	1.1051	-60.3589	0.4945	0.0529
5	1.0594	-48.3335	0.1071	0.0937
6	1.0600	-59.5562	0.3226	0.1015
7	1.0465	-88.1416	0.0151	0.0332
8	1.0800	-88.1416	0.0410	0.0376
9	1.0286	-80.3855	0.3212	0.1916
10	1.0764	-76.8121	0.1284	0.0993
11	1.1013	-68.3542	0.0666	0.0317
12	1.0790	-61.4860	0.0752	0.0489
13	1.0895	-63.1715	0.1767	0.1990
14	1.0123	-73.2454	0.2156	0.1335

II- Results of the DC converters output

Converters No.	Variables				
	V_d	I_d	T	$\cos\theta$	Φ
1	1.044	0.625	0.830	0.797	29.270
2	1.110	-0.805	1.100	0.865	60.814
3	0.952	1.023	0.961	0.593	34.083

Table 11: Load Flow solution of 14-Bus system for mode 4 with three converters

I- Voltage magnitude, angle, active, and reactive powers

Load flow Solution				
Bus	V	Ang	P(pu)	Q(pu)
1	1.0600	0.0000	0.0000	0.0000
2	1.0550	-30.1734	0.2631	0.1523
3	1.0200	-55.2522	1.0495	0.2017
4	1.0029	-68.3549	0.5789	0.1063
5	1.0574	-64.1559	0.1117	0.0436
6	1.0800	-82.2642	0.3420	0.1238
7	0.9486	-112.2126	0.0286	0.0214
8	1.0900	-112.2126	0.0537	0.0300
9	0.9537	-101.4541	0.3470	0.1857
10	0.9670	-76.8121	0.1028	0.1686
11	1.0150	-90.7587	0.0522	0.0500
12	1.0527	-84.5098	0.1004	0.0220
13	1.0353	-85.9191	0.1502	0.0941
14	0.9753	-96.0154	0.2031	0.0759

II- Results of the DC converters output

Converters No.	Variables				
	V_d	I_d	T	$\cos\theta$	Φ
1	1.086	1.231	0.952	0.818	35.781
2	1.032	-0.654	1.280	0.804	8.406
3	0.950	0.381	1.065	0.625	48.353

Table 12: Load Flow solution of 14-Bus system for mode 5 with three converters

I- Voltage magnitude, angle, active, and reactive powers

Load flow Solution				
Bus	V	Ang	P(pu)	Q(pu)
1	1.0600	0.0000	0.0000	0.0000
2	1.0450	13.2411	0.3481	0.1600
3	1.0100	16.6730	1.0000	0.2559
4	1.0690	26.5809	0.5402	0.1124
5	1.0557	29.5758	0.1070	0.0250
6	1.0700	26.8250	0.1238	0.3626
7	1.0933	33.5442	0.0069	0.0281
8	1.0900	33.5442	0.0315	0.0163
9	1.0891	29.0559	0.3720	0.2541
10	1.0794	28.3294	0.1610	0.0973
11	1.0743	27.4240	0.0525	0.0210
12	1.0603	26.1396	0.0912	0.0468
13	1.0584	26.2384	0.1730	0.0615
14	1.0575	26.7321	0.2461	0.0960

II- Results of the DC converters output

Converters No.	Variables				
	V_d	I_d	T	$\cos\theta$	Φ
1	1.229	1.288	1.042	0.791	27.824
2	1.025	- 0.079	0.965	0.948	27.225
3	1.111	0.190	1.142	0.473	25.000

Table 13: Load Flow solution of 14-Bus system for mode 6 with three converters

I- Voltage magnitude, angle, active, and reactive powers

Load flow Solution				
Bus	V	Ang	P(pu)	Q(pu)
1	1.0600	0.0000	0.0000	0.0000
2	1.0450	10.2976	0.2848	0.1686
3	1.0100	13.1357	1.0036	0.2600
4	1.0131	23.7131	0.5811	0.0823
5	1.1054	21.8012	0.0989	0.0570
6	1.0700	20.0361	0.1899	0.1928
7	1.0536	29.3713	0.0436	0.0601
8	1.0900	29.3713	0.0259	0.0187
9	1.0120	24.6630	0.3117	0.1799
10	1.0300	23.5240	0.0999	0.1354
11	1.0617	21.6336	0.1013	0.0278
12	1.0576	19.4894	0.0840	0.0640
13	1.0542	19.7912	0.2159	0.1052
14	1.0329	21.4514	0.1883	0.0827

II- Results of the DC converters output

Converters No.	Variables				
	V_d	I_d	T	$\cos\theta$	Φ
1	1.000	1.201	1.031	0.519	52.278
2	1.011	- 0.987	0.948	0.632	58.504
3	0.994	0.450	0.973	0.410	41.841

Table 14: Load Flow solution of 14-Bus system for mode 7 with three converters

I- Voltage magnitude, angle, active, and reactive powers

Load flow Solution				
Bus	V	Ang	P(pu)	Q(pu)
1	1.0600	0.0000	0.0000	0.0000
2	1.0450	10.5054	0.2342	0.3540
3	1.0100	13.5401	1.0109	0.2983
4	1.0623	23.2053	0.4979	0.0700
5	1.0533	21.3638	0.1592	0.0580
6	1.0700	19.7789	0.4084	0.2931
7	1.0856	28.6045	0.0111	0.0324
8	1.0900	28.6045	0.0180	0.0231
9	1.0463	23.8940	0.3840	0.2325
10	1.0112	22.8324	0.1028	0.1129
11	1.0736	21.1482	0.0359	0.0910
12	1.0598	19.2153	0.0800	0.0836
13	1.0583	19.4528	0.2165	0.1047
14	1.0410	20.8642	0.1710	0.1115

II- Results of the DC converters output

Converters No.	Variables				
	V_d	I_d	T	$\cos\theta$	Φ
1	1.050	1.140	1.045	0.657	14.095
2	1.008	-0.763	0.965	0.431	18.216
3	1.183	0.089	1.123	0.810	33.766

4.6 Analysis of Results for 14-Bus with three DC converter system

As a way of validating the method we proposed we tried to use the three converters with also 14 Bus systems. We also concluded that the overall active power is improved after using the converters as well as the overall reactive power for mode 1. For mode 2 to mode 7 the active and reactive power is improved for some buses but became worse for others. For example the active power at bus 3 without using the converters was 94.2 MW and became 99.92 MW after using the converters for mode 1 but it is changed to be 95.24 MW for mode 2 , 98.89 MW for mode 3, 104.95 MW for mode 4, 100 MW for mode 5, 100.36 MW for mode 6, and 101.09 MW for mode 7. Also the reactive power at bus 3 also without using the converters was 19.00 MVAR and became 27.61 MVAR for mode 1 but it is changed to be 20.01 MVAR for mode 2, 24.94 MVAR for mode 3, 20.17 MVAR for mode 4, 25.59 MVAR for mode 5, 26.00 MVAR for mode 6, 35.40MVAR for mode 7.

For bus 13 without using the converters was 13.5 MW and became 19.27 MW after using the converters for mode 1 but it is changed to be 16.11 MW for mode 2, 17.67 MW for mode 3, 15.02 MW for mode 4, 17.30 MW for mode 5, 21.59 MW for mode 6, and 21.65 MW for mode 7. Also the reactive power at bus 13 without using the converters was 5.8 MVAR and became 9.39 MVAR for mode 1 but it is changed to be 12.34 MVAR for mode 2, 19.90 MVAR for mode 3, 9.41 MVAR for mode 4, 6.15 MVAR for mode 5, 10.52 MVAR for mode 6, 10.47 MVAR for mode 7.

In comparing the three-terminal DC converters with the two-terminal DC converters on 14-bus systems, the specified variables of the DC converters for a three DC converters are indicating a reduction in the variability as shown in the tables above. Increasing the

some buses voltage level causes a slight improvement in the total losses and this will increase the overall efficiency and the decrease the voltage regulation and as a result the overall cost will be decreased. However, the converter taps (T) increases substantially.

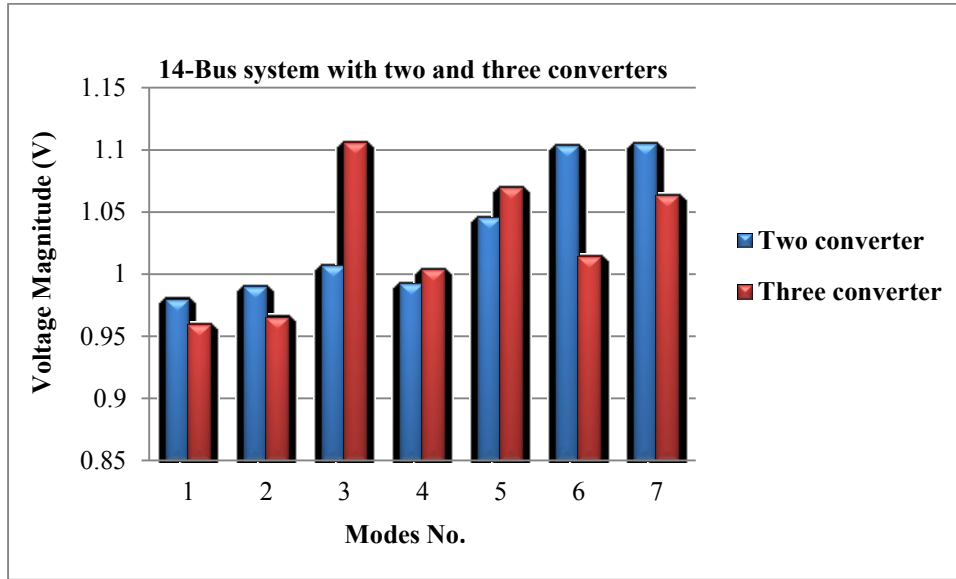


Figure 12: The relation between the voltage magnitude V_4 and modes number of 14-Bus system

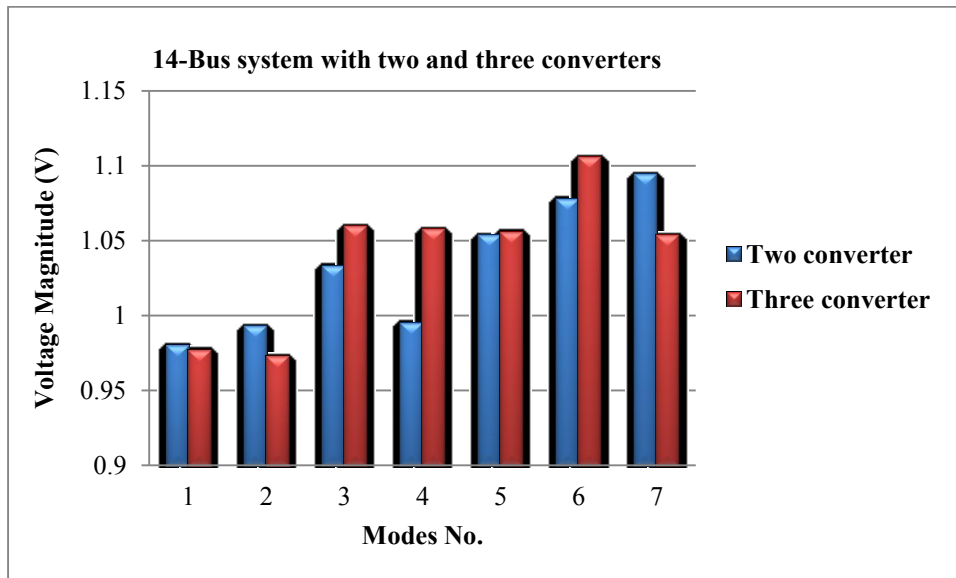


Figure 13: The relation between the voltage magnitude V_5 and modes number of 14-Bus system

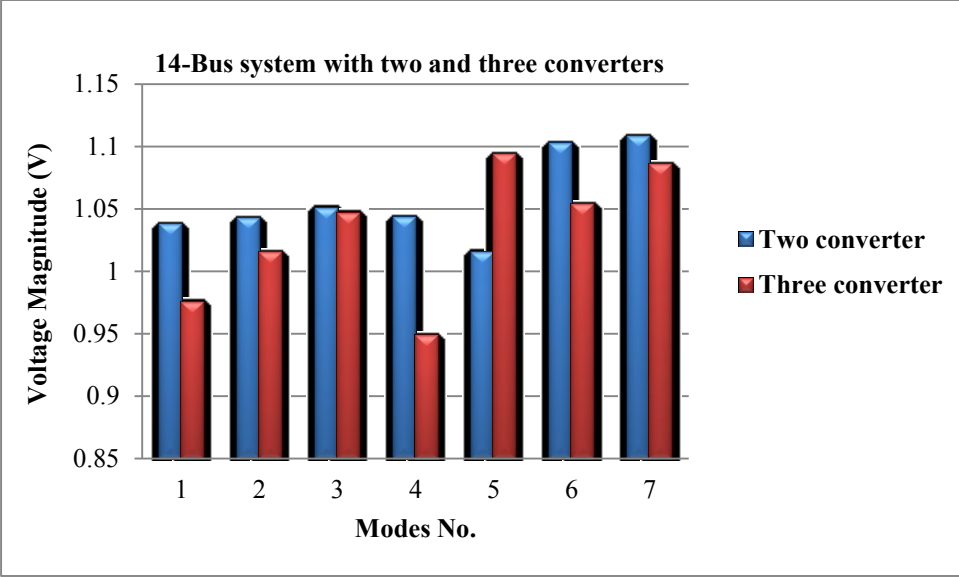


Figure 14: The relation between the voltage magnitude V_7 and modes number of 14-Bus system

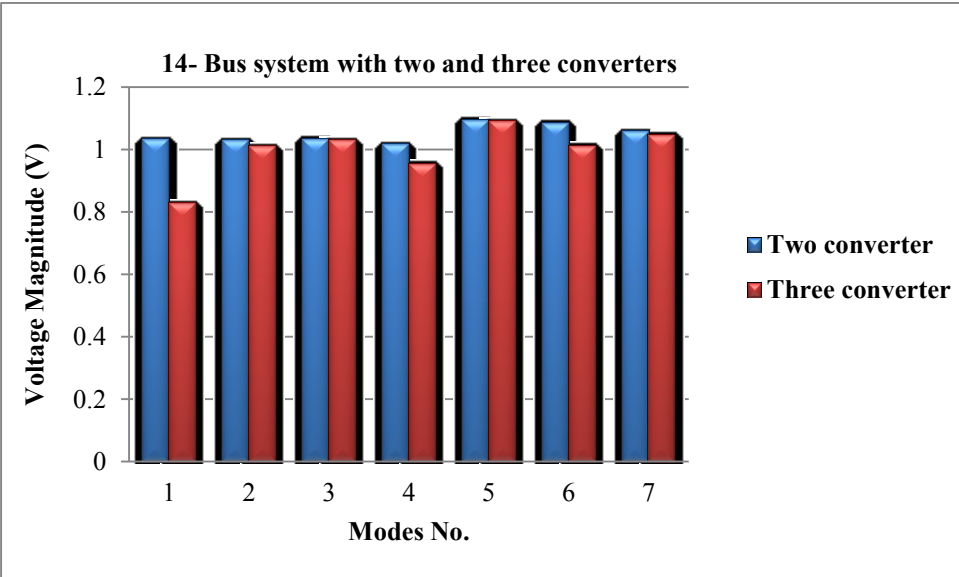


Figure 15: The relation between the voltage magnitude V_9 and modes number of 14-Bus system

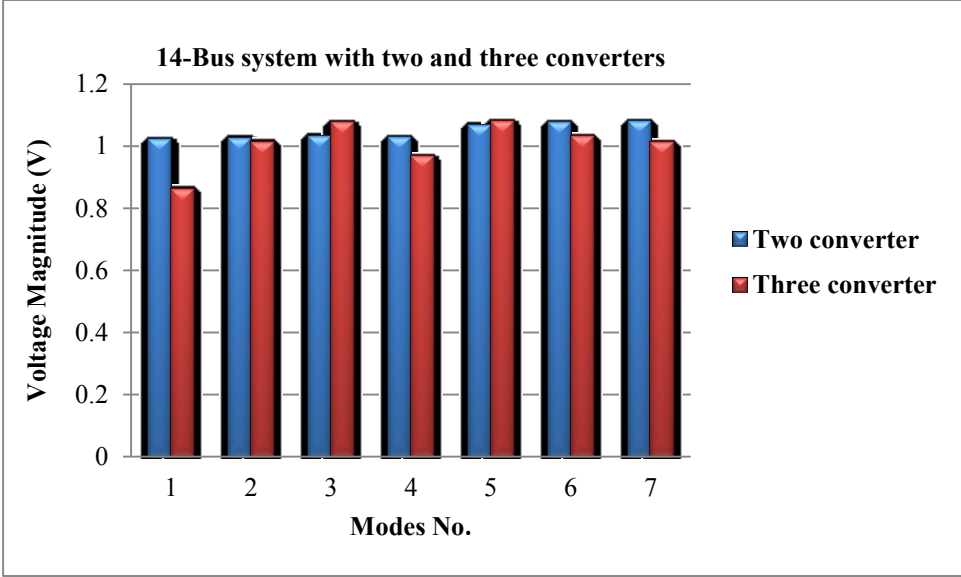


Figure 16: The relation between the voltage magnitude V_{10} and modes number of 14-Bus system

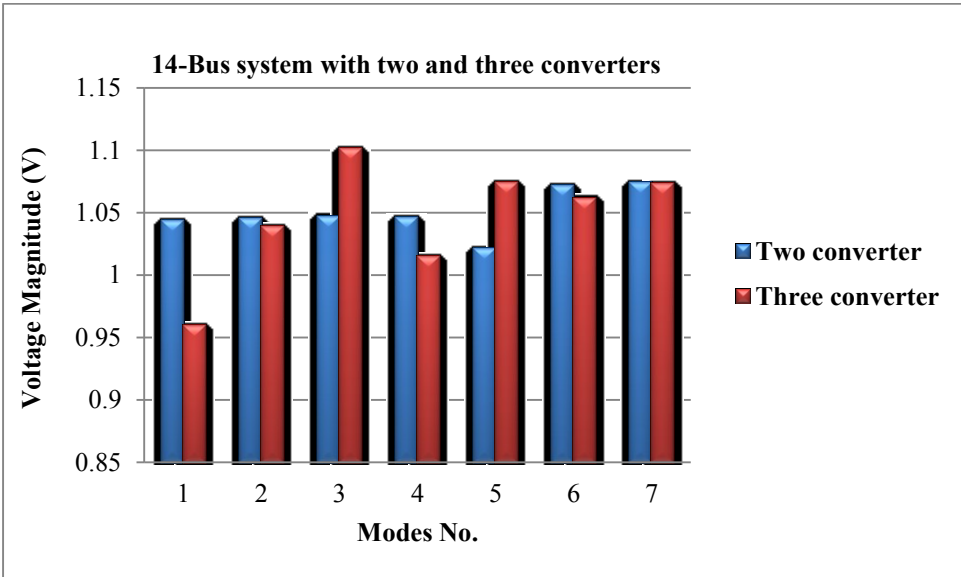


Figure 17: The relation between the voltage magnitude V_{11} and modes number of 14-Bus system

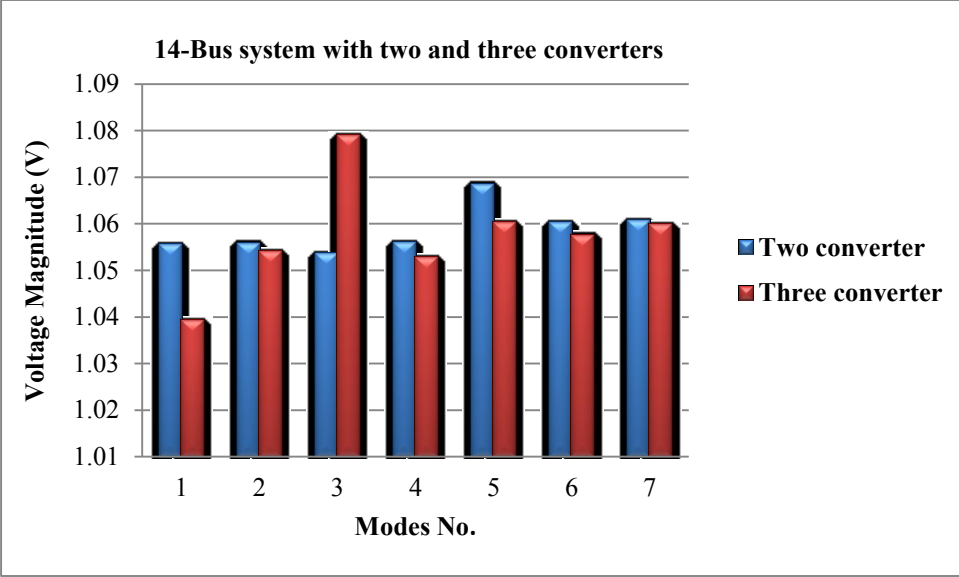


Figure 18: The relation between the voltage magnitude V_{12} and modes number of 14-Bus system

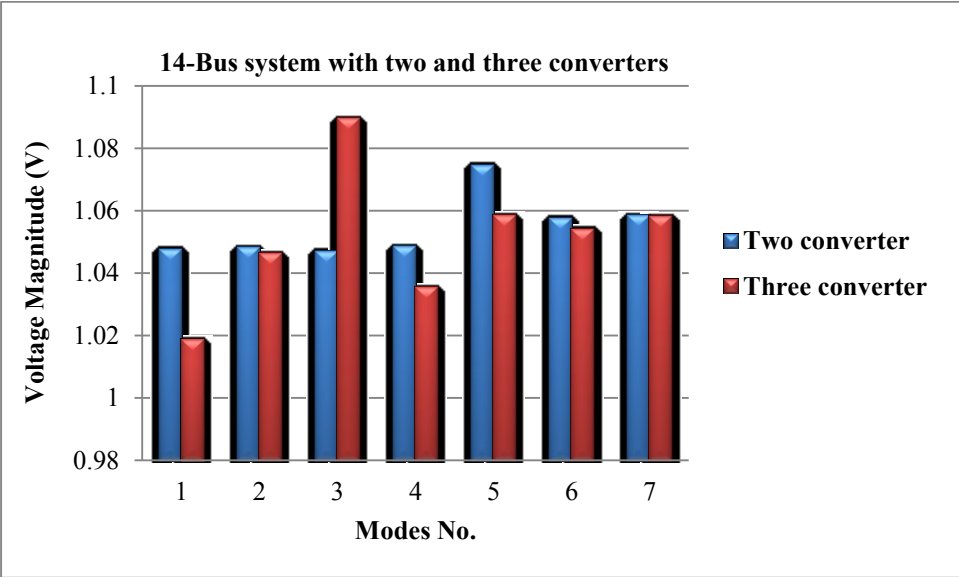


Figure 19: The relation between the voltage magnitude V_{13} and modes number of 14-Bus system

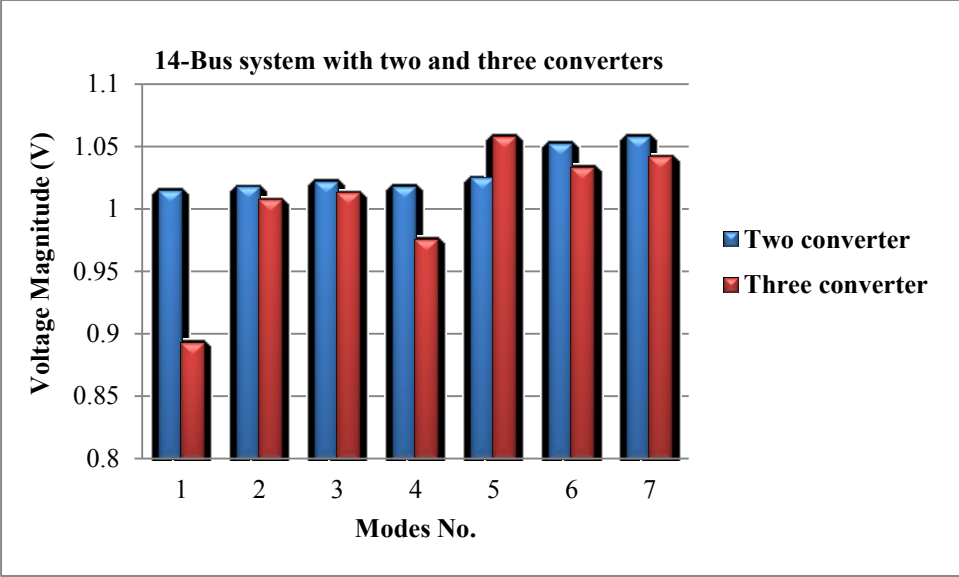


Figure 20: The relation between the voltage magnitude V_{14} and modes number of 14-Bus system

Figures (12-20) show the relation between the voltage magnitude for two converters and three converters at different buses with 14 bus systems. From which we concluded that the voltage magnitude is increased in case of two converters compared to three converters and there is a slight increase in the voltage magnitude.

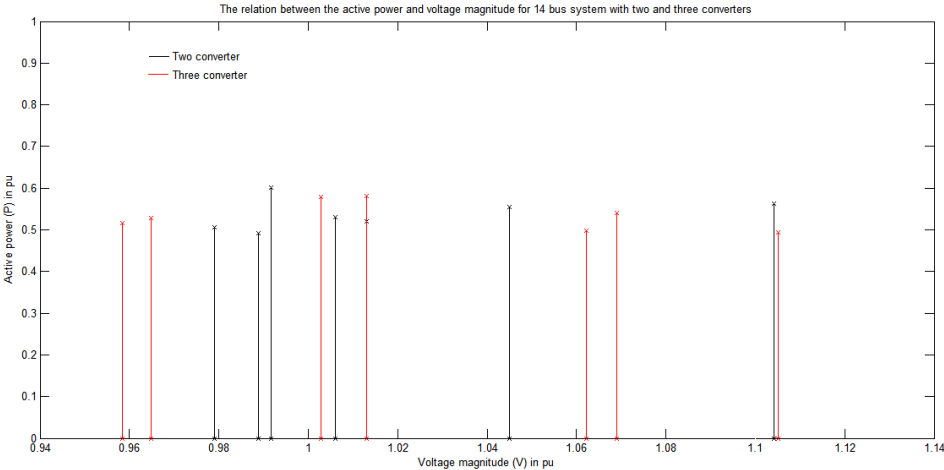


Figure 21: The relation between the active power P_4 and voltage magnitude V_4 of 14-Bus system

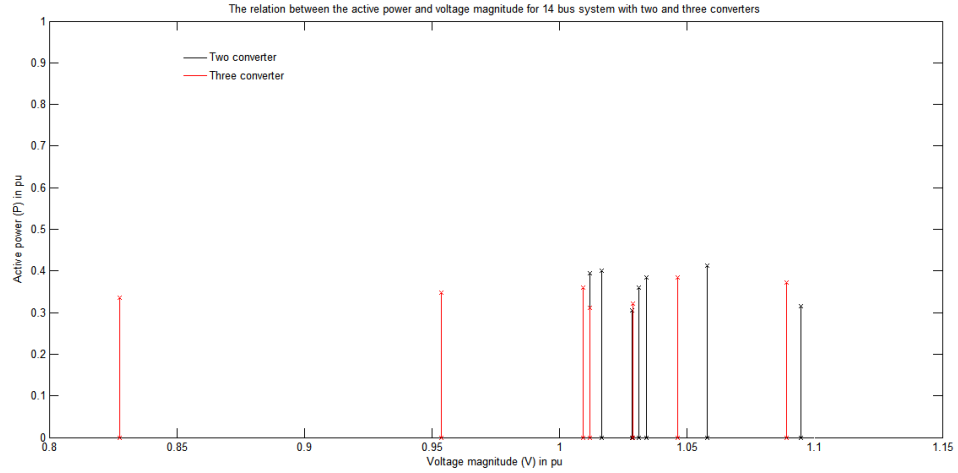


Figure 22: The relation between the active power P_9 and voltage magnitude V_9 of 14-Bus system

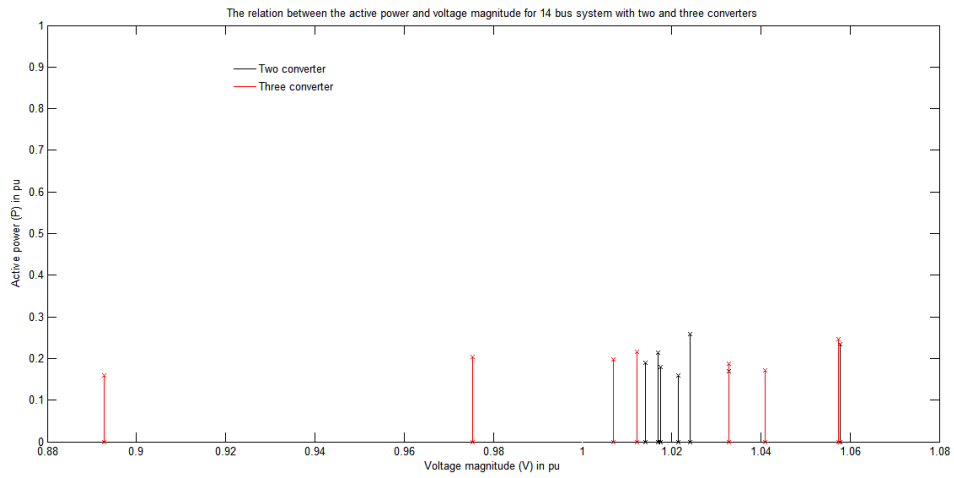


Figure 23: The relation between the active power P_{14} and voltage magnitude V_{14} of 14-Bus system

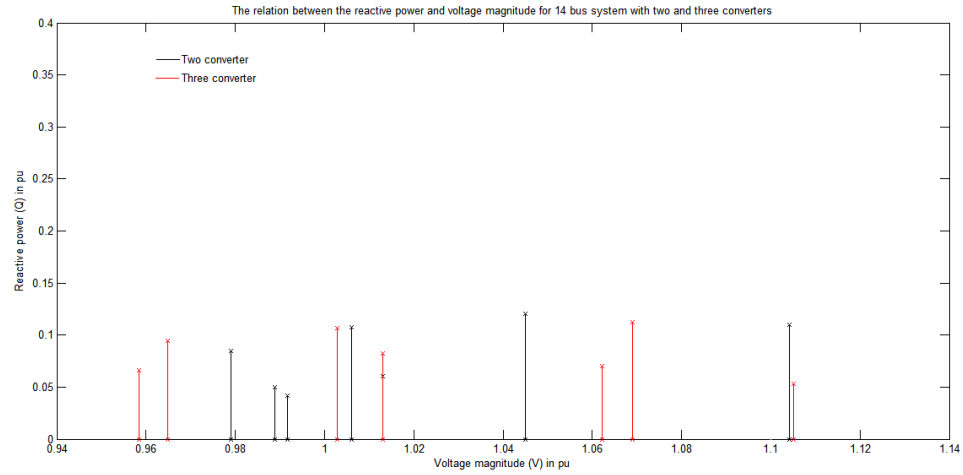


Figure 24: The relation between the reactive power Q_4 and voltage magnitude V_4 of 14-Bus system

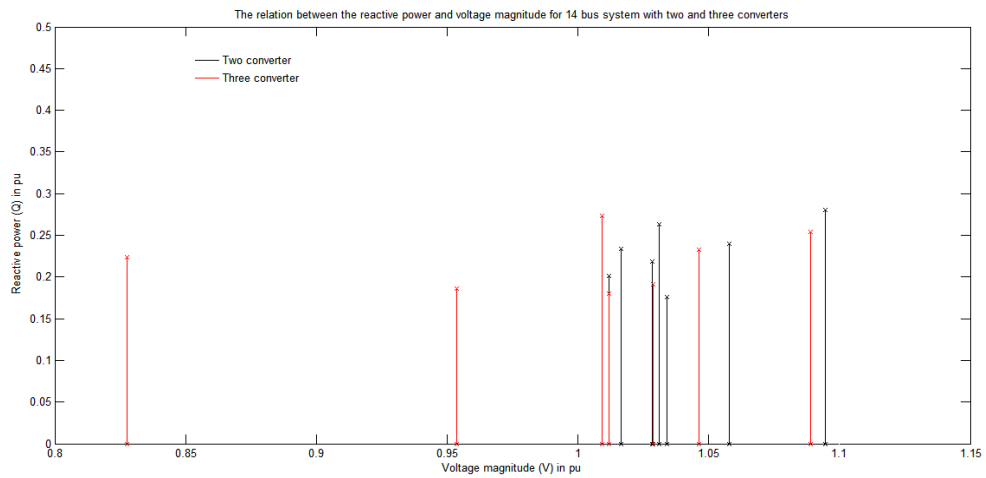


Figure 25: The relation between the reactive power Q_9 and voltage magnitude V_9 of 14-Bus system

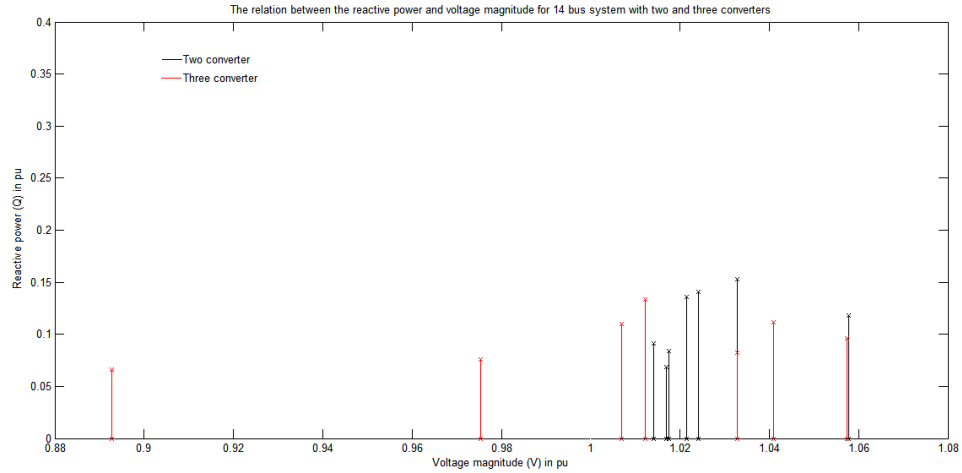


Figure 26: The relation between the reactive power Q_{14} and voltage magnitude V_{14} of 14-Bus system

Figures (21-26) show the relation between the active power and voltage magnitude for two converters and three converters at different buses with 14 bus systems. From which we concluded that the active power is increased in case of three converters compared to two converters and there is a slight increase in the voltage magnitude.

4.6.1: 30-Bus system with two terminal DC converters

Table 15: Load Flow solution of 30-Bus system for mode 1 with two converters

I- Voltage magnitude, angle, active, and reactive powers

Load Flow Solution				
Bus	V	Ang	P(pu)	Q(pu)
1	1.0600	0.0000	0.0000	0.0000
2	1.0430	-10.1663	0.3190	0.1678
3	1.0267	-16.3740	0.0512	0.0459
4	1.0135	-20.3370	0.1031	0.0713
5	1.0100	-22.1488	0.9864	0.2412
6	1.0263	-23.1617	0.0492	0.0540
7	1.0112	-23.2977	0.2803	0.2074
8	1.0100	-23.6508	0.3901	0.3881
9	1.0517	-26.1008	0.0125	0.0480
10	1.0341	-27.6901	0.1118	0.0369
11	1.0820	-26.1008	0.0271	0.0095
12	1.0595	-26.7267	0.1153	0.1521
13	1.0710	-26.7267	0.0217	0.0083
14	1.0424	-27.7283	0.0978	0.0426
15	1.0458	-27.8073	0.1256	0.0713
16	1.0412	-27.4283	0.0488	0.0572
17	1.0307	-27.8331	0.1520	0.1087
18	1.0229	-28.5075	0.0398	0.1300
19	1.0183	-28.7170	0.1101	0.0836
20	1.0215	-28.5230	0.0375	0.0911
21	1.0205	-28.2056	0.1832	0.2168
22	1.0450	-28.0025	0.0207	0.0122
23	1.0208	-28.2020	0.0635	0.0590
24	1.0727	-28.3195	0.1282	0.0973
25	1.0192	-28.1403	0.0116	0.0325
26	1.0016	-28.5671	0.0813	0.0697
27	1.0918	-27.7459	0.0420	0.0153
28	1.0215	-23.7767	0.0519	0.0448
29	1.0125	-29.0094	0.0452	0.1007
30	1.0014	-29.8888	0.2074	0.0309

II- Results of the DC converters output

Converters No.	Variables				
	V_d	I_d	T	$\cos\theta$	Φ
1	1.287	0.098	0.993	0.961	12.510
2	0.942	- 0.464	1.010	0.844	23. 856

Table 16: Load Flow solution of 30-Bus system for mode 2 with two converters

I- Voltage magnitude, angle, active, and reactive powers

Load Flow Solution				
Bus	V	Ang	P(pu)	Q(pu)
1	1.0600	0.0000	0.0000	0.0000
2	1.0430	-10.1025	0.2643	0.2119
3	1.0068	-15.9004	0.0816	0.0506
4	0.9893	-19.7297	0.1509	0.0855
5	1.0100	-22.0785	0.9683	0.2516
6	0.9853	-22.2147	0.0366	0.0280
7	0.9871	-22.6749	0.3070	0.1439
8	1.0100	-23.3803	0.3382	0.4494
9	1.0295	-25.1965	0.0000	0.0000
10	1.0118	-26.8090	0.0767	0.0793
11	1.0010	-25.1965	0.0254	0.0510
12	1.0451	-26.0949	0.1592	0.0892
13	1.0710	-26.0949	0.0130	0.0145
14	1.0266	-27.0673	0.1167	0.0591
15	1.0187	-27.0825	0.1550	0.0968
16	1.0236	-26.6853	0.0478	0.0273
17	1.0098	-26.9915	0.1131	0.0782
18	1.0039	-27.7267	0.0732	0.1054
19	0.9983	-27.9029	0.1462	0.0638
20	1.0009	-27.6911	0.0830	0.1161
21	0.9991	-27.3572	0.2874	0.1735
22	1.0622	-27.1310	0.0492	0.0233
23	0.9996	-27.3645	0.0529	0.0858
24	0.9872	-27.4560	0.1603	0.1567
25	0.9920	-27.2512	0.0580	0.0312
26	0.9743	-27.6780	0.0745	0.0210
27	1.0022	-26.8460	0.0201	0.0222

Load Flow Solution				
Bus	V	Ang	P(pu)	Q(pu)
28	0.9902	-22.9650	0.0397	0.0157
29	0.9829	-28.1095	0.0946	0.1421
30	0.9607	-28.9889	0.1643	0.0473

II- Results of the DC converters output

Converters No.	Variables				
	V_d	I_d	T	$\cos\theta$	Φ
1	1.259	0.0857	0.962	0.789	42.753
2	1.241	-0.0635	1.016	0.924	19.901

Table 17: Load Flow solution of 30-Bus system for mode 3 with two converters

I- Voltage magnitude, angle, active, and reactive powers

Load Flow Solution				
Bus	V	Ang	P(pu)	Q(pu)
1	1.0600	0.0000	0.0000	0.0000
2	1.0430	-8.7401	0.3595	0.1836
3	1.0274	-14.0960	0.0793	0.0942
4	1.0150	-17.4951	0.0941	0.0341
5	1.0100	-19.6924	1.0217	0.2298
6	1.0268	-19.5600	0.0440	0.0193
7	1.0118	-20.1672	0.2332	0.1758
8	1.0100	-20.0418	0.3445	0.4034
9	1.0524	-22.6359	0.0169	0.0270
10	1.0351	-24.2992	0.0922	0.0490
11	1.0810	-22.6359	0.0378	0.0112
12	1.0390	-23.5877	0.1950	0.1138
13	1.0710	-23.5877	0.0168	0.0155
14	1.0425	-24.5436	0.0836	0.0944
15	1.0363	-24.5788	0.1414	0.0873
16	1.0418	-24.1834	0.0301	0.0521
17	1.0316	-24.4865	0.1710	0.1192
18	1.0235	-25.2221	0.0615	0.1547
19	1.0090	-25.3979	0.1382	0.0491
20	1.0224	-25.1861	0.0496	0.0804
21	1.0214	-24.8454	0.2270	0.1495

Load Flow Solution				
Bus	V	Ang	P(pu)	Q(pu)
22	1.0362	-24.6070	0.0301	0.0620
23	1.0217	-24.8517	0.0734	0.0359
24	1.0446	-24.9176	0.1020	0.0873
25	1.0203	-24.6630	0.0431	0.0159
26	1.0026	-25.0898	0.0553	0.0428
27	1.0329	-24.2217	0.0391	0.0105
28	1.0219	-20.1831	0.0026	0.0101
29	1.0136	-25.4851	0.0753	0.1157
30	1.0024	-26.3646	0.1376	0.0669

II- Results of the DC converters output

Converters No.	Variables				
	V_d	I_d	T	$\cos\theta$	Φ
1	0.994	0.0547	1.000	0.566	14.916
2	1.131	-0.0541	1.210	0.870	39.214

Table 18: Load Flow solution of 30-Bus system for mode 4 with two converters

I- Voltage magnitude, angle, active, and reactive powers

Load Flow Solution				
Bus	V	Ang	P(pu)	Q(pu)
1	1.0600	0.0000	0.0000	0.0000
2	1.0430	-8.6989	0.2390	0.1467
3	1.0142	-13.7862	0.0620	0.0721
4	0.9991	-17.0977	0.1173	0.0589
5	1.0100	-19.6468	1.0080	0.2603
6	1.0005	-18.9495	0.0229	0.0187
7	0.9963	-19.7656	0.2531	0.1361
8	1.0100	-19.8669	0.3618	0.3374
9	1.0381	-22.0522	0.0124	0.0022
10	1.0207	-23.7300	0.1007	0.1095
11	1.0820	-22.0522	0.0131	0.0378
12	1.0102	-23.1761	0.2085	0.1440
13	1.0710	-23.1761	0.0174	0.0611
14	1.0322	-24.1135	0.1221	0.0860

Load Flow Solution				
Bus	V	Ang	P(pu)	Q(pu)
15	1.0552	-24.1083	0.0935	0.0421
16	1.0303	-23.7014	0.1942	0.1809
17	1.0181	-23.9422	0.1287	0.0937
18	1.0112	-24.7162	0.0954	0.1690
19	1.0062	-24.8709	0.1720	0.0926
20	1.0090	-24.6480	0.0563	0.1042
21	1.0076	-24.2969	0.2621	0.1299
22	1.0013	-24.0439	0.0346	0.0180
23	1.0080	-24.3100	0.0908	0.0631
24	0.9985	-24.3597	0.1330	0.1042
25	1.0027	-24.0892	0.0210	0.0293
26	0.9850	-24.5160	0.0488	0.0876
27	1.0138	-23.6413	0.0151	0.0339
28	1.0018	-19.6596	0.0170	0.0641
29	0.9945	-24.9047	0.0857	0.1589
30	0.9833	-25.7842	0.1502	0.0700

II- Results of the DC converters output

Converters No.	Variables				
	V_d	I_d	T	$\cos\theta$	Φ
1	1.200	0.016	0.956	0.722	42.401
2	1.247	-0.048	1.028	0.492	22.949

Table 19: Load Flow solution of 30-Bus system for mode 5 with two converters

I- Voltage magnitude, angle, active, and reactive powers

Load Flow Solution				
Bus	V	Ang	P(pu)	Q(pu)
1	1.0600	0.0000	0.0000	0.0000
2	1.0330	-6.9342	0.2936	0.1703
3	0.9996	-10.4031	0.0449	0.0886
4	0.9863	-12.9320	0.0851	0.1004
5	1.0100	-16.6872	1.1000	0.2810
6	0.9851	-14.1147	0.0112	0.0481
7	0.9876	-15.6845	0.2914	0.1274
8	1.0200	-15.2795	0.3202	0.6577
9	1.0260	-17.3564	0.0399	0.0269
10	1.0074	-19.0726	0.0895	0.0584
11	1.0820	-17.3564	0.0134	0.0101
12	1.0084	-18.7766	0.1782	0.1280
13	1.0710	-18.7766	0.0490	0.0132
14	1.0200	-19.6362	0.1517	0.0395
15	1.0027	-19.5907	0.1891	0.0533
16	1.0180	-19.1784	0.2046	0.1587
17	1.0051	-19.3219	0.1953	0.0925
18	0.9983	-20.1453	0.1097	0.1246
19	0.9931	-20.2729	0.1624	0.0274
20	0.9958	-20.0324	0.0703	0.0036
21	0.9942	-19.6695	0.2450	0.1673
22	0.9995	-19.3938	0.0220	0.0275
23	0.9946	-19.6925	0.1028	0.0428
24	0.9841	-19.7226	0.1456	0.1153
25	0.9864	-19.4287	0.0142	0.0608
26	0.9682	-19.8747	0.0685	0.0156
27	0.9967	-18.9649	0.0099	0.0128
28	0.9890	-14.8795	0.0214	0.0510
29	0.9764	-20.2617	0.0393	0.1365
30	0.9546	-21.1920	0.1479	0.0378

II- Results of the DC converters output

Converters No.	Variables				
	V_d	I_d	T	$\cos\theta$	Φ
1	0.804	0.127	1.000	0.581	30.288
2	0.799	-0.127	1.002	0.416	21.640

Table 20: Load Flow solution of 30-Bus system for mode 6 with two converters

I- Voltage magnitude, angle, active, and reactive powers

Load Flow Solution				
Bus	V	Ang	P(pu)	Q(pu)
1	1.0600	0.0000	0.0000	0.0000
2	1.0430	-24.8246	0.2217	0.1990
3	1.1077	-34.9800	0.0972	0.0636
4	1.0849	-43.7270	0.1490	0.0421
5	1.0100	-50.9004	1.0950	0.1948
6	1.1041	-70.0274	0.0470	0.0422
7	1.0705	-62.8139	0.2436	0.1931
8	1.0100	-68.6827	0.4149	0.5552
9	1.1044	-68.6302	0.0612	0.0291
10	1.1014	-67.8746	0.1498	0.0812
11	1.0820	-68.6302	0.0162	0.0110
12	1.0708	-59.4282	0.1243	0.1643
13	1.0710	-59.4282	0.0300	0.0201
14	1.1000	-61.8166	0.1093	0.0749
15	1.1002	-63.1574	0.1772	0.1089
16	1.0323	-63.2663	0.2548	0.2210
17	1.1046	-66.6943	0.2172	0.1362
18	1.1074	-65.5513	0.0626	0.2024
19	1.0970	-66.7628	0.2043	0.0389
20	1.0971	-67.0965	0.0915	0.0082
21	1.0936	-67.4741	0.2537	0.2310
22	1.0974	-68.3255	0.0106	0.0218
23	1.0958	-67.1813	0.0878	0.0955
24	1.0843	-68.8363	0.1801	0.0759
25	1.0888	-70.9110	0.0263	0.0228
26	1.0712	-71.3378	0.1021	0.0239
27	1.0511	-71.9181	0.0235	0.0576

Load Flow Solution				
Bus	V	Ang	P(pu)	Q(pu)
28	1.1043	-69.9842	0.0104	0.0611
29	1.0828	-73.1815	0.0557	0.1777
30	1.0716	-74.0610	0.1260	0.0600

II- Results of the DC converters output

Converters No.	Variables				
	V_d	I_d	T	$\cos\theta$	Φ
1	1.000	0.109	0.766	0.935	16.371
2	0.999	-0.218	0.811	0.672	29.852

Table 21: Load Flow solution of 30-Bus system for mode 7 with two converters

I- Voltage magnitude, angle, active, and reactive powers

Load Flow Solution				
Bus	V	Ang	P(pu)	Q(pu)
1	1.0600	0.0000	0.0000	0.0000
2	1.0430	-24.8986	0.3462	0.2217
3	1.0662	-35.6137	0.1000	0.0352
4	1.0995	-44.5412	0.1324	0.0901
5	1.0100	-50.9875	0.9579	0.2760
6	1.1003	-71.1102	0.0026	0.0100
7	1.0977	-63.5283	0.3694	0.2228
8	1.0100	-69.0024	0.3810	0.4344
9	1.0400	-69.6801	0.0267	0.0212
10	1.1076	-68.9068	0.1355	0.0620
11	1.0820	-69.6801	0.0472	0.0196
12	1.0992	-60.2402	0.2116	0.0924
13	1.0710	-60.2402	0.0158	0.0317
14	1.0700	-62.6531	0.1700	0.1005
15	1.1014	-64.0518	0.0899	0.1124
16	1.1040	-64.1771	0.2837	0.1651
17	1.0294	-67.6920	0.2113	0.0877
18	1.0304	-66.4952	0.0917	0.1890
19	1.0210	-67.7361	0.1333	0.0312
20	1.0216	-68.0855	0.1019	0.0059

Load Flow Solution				
Bus	V	Ang	P(pu)	Q(pu)
21	1.0190	-68.4769	0.2171	0.1946
22	1.0311	-69.3471	0.0000	0.0000
23	1.0209	-68.1744	0.1139	0.0743
24	1.0117	-69.8489	0.1000	0.1345
25	1.0202	-71.9395	0.0073	0.0002
26	1.0026	-72.3663	0.0925	0.0241
27	1.0350	-72.9511	0.0362	0.0180
28	1.0397	-70.9156	0.0149	0.0571
29	1.0257	-74.2145	0.0622	0.1286
30	1.0145	-75.0940	0.1764	0.0590

II- Results of the DC converters output

Converters No.	Variables				
	V_d	I_d	T	$\cos\theta$	Φ
1	1.400	0.094	0.957	0.743	27.120
2	1.199	-0.092	0.970	0.505	61.016

4.7 Analysis of Results for 30-Bus with two DC converter system

We tried also to use 30 bus systems. After using three converters, we concluded also that the overall active power is improved after using the converters as well as the overall reactive power for mode 1. For mode 2 to mode 7 the active and reactive power is improved for some buses but became worse for others. For example the active power at bus 5 without using the converters was 94.2 MW and became 98.64 MW after using the converters for mode 1 but it is changed to be 96.83 MW for mode 2, 102.17 MW for mode 3, 100.80 MW for mode 4, 110 MW for mode 5, 109.50 MW for mode 6, and 95.79 MW for mode 7. Also the reactive power at bus 5 also without using the converters was 19.00 MVAR and became 24.12 MVAR for mode 1 but it is changed to be 25.16

MVAR for mode 2, 22.98 MVAR for mode 3, 26.03 MVAR for mode 4, 28.10 MVAR for mode 5, 19.48 MVAR for mode 6, 27.60 MVAR for mode 7.

For bus 15 without using the converters was 8.2 MW and became 12.56 MW after using the converters for mode 1 but it is changed to be 15.50 MW for mode 2, 14.14 MW for mode 3, 9.35 MW for mode 4, 18.91 MW for mode 5, 17.72 MW for mode 6, and 8.99 MW for mode 7. Also the reactive power at bus 15 without using the converters was 2.5 MVAR and became 7.13 MVAR for mode 1 but it is changed to be 9.68 MVAR for mode 2, 8.73 MVAR for mode 3, 4.21 MVAR for mode 4, 5.33 MVAR for mode 5, 10.89 MVAR for mode 6, 11.24 MVAR for mode 7.

4.7.1 30-Bus system with three terminal DC converters

Table 22: Load Flow solution of 30-Bus system for mode 1 with three converters

I- Voltage magnitude, angle, active, and reactive powers

Load Flow Solution				
Bus	V	Ang	P(pu)	Q(pu)
1	1.0600	0.0000	0.0000	0.0000
2	1.0430	-3.6263	0.2473	0.1714
3	0.9309	0.1012	0.0761	0.0637
4	0.9872	-2.0159	0.1244	0.0451
5	1.0100	-11.2891	1.0803	0.2601
6	0.8927	-4.6154	0.0310	0.0432
7	0.9338	-7.7927	0.2738	0.1386
8	1.0100	-7.3135	0.3416	0.3399
9	0.9693	-7.6424	0.0331	0.0250
10	0.9412	-9.2792	0.1042	0.0570
11	1.0820	-7.6424	0.0580	0.0863
12	0.9666	-8.3674	0.1626	0.1015
13	1.0710	-8.3674	0.0347	0.0610
14	0.9495	-9.3621	0.0571	0.0154
15	0.9428	-9.4314	0.0777	0.0219
16	0.9484	-9.0471	0.0932	0.0667
17	0.9378	-9.4311	0.1471	0.1050
18	0.9299	-10.1194	0.0624	0.1581
19	0.9254	-10.3216	0.1438	0.0795
20	0.9286	-10.1238	0.0198	0.0061
21	0.9272	-9.8065	0.2345	0.1330
22	0.9309	-9.6100	0.0379	0.0304
23	0.9273	-9.8066	0.0812	0.0640
24	0.9159	-9.9392	0.1274	0.0926
25	0.9176	-9.7988	0.0500	0.0381
26	0.9000	-10.2256	0.0806	0.0713
27	0.9267	-9.4361	0.0333	0.0454
28	0.9183	-5.6675	0.0424	0.0611
29	0.9074	-10.6996	0.0702	0.0363
30	0.8962	-11.5790	0.1578	0.0585

II- Results of the DC converters output

Converters No.	Variables				
	V_d	I_d	T	$\cos\theta$	Φ
1	1.298	0.401	1.005	0.817	28.092
2	1.210	-0.049	1.012	0.953	55.017
3	1.000	0.390	0.987	0.862	11.280

Table 23: Load Flow solution of 30-Bus system for mode 2 with three converters

I- Voltage magnitude, angle, active, and reactive powers

Load Flow Solution				
Bus	V	Ang	P(pu)	Q(pu)
1	1.0600	0.0000	0.0000	0.0000
2	1.0430	-2.8720	0.2376	0.1461
3	0.9561	-1.9314	0.1044	0.0682
4	0.9677	-3.3467	0.0571	0.0420
5	1.0100	-10.0925	1.0220	0.2239
6	0.9947	-5.0867	0.6510	0.0991
7	0.9940	-7.6684	0.2451	0.2120
8	1.0100	-6.1009	0.3120	0.3611
9	1.0331	-8.2274	0.0144	0.0309
10	1.0139	-9.9258	0.0656	0.0177
11	1.0820	-8.2274	0.0293	0.0510
12	1.0293	-9.3389	0.1820	0.1237
13	1.0710	-9.3389	0.0137	0.0111
14	1.0220	-10.2751	0.0652	0.0149
15	1.0100	-10.2853	0.0866	0.0223
16	1.0211	-9.8811	0.0370	0.0175
17	1.0106	-10.1343	0.1548	0.1061
18	1.0027	-10.9004	0.0326	0.0085
19	0.9950	-11.0594	0.0949	0.0338
20	1.0013	-10.8388	0.0227	0.0060
21	1.0002	-10.4886	0.2562	0.1539
22	1.0044	-10.2372	0.0000	0.0000
23	1.0005	-10.5002	0.0323	0.0159
24	0.9916	-10.5496	0.1363	0.1276

Load Flow Solution				
Bus	V	Ang	P(pu)	Q(pu)
25	0.9966	-10.2758	0.0356	0.0124
26	0.9789	-10.7026	0.0342	0.0225
27	1.0782	-9.8248	0.0260	0.0237
28	0.9972	-5.8182	0.0471	0.0189
29	0.9889	-11.0883	0.0343	0.1178
30	0.9777	-11.9678	0.1599	0.0900

II- Results of the DC converters output

Converters No.	Variables				
	V_d	I_d	T	$\cos\theta$	Φ
1	1.293	0.449	0.970	0.802	16.798
2	1.279	-0.250	1.000	0.845	24.012
3	1.151	1.008	1.168	0.631	13.778

Table 24: Load Flow solution of 30-Bus system for mode 3 with three converters

I- Voltage magnitude, angle, active, and reactive powers

Load Flow Solution				
Bus	V	Ang	P(pu)	Q(pu)
1	1.0600	0.0000	0.0000	0.0000
2	1.0430	-0.6382	0.2647	0.1503
3	0.9096	6.9896	0.0349	0.0190
4	0.9164	4.4221	0.1012	0.0277
5	1.0100	-7.0485	0.9580	0.2943
6	0.9450	-0.0779	0.0192	0.0356
7	0.9650	-3.4234	0.3140	0.1853
8	1.0100	-1.9070	0.3097	0.3400
9	1.0035	-2.7128	0.0114	0.0501
10	0.9816	-4.1376	0.0981	0.0270
11	1.0820	-2.7128	0.0530	0.0341
12	1.0169	-2.7393	0.1501	0.0946
13	1.0710	-2.7393	0.0000	0.0000
14	0.9983	-3.8357	0.0306	0.0104
15	0.9896	-3.9709	0.0275	0.0357
16	0.9944	-3.6179	0.0310	0.0416

Load Flow Solution				
Bus	V	Ang	P(pu)	Q(pu)
17	0.9799	-4.2001	0.1114	0.0782
18	0.9744	-4.7697	0.0145	0.0105
19	0.9686	-5.0372	0.0527	0.0405
20	0.9710	-4.8737	0.0106	0.0095
21	0.9690	-4.6040	0.2778	0.2011
22	0.9718	-4.4775	0.0000	0.0000
23	0.9696	-4.5853	0.0120	0.0148
24	0.9584	-4.8229	0.1534	0.1825
25	0.9593	-4.8367	0.0121	0.0063
26	0.9416	-5.2635	0.0239	0.0081
27	0.9684	-4.5697	0.0000	0.0000
28	0.9589	-0.9335	0.1185	0.0940
29	0.9492	-5.8331	0.0153	0.0298
30	0.9380	-6.7126	0.1641	0.0310

II- Results of the DC converters output

Converters No.	Variables				
	V_d	I_d	T	$\cos\theta$	Φ
1	0.998	1.000	0.984	0.597	30.714
2	1.102	-0.870	0.974	0.713	11.620
3	1.299	0.069	1.066	0.851	11.186

Table 25: Load Flow solution of 30-Bus system for mode 4 with three converters

I- Voltage magnitude, angle, active, and reactive powers

Load Flow Solution				
Bus	V	Ang	P(pu)	Q(pu)
1	1.0600	0.0000	0.0000	0.0000
2	1.0430	-0.0777	0.2793	0.1362
3	1.0767	5.4831	0.0341	0.0175
4	1.0563	3.3178	0.1109	0.0526
5	1.0100	-6.1487	1.0536	0.2225
6	1.0322	-0.6499	0.0175	0.0342
7	1.0165	-3.4674	0.2859	0.1511
8	1.0100	-1.0375	0.4070	0.3506
9	1.0572	-3.3561	0.0199	0.0157
10	1.0417	-4.8195	0.0334	0.0206
11	1.0820	-3.3561	0.0147	0.0542
12	1.0747	-3.5858	0.2198	0.1166
13	1.0710	-3.5858	0.0413	0.0189
14	1.0564	-4.6478	0.0569	0.0152
15	1.0093	-4.7587	0.0744	0.0272
16	1.0532	-4.3964	0.3310	0.0284
17	1.0396	-4.9118	0.1832	0.1078
18	1.0336	-5.5205	0.0293	0.0414
19	1.0281	-5.7663	0.0881	0.0346
20	1.0307	-5.5913	0.0203	0.0170
21	1.0291	-5.3022	0.2125	0.2591
22	1.0427	-5.1422	0.0177	0.0259
23	1.0297	-5.2887	0.0292	0.0160
24	1.0514	-5.4728	0.1924	0.1327
25	1.0255	-5.3961	0.0482	0.0145
26	1.0011	-5.8228	0.0331	0.0227
27	1.0373	-5.0671	0.0000	0.0000
28	1.0263	-1.2292	0.0179	0.0138
29	1.0180	-6.3306	0.0236	0.0910
30	1.0068	-7.2100	0.1804	0.1032

II- Results of the DC converters output

Converters No.	Variables				
	V_d	I_d	T	$\cos\theta$	Φ
1	1.003	0.047	0.962	0.623	40.506
2	1.291	-0.180	1.010	0.512	40.319
3	1.015	0.055	1.073	0.911	35.184

Table 26: Load Flow solution of 30-Bus system for mode 5 with three converters

I- Voltage magnitude, angle, active, and reactive powers

Load Flow Solution				
Bus	V	Ang	P(pu)	Q (pu)
1	1.0600	0.0000	0.0000	0.0000
2	1.0430	30.5322	0.2495	0.2077
3	1.1083	55.4963	0.1022	0.0451
4	1.0315	62.4151	0.1376	0.1627
5	1.0100	47.5104	1.0809	0.2458
6	0.9830	79.9352	0.0214	0.0016
7	0.9944	66.0949	0.2676	0.1634
8	1.0100	78.6905	0.3851	0.4023
9	1.0384	73.3665	0.0100	0.0152
10	1.0307	69.8145	0.0559	0.0330
11	1.0820	73.3665	0.0387	0.0164
12	1.0655	63.8019	0.1490	0.1575
13	1.0710	63.8019	0.0451	0.0400
14	1.0267	64.0411	0.0637	0.0148
15	1.0269	65.2083	0.0756	0.0201
16	1.0333	66.0459	0.0310	0.0126
17	1.0265	68.4526	0.1049	0.1571
18	1.0162	66.0848	0.0315	0.0084
19	1.0330	66.8088	0.0967	0.0526
20	1.0169	67.4949	0.0235	0.0015
21	1.0158	68.4451	0.1916	0.1783
22	1.0382	69.6106	0.0431	0.0300
23	1.0156	68.1773	0.0266	0.0108
24	1.0070	69.4451	0.0962	0.1758
25	1.0094	71.6364	0.0155	0.0130

Load Flow Solution				
Bus	V	Ang	P(pu)	Q (pu)
26	0.9918	71.2097	0.0348	0.0427
27	1.0093	73.2755	0.0210	0.0035
28	0.9895	78.9202	0.0196	0.0128
29	1.0001	72.0120	0.1447	0.3089
30	0.9889	71.1326	0.1263	0.0221

II- Results of the DC converters output

Converters No.	Variables				
	V_d	I_d	T	$\cos\theta$	Φ
1	1.397	0.078	1.000	0.679	12.091
2	1.040	-0.775	0.959	0.843	43.738
3	1.022	1.139	0.987	0.589	25.000

Table 27: Load Flow solution of 30-Bus system for mode 6 with three converters

I- Voltage magnitude, angle, active, and reactive powers

Load Flow Solution				
Bus	V	Ang	P(pu)	Q(pu)
1	1.0600	0.0000	0.0000	0.0000
2	1.0430	28.9947	0.3452	0.2849
3	1.0228	49.7665	0.0810	0.0574
4	1.0169	60.0272	0.1874	0.0782
5	1.0100	44.7160	1.1510	0.4356
6	0.9781	75.8333	0.0100	0.0042
7	0.9912	62.5347	0.2599	0.1890
8	1.0100	74.5111	0.3244	0.3261
9	1.0343	69.5684	0.0313	0.0178
10	1.0252	66.1807	0.0727	0.1280
11	1.0820	69.5684	0.0059	0.0132
12	1.0112	60.7528	0.1900	0.0821
13	1.0710	60.7528	0.0149	0.0120
14	1.0225	60.8874	0.0512	0.3195

Load Flow Solution				
Bus	V	Ang	P(pu)	Q(pu)
15	1.0421	61.9508	0.0821	0.2655
16	1.0283	62.7502	0.3049	0.1747
17	1.0212	64.9212	0.1559	0.0431
18	1.0111	62.6952	0.0268	0.1086
19	1.0078	63.3409	0.0877	0.2848
20	1.0116	63.9858	0.0599	0.0599
21	1.0104	64.8825	0.2213	0.1875
22	1.0146	65.9663	0.0410	0.0163
23	1.0103	64.6374	0.1194	0.1960
24	1.0006	65.7869	0.1604	0.1610
25	1.0039	67.8051	0.0231	0.0076
26	0.9862	67.3783	0.0581	0.1182
27	1.0107	69.3365	0.0227	0.0134
28	0.9856	74.8243	0.0164	0.0085
29	0.9944	68.0730	0.2071	0.2942
30	0.9832	67.1936	0.3029	0.0894

II- Results of the DC converters output

Converters No.	Variables				
	V_d	I_d	T	$\cos\theta$	Φ
1	1.000	0.459	1.061	0.831	41.180
2	1.000	-0.222	0.996	0.791	47.633
3	0.964	1.035	1.188	0.489	32.915

Table 28: Load Flow solution of 30-Bus system for mode 7 with three converters

I- Voltage magnitude, angle, active, and reactive powers

Load Flow Solution				
Bus	V	Ang	P(pu)	Q(pu)
1	1.0600	0.0000	0.0000	0.0000
2	1.0430	29.0216	0.4232	0.3005
3	1.0273	49.7648	0.0251	0.0244
4	1.0128	60.2044	0.0940	0.0398
5	1.0100	44.7240	0.9626	0.2214
6	0.9480	76.4602	0.0000	0.0000
7	0.9734	62.9338	0.3381	0.1250
8	1.0100	74.6400	0.3753	0.3940
9	1.0189	70.1377	0.0110	0.0139
10	1.0108	66.7189	0.3794	0.0921
11	1.0820	70.1377	0.0028	0.0422
12	1.0249	60.9980	0.1374	0.1354
13	1.0710	60.9980	0.0340	0.0161
14	1.0145	61.1695	0.0702	0.0564
15	1.0129	62.3049	0.2879	0.0813
16	1.0186	63.1252	0.0426	0.0168
17	1.0081	65.4123	0.1440	0.1209
18	1.0000	63.1151	0.0582	0.0502
19	0.9957	63.7999	0.1009	0.0647
20	0.9989	64.4656	0.0406	0.0258
21	0.9969	65.3830	0.2057	0.2410
22	0.9998	66.4969	0.0215	0.0137
23	0.9970	65.1255	0.1142	0.1767
24	0.9853	66.3113	0.1965	0.1456
25	0.9851	68.3714	0.0378	0.0108
26	0.9675	67.9446	0.0250	0.0292
27	0.9928	69.9242	0.0198	0.0173
28	0.9626	75.3498	0.0630	0.0245
29	0.9735	68.6607	0.0149	0.0781
30	0.9523	67.7813	0.2880	0.1009

II- Results of the DC converters output

Converters No.	Variables				
	V_d	I_d	T	$\cos\theta$	Φ
1	1.290	1.384	1.059	0.545	27.910
2	1.276	-0.889	1.077	0.823	23.497
3	1.168	0.495	1.041	0.512	36.445

4.8 Analysis of Results for 30-Bus with three DC converter system

We tried also to use 30 bus systems. After using three converters, we concluded also that the overall active power is improved after using the converters as well as the overall reactive power for mode 1. For mode 2 to mode 7, the active and reactive power is improved for some buses but became worse for others. For example the active power at bus 8 without using the converters was 30.00 MW and became 34.16 MW after using the converters for mode 1 but it is changed to be 31.20 MW for mode 2, 30.97 MW for mode 3, 40.70 MW for mode 4, 38.51 MW for mode 5, 32.44 MW for mode 6, and 37.53 MW for mode 7.

Also the reactive power at bus 8 without using the converters was 30.00 MVAR and became 33.99 MVAR for mode 1 but it is changed to be 36.11 MVAR for mode 2, 34.00 MVAR for mode 3, 35.06 MVAR for mode 4, 40.23 MVAR for mode 5, 32.61 MVAR for mode 6, 39.40 MVAR for mode 7.

For bus 30 without using the converters was 10.6 MW and became 15.78 MW after using the converters for mode 1 but it is changed to be 15.99 MW for mode 2, 16.41 MW for mode 3, 18.04 MW for mode 4, 12.63 MW for mode 5, 30.29 MW for mode 6, and 28.80 MW for mode 7. Also the reactive power at bus 30 also without using the converters was 1.9 MVAR and became 5.85 MVAR for mode 1 but it is changed to be 9.00 MVAR for

mode 2, 3.10 MVAR for mode 3, 10.32 MVAR for mode 4, 2.21 MVAR for mode 5, 8.94 MVAR for mode 6, 10.09 MVAR for mode 7.

In comparing the three-terminal DC converters with the two-terminal DC converters on 30-bus systems, the specified variables of the DC converters for a three-terminal DC links are indicating a reduction in the variability as shown in the tables above. Increasing the some buses voltage level causes a slight improvement in the total losses and this will increase the overall efficiency and the decrease the voltage regulation and as a result the overall cost will be decreased. However, the converter taps (T) increases substantially.

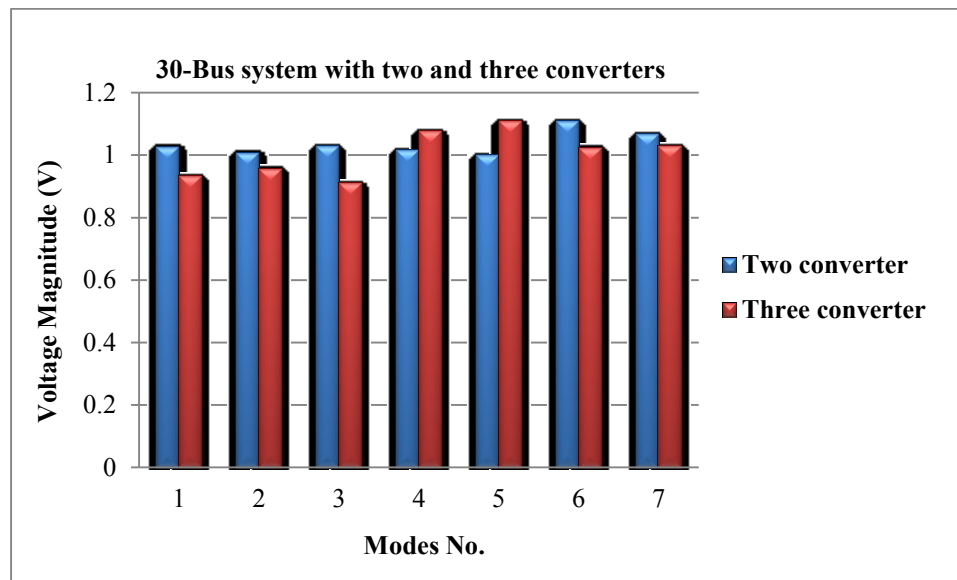


Figure 27: The relation between the voltage magnitude V_3 and modes number of 30 Bus system

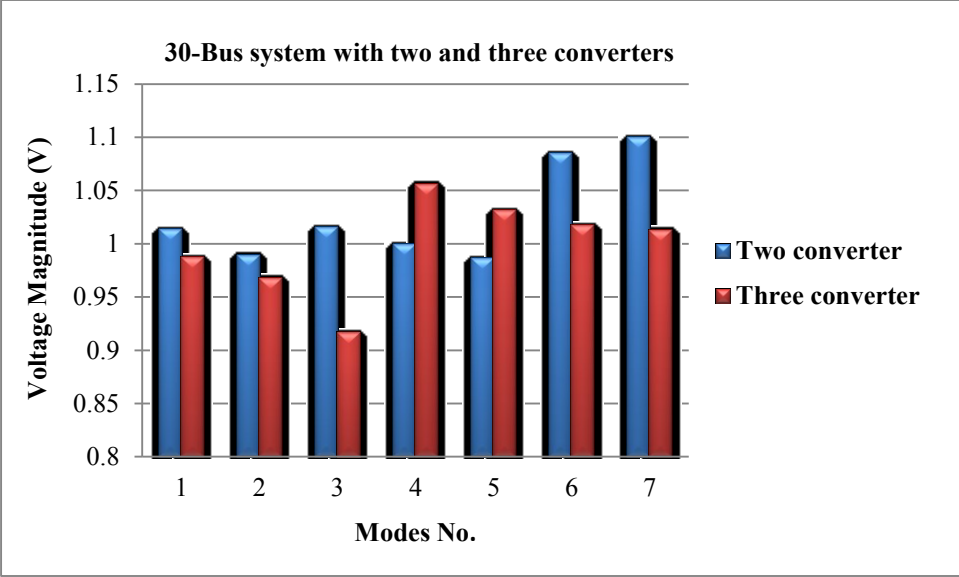


Figure 28: The relation between the voltage magnitude V_4 and modes number of 30 Bus system

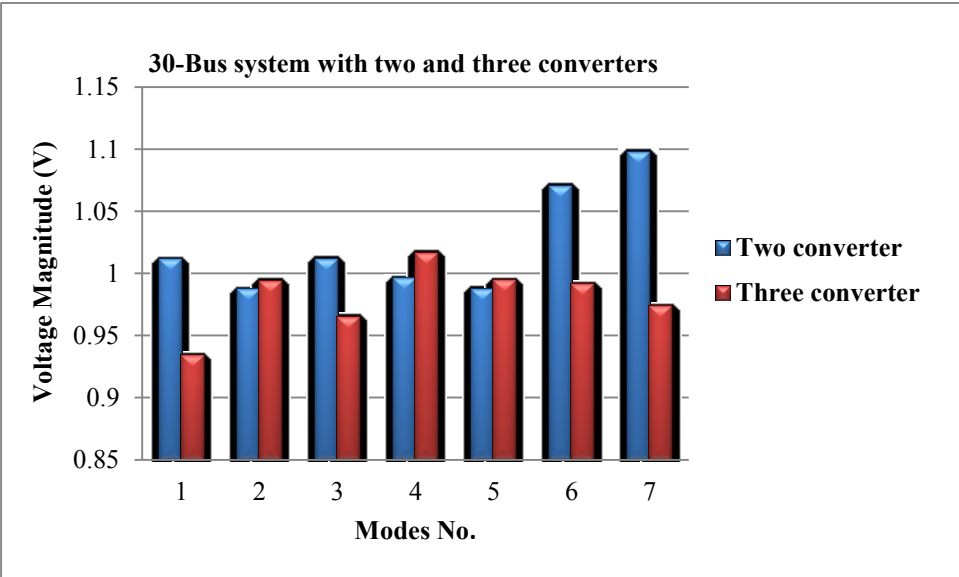


Figure 29: The relation between the voltage magnitude V_7 and modes number of 30 Bus system

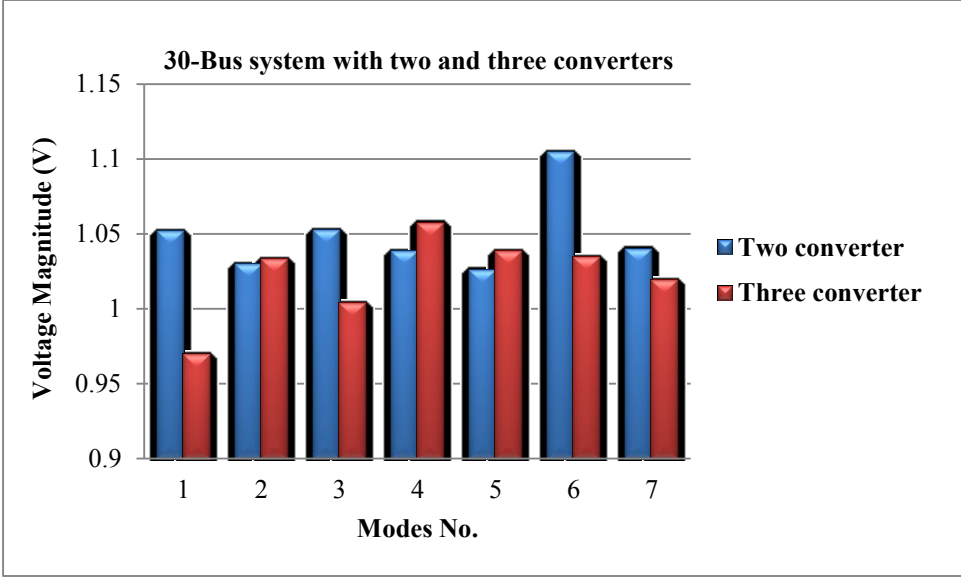


Figure 30: The relation between the voltage magnitude V_9 and modes number of 30 Bus system

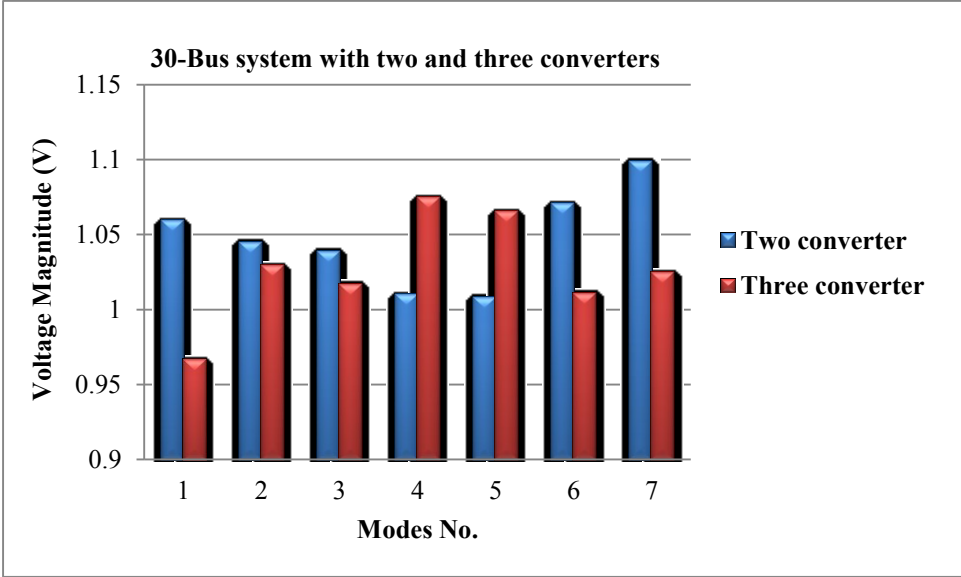


Figure 31: The relation between the voltage magnitude V_{12} and modes number of 30 Bus system

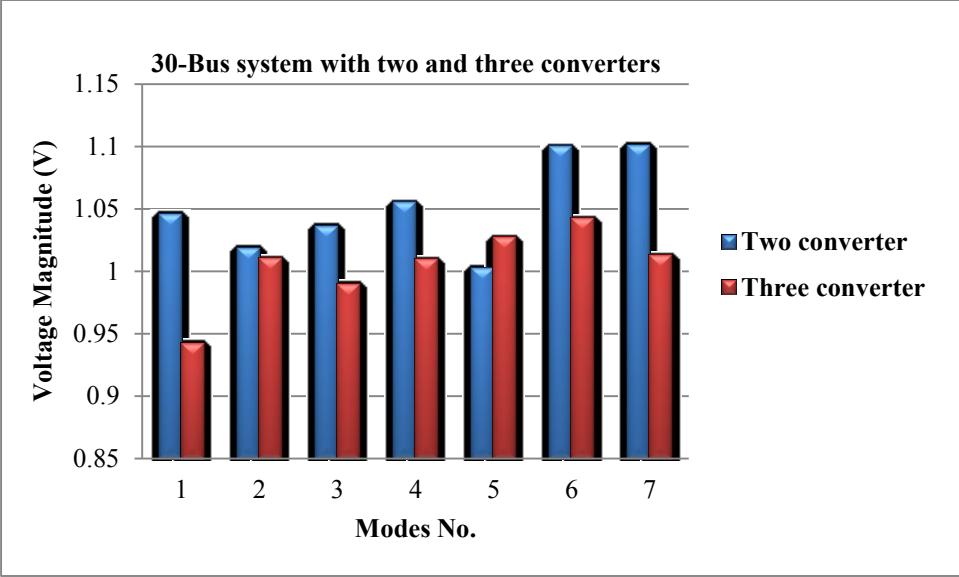


Figure 32: The relation between the voltage magnitude V_{15} and modes number of 30 Bus system

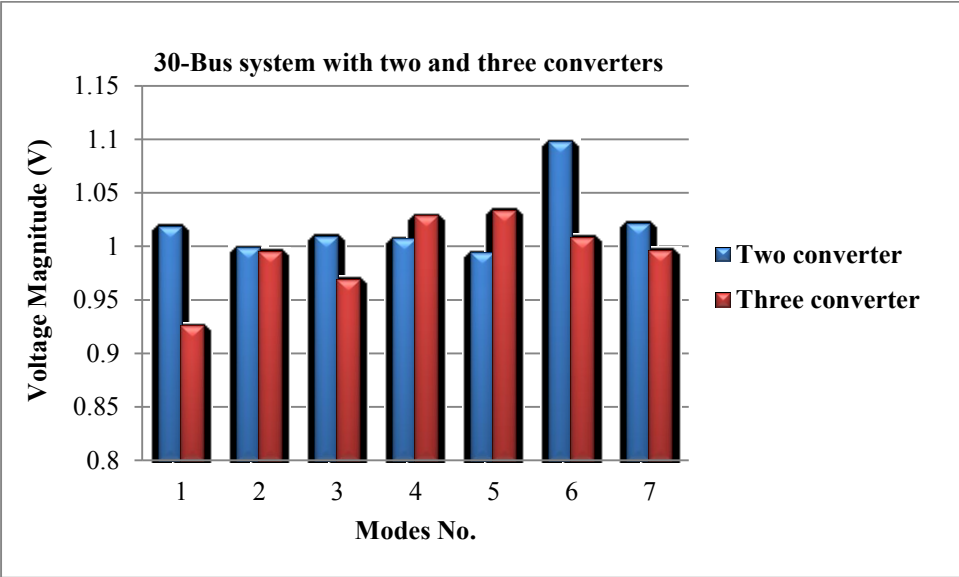


Figure 33: The relation between the voltage magnitude V_{19} and modes number of 30 Bus system

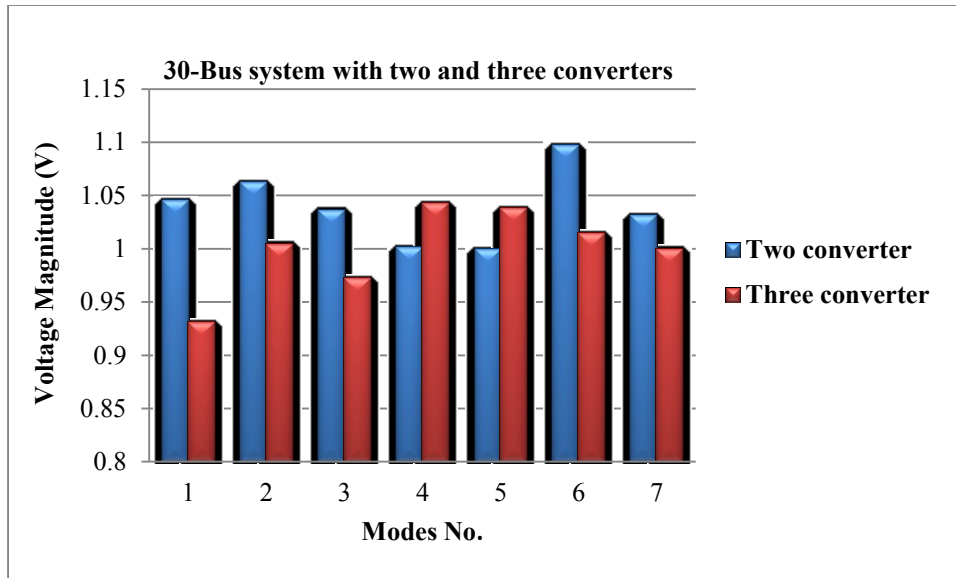


Figure 34: The relation between the voltage magnitude V_{22} and modes number of 30 Bus system

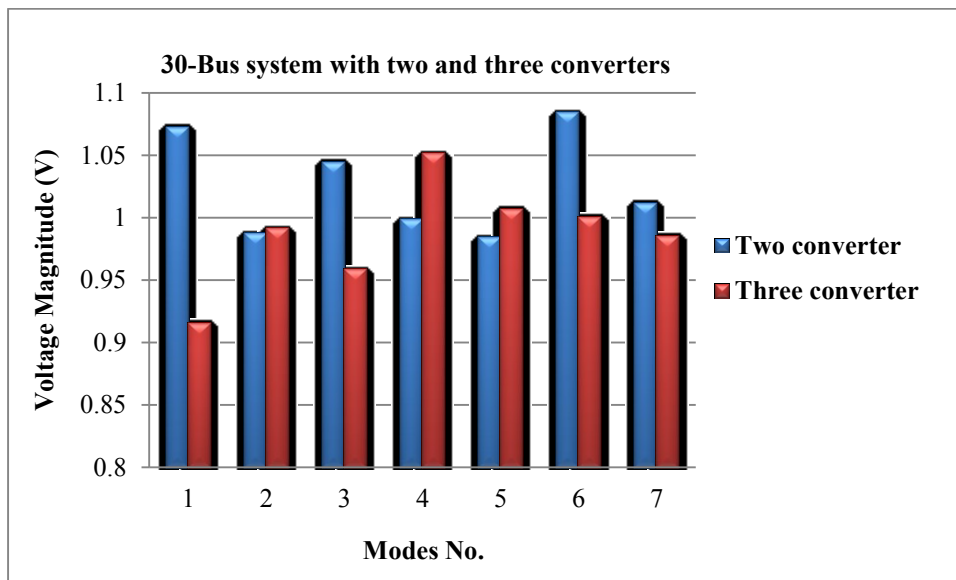


Figure 35: The relation between the voltage magnitude V_{24} and modes number of 30 Bus system

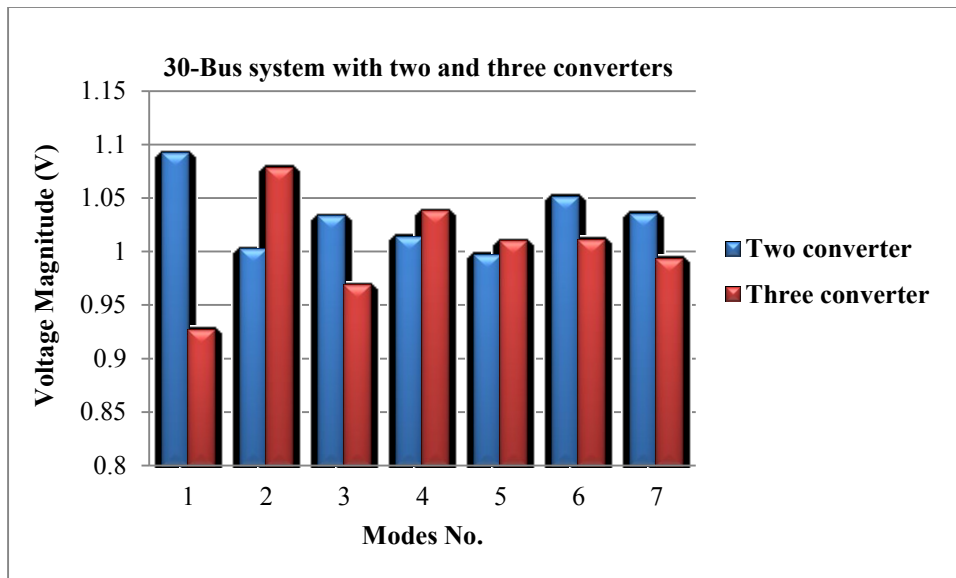


Figure 36: The relation between the voltage magnitude $_V_{27}$ and modes number of 30 Bus system

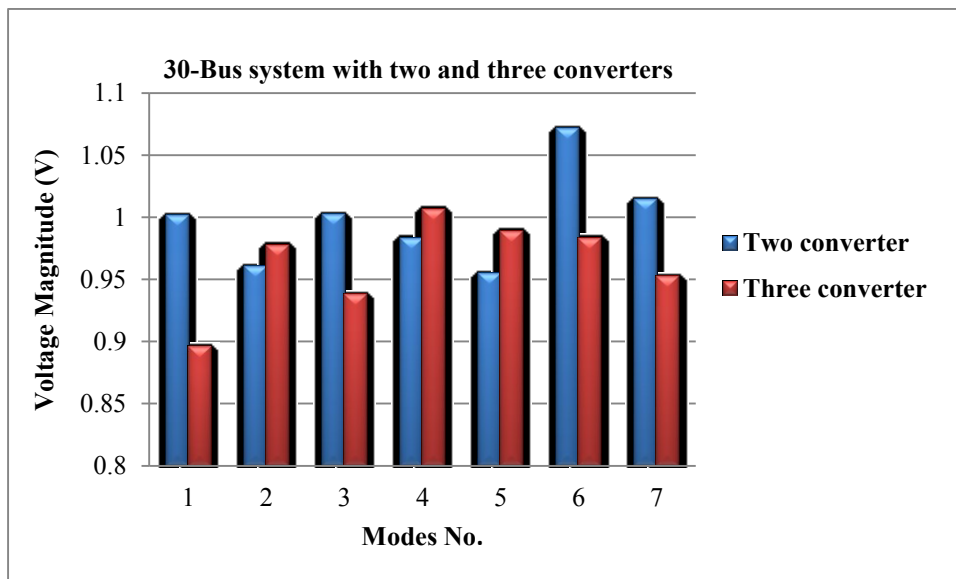


Figure 37: The relation between the voltage magnitude $_V_{30}$ and modes number of 30 Bus system

Figures (27-37) show the relation between the voltage magnitude for two converters and three converters at different buses with 30 bus systems. From which we concluded that the voltage magnitude is increased in case of two converters compared to three converters and there is a slight increase in the voltage magnitude.

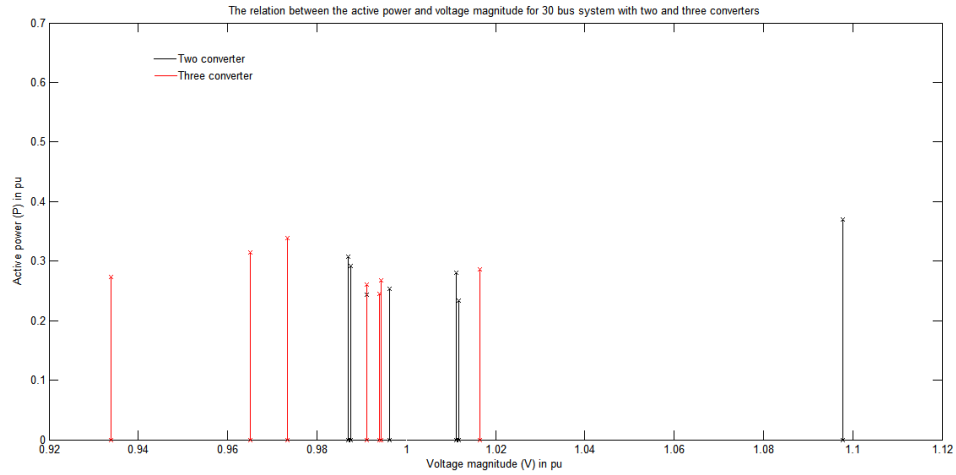


Figure 38: The relation between the active power P_7 and voltage magnitude V_7 of 30 Bus system

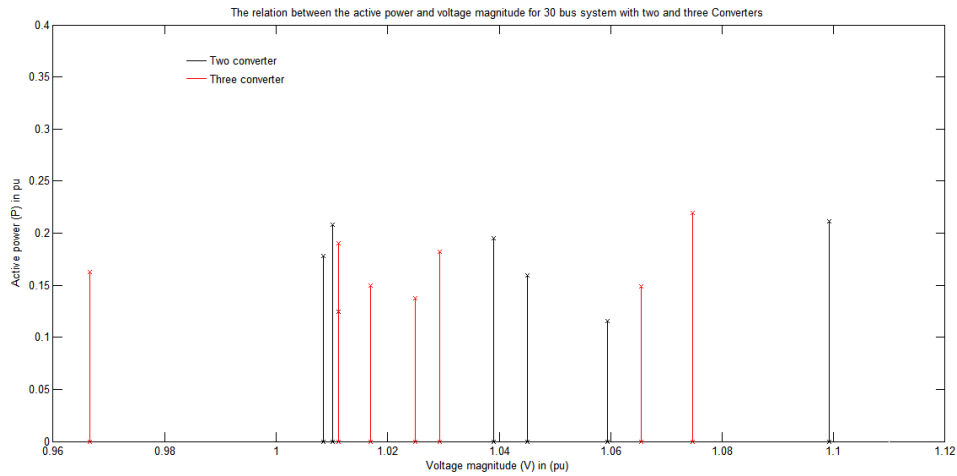


Figure 39: The relation between the active power P_{12} and voltage magnitude V_{12} of 30 Bus system

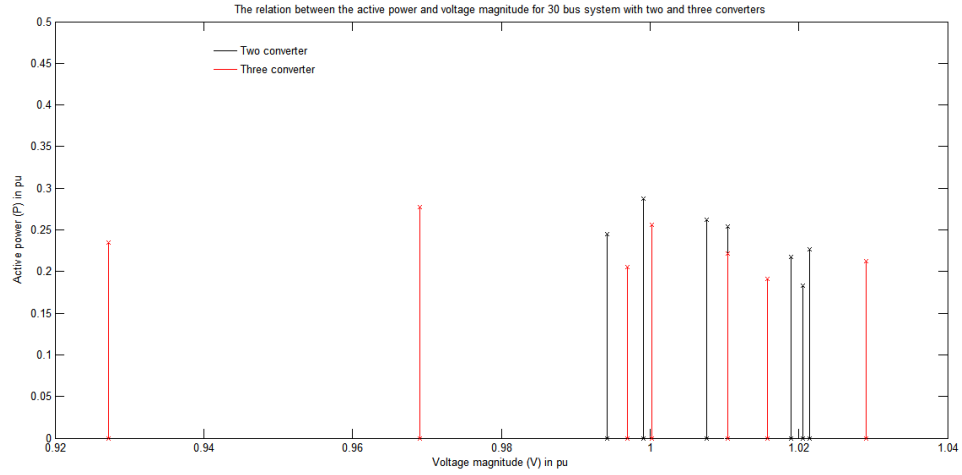


Figure 40: The relation between the active power P_{21} and voltage magnitude V_{21} of 30 Bus system

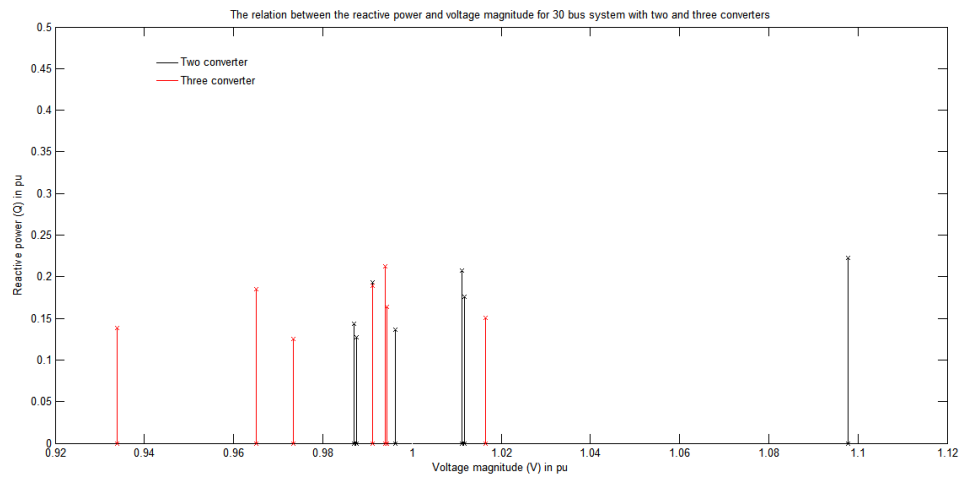


Figure 41: The relation between the reactive power Q_7 and voltage magnitude V_7 of 30 Bus system

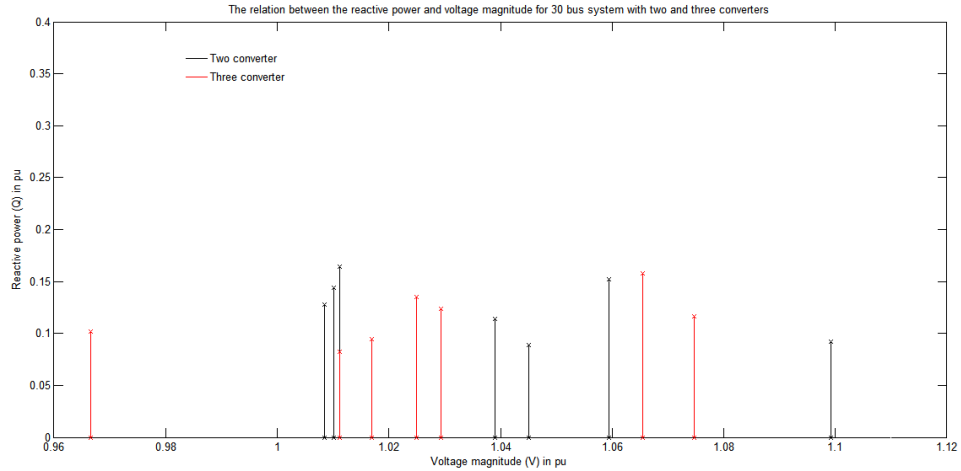


Figure 42: The relation between the reactive power Q_{12} and voltage magnitude V_{12} of 30 Bus system

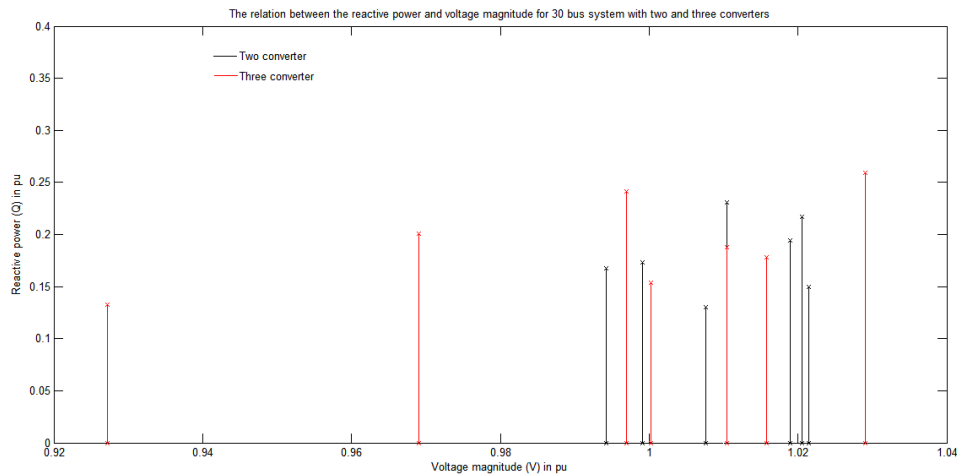


Figure 43: The relation between the reactive power Q_{21} and voltage magnitude V_{21} of 30 Bus system

Figures (38-43) show the relation between the active power and voltage magnitude for two converters and three converters at different buses with 30 bus systems . From which we concluded that the active power is increased in case of three converters compared to two converters and there is a slight increase in the voltage magnitude.

Chapter 5: Conclusion and Future Work

5.1 Conclusion and Contributions

HVDC power systems may have two or three-terminal DC link configurations for the DC portion for improving the voltage, decreasing the power losses and as a result increasing the overall efficiency. Most of the previous work used two converters. In this work we tried to use two and three converters and made a comparison between them for different systems. The three systems are used in this thesis to evaluate the performance of the proposed method, IEEE 14-bus and 30-bus systems. The DC system is formulated in a general format that allows any multi-terminal system configuration to be easily accommodated. Accordingly, a MATLAB program was used to find the control setting of HVDC for the pre-specified real and reactive power flows between any buses. Consequently, the effects of power flow between the lines of the HVDC systems were observed. Because a power flow method is acceptable only when it performs satisfactorily under various realistic operating modes, the converters must be capable of functioning under different control parameters to ensure efficiency and effectiveness.

The HVDC power flow method possessing all of the capabilities of the conventional Newton-Raphson method is shown to have the qualities of simultaneous and sequential solution of the AC/DC method combined. Furthermore, its storage requirement for the DC solution is minimal compared to that of the Jacobian in the conventional Newton-Raphson method. The numerical method for calculating the transit of power in electrical HVDC networks is easily implemented with minimal convergence point problems.

The power flow of a power system with multi-terminal DC links was analyzed, with the DC system under converter control specifications showing a distinctive solution known

as the DC power flow solution. As well, the DC system was forced into the AC system as the load on the buses increased. At this stage, the voltage has varying values when compared with the different bus systems.

In systems with heavy reactive loads, the proposed method performs very closely to the other method considered in this thesis (i.e., the Newton-Raphson load flows). The algorithms are capable of handling two-terminal as well as multi-terminal DC networks. An enhanced version of the Newton-Raphson method based on the polar coordinates formulation and requiring less solution time using five equations per converter, was developed and presented. The proposed method was found to be valid under different control systems on converters and to have reliable convergence. The problem has been treated recently.

In conclusion, the five variable models for the converter enable us to account for losses in the interface converter system. The analysis of the simulation results indicates that the proposed method exhibits more convergence patterns, accuracy and stability than the existing Newton-Raphson AC-DC model. In this section, those schemes which that the DC variables are strongly related to the terminal voltage give the fastest and most reliable performance. The main objective of power flow studies is to compute voltage magnitudes and phase angles at the load buses and reactive powers and voltage phase angles at the generating buses. A by-product of this calculation is active and reactive power flows in the transformers, transmission lines and system loss. A comprehensive treatment for AC power flow, including HVDC interconnections has been presented in this thesis. Thus, because of its ability to perform accurately, efficiently and reliably under all operating

modes and different converter control specifications, the proposed method is seen to be practically viable.

The main contribution is the improvement of the Jacobian elements approximation. In addition, I used two and three DC converters, and with these converters the overall active power is improved after using the converter as well as the overall reactive power for mode 1. Conversely, in the other modes (i.e. Mode 2 until 7) the active and reactive powers are improved for some buses, but comes out to be worse for others. Consequently, we found a graph that is describing the relation between the voltage magnitude with a number of modes and the active, reactive power with the voltage magnitude, for different buses for different systems.

5.2 Suggestions for Future Work

This thesis involved the formulation, development and simulation of HVDC power flow as applied to electrical power systems. Aspects relating to future research are outlined below:

- There are ten variables in HVDC converter models, of which only a minimal amount have been used. This is sufficient to represent the converter model. A minimum number of variables were chosen in order to reduce the program complexity. Nevertheless, the use of all ten variables could be the subject of future studies.
- Converter and transformer losses were ignored while developing the mathematical models for this thesis. This may produce some errors in the solution. Incorporating these features (i.e., converter and transformer losses) in

the mathematical model may also be of considerable research interest for the future.

- For an AC power system, the stability problem for both static and dynamic is always an issue for the electric power utility. Thus, it would be interesting to investigate, for instance, the risk of voltage collapse for the inclusion of HVDC links.

References

- [1] W. Xi-Fan, S. Yonghua and I. Malcolm, Modern Power Systems Analysis, ISBN 978-0-387-72852-0, 2009.
- [2] G. John and S. William, Power System Analysis, Mcgraw-Hill: ISBN 0-07-061293-5, 1994.
- [3] Glenn W. Stagg, Ahmed H. El-Abiad, Computer Methods in Power Systems, Mcgraw-Hill, 1968.
- [4] H. E. Brown, G. K. Carter, H. H. Happ and C. E. Person, "Power Flow. Solution By Impedance Matrix Method," IEEE Trans. Power Apparatus and System, April 1963.
- [5] Robert G. Andretich, Homxier E. Brown, Harvey H. Happ and Conrad E. Person, "The Piecewise Solution of The Impedance Matrix Load Flow," IEEE Transactions on Power Apparatus And Systems, October 1968, Vol. PAS-87, No. 10, pp.1877-1882.
- [6] William F. Tinney and Clifford E. Hart, "Power Flow Solution By Newton's Method," IEEE Transactions On Power Apparatus And Systems, Nov. 1967.
- [7] Stott. B. and Alasc. O., "Fast Decoupled Load Flow," IEEE Transactions On Power Apparatus And Systems, PAS-93, pp.859-869, 1974.
- [8] J. W. Allen and F. W. Bruce, power Generation, Operation, And Control, Wiley, ISBN:978-0471586999, 1996.
- [9] P. S. R. Murty, Operation And Control In Power Systems, Taylor And Francis: ISBN: 9780415665650, 2011.
- [10] T. Nguyen, "Neural Network Load-Flow," IEEE Proceedings of Generation Transmission Distribution, Vol. 142, No. 1, Jan. 1995, pp. 51-58.

- [11] W. L. Chan, A. T. P. So and L. L. La, "Initial Applications Of Complex Artificial Neural Networks To Load-Flow Analysis," IEEE Proceedings Of Generation Transmission Distribution, Vol. 147, No. 6, July 2000, pp. 361-366.
- [12] K. P. Wong, A. Li and T. M. Y. Law, " Advanced Constrained Genetic Algorithm Load Flow Method," IEE Proceedings Of Generation Transmission Distribution, Vol.146, No.6, November 1999, pp.609-616.
- [13] K. L. Lo, Y. J. Lin and W. H. Siew, " Fuzzy-Logic Method For Adjustment Of Variable Parameters in Load Flow Calculation," IEE Proceedings of Generation Transmission Distribution, 146(3), 276–282, 1999.
- [14] Ray Daniel Zimmerman, Carlos Edmundo Murillo-Sánchez and Robert John Thomas "Matpower: Steady-State Operations, Planning And Analysis Tools For Power Systems Research And Education," IEEE Transactions on Power Systems, Feb. 2011.
- [15] Arrillaga, J.; Arnold, C., Computer Analysis of Power Systems, London: John Wiley and Sons Ltd, 1990.
- [16] Arrillaga, J. and Bodger, P. , "AC-DC load flows with a realistic representation of converting plant," Proc. IEEE, Vol. 125, No.1, January 1978, pp. 41-46.
- [17] Arritlaga, J. ; Harker, B.J. ; Turner, K.S. , "Clarifying an Ambiguity in recent AC-DC load flow formulations," Proc. IEEE, Vol. 127 Pt.C., No. 5, September 1980, pp. 324-325.
- [18] Arrillaga, J. ; Bodger, P. , "Integration of HVDC links with fast-decoupled load flow solutions," IEEE Proc., 124 (5), 463–468, 1977.

- [19] Reeve, J. ; Fahny, G. ; Stott, B., "Versatile Load flow method for Multi-terminal HVDC Systems," IEEE Transaction Power Apparatus And Systems, 96(3), 925–932, May/June 1977.
- [20] J. Reeve and J. Carr, "Review of Techniques For HVDC Multi-Terminal Systems," IEEE Int. Conference Publication, HV AC/DC Transmission, London, December 1973.
- [21] El-Marsafawy, M.M. ; Mathur, R.M. , "A new technique for load flow solution of integrated multiterminal AC-DC systems," IEEE Transactions on Power Apparatus And Systems, Vol. PAS-99, No. 1, pp. 246-255, Jan./ Feb. 1980,.
- [22] M. E. El-Hawary; S. Ibrahim, "A New Approach to AC-DC Load Flow Analysis," Electric Power Sytems Research, Volume 33, Number 3, June 1995, pp. 193-200(8).
- [23] Ding, Q. F. ; Zhang, B. M. , "A New Approach To AC/MTDC Power Flow," Proceedings of the 4th International Conference on Advances in Power System Control, Operation and Management, Hong Kong, Vol. 2, No. 450, pp. 689-694, November 1997.
- [24] Mustafa, M.W. and A. F. Abdul Kadir, "A Modified Approach For Load Flow Analysis of Integrated AC-DC Power Systems," IEEE Trans. Power Apparatus And Systems, Page(s): 108 - 113 vol. 2, 2000.
- [25] U. Arifoglu, "The Power Flow Algorithm For Balanced And Unbalanced Bipolar Multiterminal AC-DC Systems," Electric Power Systems Research, Vol-46, No. 3, March 2003, pp. 239-246.
- [26] Minassians, A. D. and Gharehpetian, G. B., "Decoupled AC/DC Load Flow For Monte Carlo Simulation Of Metro Power System," Iranian Journal of Science & Technology, Transaction B, pp. 305-314, June 2004.

- [27] Panosyan, A. and Oswald, B.R. , "Modified Newton-Raphson Load Flow Analysis For Integrated AC/DC Power Flow," Institute of Electric Power Systems, vol. 2, 2004, pp. 1223 - 1227.
- [28] Osaloni, O. and Radman, G. , "Integrated AC/DC Systems, Power Flow Solution Using Newton-Raphson And Broyden approaches," IEEE Trans. Power Apparatus and System, 2005, pp. : 225 - 229.
- [29] R. Lis, "Power Limitations of The HVDC Transmission Power System," Proceedings of the 7th WSEAS International Conference on Power Systems, Beijing, September 15-17,2007.
- [30] Beerten, J. ; Cole, S. ; Belmans, R. , "A Sequential AC/DC Power Flow Algorithm For Networks Containing Multiterminal VSC HVDC Systems," IEEE Transactions Power Apparatus and Systems, 2010, pp. :1 - 7.
- [31] Shuai Lu ; Ning Zhou ; Kumar, N.P. ; Samaan, N. ;Chakrabarti, B.B. , "Improved DC Power Flow Method Based on Empirical Knowledge of The System," Transmission and Distribution Conference and Exposition, IEEE, USA, 2010, pp.: 1 - 6.
- [32] Soobae Kim and Overbye, T.J. , "Hybrid Power Flow Analysis: Combination of AC and DC Models," IEEE Trans. Power Apparatus and Systems, Urbana, IL 61801 USA, 2011, pp.1 - 4.
- [33] Haileselassie, T.M. and Uhlen, K. , "Power Flow Analysis of Multiterminal HVDC Networks," IEEE Trondheim PowerTech, Norway, 19-23 June 2011, pp. 1 - 6.
- [34] Ayan, K. ; Arifoglu, U. ; Kilic, U. , "Integrated AC/DC Systems Load Flow Using Genetic Algorithm," The 5th International Power Engineering and Optimization Conference, Shah Alam, Selangor, Malaysia, 6-7 June 2011, pp. 404 - 409 .

[35] Zhijun Qin and Yunhe Hou , "Application of Non-linear Programming For Large-Scale AC-DC Power Flow Analysis," IEEE Trans. Power Apparatus and Systems, 2012,pp. 1 - 8.

[36] www.ee.washington.edu/research/pstca/

APPENDICES

Appendix A

A.1: Derivation of Power Network Equations Using a Sample Network

In this section, the equations for the power calculations for a node will be inspected. Let's consider a sample power network as shown in the figure below

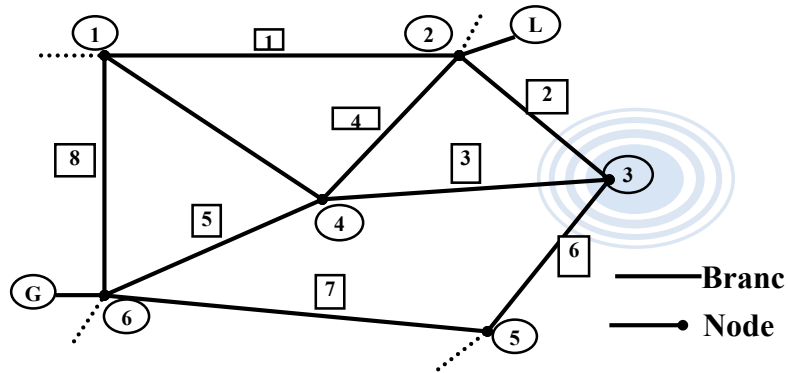


Figure 44: Tree of the Connected Graph of a Sample Power Network

Here all the complex power injections for one node are going to be written and it could be applied to all the nodes in the network. We consider node 3 and all the branches connected to it (Figure below):

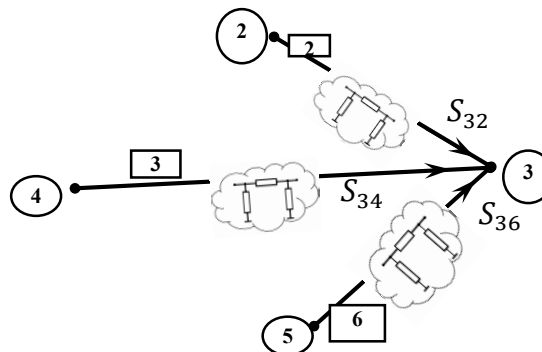


Figure 45: The Node 3 in the Sample Power Network Along with the all Branches Connected and the Illustration of the Equivalent pi Model for each Branch

To find the power injections S_2 and S_3 and S_6 we use the equivalent pi model described in the previous section. The power injection equations will be:

$$\bar{S}_{32} = (\bar{y}_2 + \bar{y}_{30})^* \bar{V}_3 \bar{V}_3^* - \bar{y}_2^* \bar{V}_3 \bar{V}_2^*$$

$$\bar{S}_{34} = (\bar{y}_3 + \bar{y}_{30})^* \bar{V}_3 \bar{V}_3^* - \bar{y}_3^* \bar{V}_3 \bar{V}_4^*$$

$$\bar{S}_{36} = (\bar{y}_6 + \bar{y}_{30})^* \bar{V}_3 \bar{V}_3^* - \bar{y}_6^* \bar{V}_3 \bar{V}_6^*$$

The relationship between the injected complex powers in a node is $\sum \bar{S} = 0$. For node 3 it will be:

$$\bar{S}_{32} + \bar{S}_{34} + \bar{S}_{36} = 0$$

$$(\bar{y}_2 + \bar{y}_{30})^* \bar{V}_3 \bar{V}_3^* - \bar{y}_2^* \bar{V}_3 \bar{V}_2^* + (\bar{y}_3 + \bar{y}_{30})^* \bar{V}_3 \bar{V}_3^* - \bar{y}_3^* \bar{V}_3 \bar{V}_4^* + (\bar{y}_6 + \bar{y}_{30})^* \bar{V}_3 \bar{V}_3^* - \bar{y}_6^* \bar{V}_3 \bar{V}_6^* = 0$$

$$(\bar{y}_2 + \bar{y}_3 + \bar{y}_6 + 3\bar{y}_{30})^* |\bar{V}_3|^2 - [\bar{y}_2^* \bar{V}_2^* + \bar{y}_3^* \bar{V}_4^* + \bar{y}_6^* \bar{V}_6^*] \bar{V}_3 = 0$$

The last equation is the desired non-linear function that relates the states to the physical admittances for the sample power network.

A.2: Generalization of Power Equations

The total power flux equation for the sample network will be written in order to conclude the equations for a general network easier. The injected powers in nodes are the measured quantities.

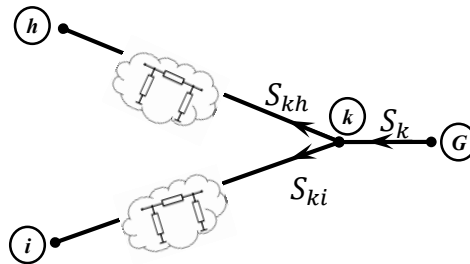


Figure 46: Sample Network with Two Branches Connected to a Generator (Power Injector) Along with the Illustration of Equivalent pi Model

$$\bar{S}_{kh} = (\bar{y}_{kh} + \bar{y}_{k0})^* \bar{V}_k \bar{V}_k^* - \bar{y}_{kh}^* \bar{V}_k \bar{V}_h^*$$

$$\bar{S}_{ki} = (\bar{y}_{ki} + \bar{y}_{k0})^* \bar{V}_k \bar{V}_k^* - \bar{y}_{ki}^* \bar{V}_k \bar{V}_i^*$$

In node k , the injected power, G is equal to the total power fluxes:

$$\bar{S}_k = \bar{S}_{kh} + \bar{S}_{ki}$$

$$\bar{S}_k = (\bar{y}_{kh} + \bar{y}_{k0})^* \bar{V}_k \bar{V}_k^* - \bar{y}_{kh}^* \bar{V}_k \bar{V}_h^* + (\bar{y}_{ki} + \bar{y}_{k0})^* \bar{V}_k \bar{V}_k^* - \bar{y}_{ki}^* \bar{V}_k \bar{V}_i^*$$

$$\bar{S}_k = (\bar{y}_{kh} + \bar{y}_{ki} + 2\bar{y}_{k0})^* |\bar{V}_k|^2 - (\bar{y}_{kh} \bar{V}_h + \bar{y}_{ki} \bar{V}_i)^* \bar{V}_k$$

The elements of node admittance can be written as:

$$\bar{y}_{kh} = g_{kh} + jb_{kh}$$

Note that \bar{y}_{kh} is equal to \bar{y}_{hk} and accordingly $g_{kh} = g_{hk}$ and $b_{kh} = b_{hk}$.

Consequently the complex node power injection can be expressed as:

$$P_k + jQ_k = (g_{kh} + jb_{kh} + g_{ki} + jb_{ki} + 2g_{k0} + j2b_{k0})^* |\bar{V}_k|^2 - (g_{kh} \bar{V}_h + jb_{kh} \bar{V}_h + g_{ki} \bar{V}_i + jb_{ki} \bar{V}_i)^* \bar{V}_k$$

$$P_k + jQ_k = (g_{kh} - jb_{kh} + g_{ki} - jb_{ki} + 2g_{k0} - j2b_{k0}) |\bar{V}_k|^2 - g_{kh} \bar{V}_k \bar{V}_h^* + jb_{kh} \bar{V}_k \bar{V}_h^* - g_{ki} \bar{V}_k \bar{V}_i^* + jb_{ki} \bar{V}_k \bar{V}_i^*$$

And using polar form of voltage it will be:

$$P_k + jQ_k = (g_{kh} - jb_{kh} + g_{ki} - jb_{ki} + 2g_{k0} - j2b_{k0}) |\bar{V}_k|^2 - g_{kh} |\bar{V}_k| |\bar{V}_h| e^{j\theta_{kh}} + jb_{kh} |\bar{V}_k| |\bar{V}_h| e^{j\theta_{kh}} - g_{ki} |\bar{V}_k| |\bar{V}_i| e^{j\theta_{ki}} + jb_{ki} |\bar{V}_k| |\bar{V}_i| e^{j\theta_{ki}}$$

Using Euler rule: $e^{j\theta} = \cos \theta + j \sin \theta$ we will have:

$$\begin{aligned}
P_k + jQ_k &= (g_{kh} + g_{ki} + 2g_{k0} - j(b_{kh} + b_{ki} + 2b_{k0}))|\bar{V}_k|^2 \\
&\quad - g_{kh}|\bar{V}_k||\bar{V}_h|(\cos \theta_{kh} + j \sin \theta_{kh}) + jb_{kh}|\bar{V}_k||\bar{V}_h|(\cos \theta_{kh} + j \sin \theta_{kh}) \\
&\quad - g_{ki}|\bar{V}_k||\bar{V}_i|(\cos \theta_{ki} + j \sin \theta_{ki}) + jb_{ki}|\bar{V}_k||\bar{V}_i|(\cos \theta_{ki} + j \sin \theta_{ki}) \\
P_k + jQ_k &= (g_{kh} + g_{ki} + 2g_{k0})|\bar{V}_k|^2 - j(b_{kh} + b_{ki} + 2b_{k0})|\bar{V}_k|^2 - g_{kh}|\bar{V}_k||\bar{V}_h| \cos \theta_{kh} \\
&\quad - jg_{kh}|\bar{V}_k||\bar{V}_h| \sin \theta_{kh} + jb_{kh}|\bar{V}_k||\bar{V}_h| \cos \theta_{kh} - b_{kh}|\bar{V}_k||\bar{V}_h| \sin \theta_{kh} \\
&\quad - g_{ki}|\bar{V}_k||\bar{V}_i| \cos \theta_{ki} - jg_{ki}|\bar{V}_k||\bar{V}_i| \sin \theta_{ki} + jb_{ki}|\bar{V}_k||\bar{V}_i| \cos \theta_{ki} \\
&\quad - b_{ki}|\bar{V}_k||\bar{V}_i| \sin \theta_{ki} \\
P_k + jQ_k &= (g_{kh} + g_{ki} + 2g_{k0})|\bar{V}_k|^2 - g_{kh}|\bar{V}_k||\bar{V}_h| \cos \theta_{kh} - b_{kh}|\bar{V}_k||\bar{V}_h| \sin \theta_{kh} \\
&\quad - g_{ki}|\bar{V}_k||\bar{V}_i| \cos \theta_{ki} - b_{ki}|\bar{V}_k||\bar{V}_i| \sin \theta_{ki} \\
&\quad + j[-(b_{kh} + b_{ki} + 2b_{k0})|\bar{V}_k|^2 - g_{kh}|\bar{V}_k||\bar{V}_h| \sin \theta_{kh} \\
&\quad + b_{kh}|\bar{V}_k||\bar{V}_h| \cos \theta_{kh} - g_{ki}|\bar{V}_k||\bar{V}_i| \sin \theta_{ki} + b_{ki}|\bar{V}_k||\bar{V}_i| \cos \theta_{ki}]
\end{aligned}$$

Splitting above equation into real and imaginary parts gives the active and the reactive node power injection at node k in polar form.

$$\begin{aligned}
P_k &= (g_{kh} + g_{ki} + 2g_{k0})|\bar{V}_k|^2 - g_{kh}|\bar{V}_k||\bar{V}_h| \cos \theta_{kh} - b_{kh}|\bar{V}_k||\bar{V}_h| \sin \theta_{kh} \\
&\quad - g_{ki}|\bar{V}_k||\bar{V}_i| \cos \theta_{ki} - b_{ki}|\bar{V}_k||\bar{V}_i| \sin \theta_{ki}
\end{aligned}$$

$$\begin{aligned}
Q_k &= -(b_{kh} + b_{ki} + 2b_{k0})|\bar{V}_k|^2 - g_{kh}|\bar{V}_k||\bar{V}_h| \sin \theta_{kh} + b_{kh}|\bar{V}_k||\bar{V}_h| \cos \theta_{kh} \\
&\quad - g_{ki}|\bar{V}_k||\bar{V}_i| \sin \theta_{ki} + b_{ki}|\bar{V}_k||\bar{V}_i| \cos \theta_{ki}
\end{aligned}$$

The above equations are the total power flux equations for the sample network (top figure). To conclude it for a general network, we simplify and then use a summation notation to include all nodes. Therefore, firstly for active node power it can be written that:

$$P_k = (g_{kh} + g_{ki} + 2g_{k0})|\bar{V}_k|^2 - (g_{kh} \cos \theta_{kh} + b_{kh} \sin \theta_{kh})|\bar{V}_k||\bar{V}_h| - (g_{ki} \cos \theta_{ki} + b_{ki} \sin \theta_{ki})|\bar{V}_k||\bar{V}_i|$$

$$P_k = G_{kk}|\bar{V}_k|^2 - \sum_{\substack{j=1 \\ j \neq k}}^n |\bar{V}_k||\bar{V}_j|(g_{kj} \cos \theta_{kj} + b_{kj} \sin \theta_{kj})$$

Where the index j is the node number from 1 to n . For reactive node power it can be written in a similar way that:

$$Q_k = -B_{kk}|\bar{V}_k|^2 - \sum_{\substack{j=1 \\ j \neq k}}^n |\bar{V}_k||\bar{V}_j|(g_{kj} \sin \theta_{kj} - b_{kj} \cos \theta_{kj})$$

Appendix B: Data for DC converters

Table B.1: Data of Two Converters for 14-bus system

Bus 4 (Rectifier)	Bus 5 (Inverter)
$X_c=0.054831$	$X_c=0.054831$
$T=1.00$	$T=1.10$
$\alpha=5$ degree	$\gamma=25$ degree
$V_{dc}=1.00$ (p.u.)	$V_{dc}=0.96$ (p.u.)
$I_{dc}=0.068$ (p.u.)	$I_{dc}=1.00$ (p.u.)
$P_{dc}=0.066$ (p.u.)	$P_{dc}=-1.00$ (p.u.)
$\Phi=25$ degree	$\Phi=25$ degree

Table B.2: Data of Three Converters for 14-bus system

Bus 2 (Rectifier)	Bus 4 (Rectifier)	Bus 5 (Inverter)
$X_c=0.054831$	$X_c=0.054831$	$X_c=0.054831$
$T=1.00$	$T=0.99$	$T=0.99$
$\alpha=5$ degree	$\gamma=25$ degree	$\alpha=5$ degree
$V_{dc}=1.00$ (p.u.)	$V_{dc}=1$ (p.u.)	$V_{dc}=0.96$ (p.u.)
$I_{dc}=1.00$ (p.u.)	$I_{dc}=1.00$ (p.u.)	$I_{dc}=0.68$ (p.u.)
$P_{dc}=0.066$ (p.u.)	$P_{dc}=-1.00$ (p.u.)	$P_{dc}=1.00$ (p.u.)
$\Phi=25$ degree	$\Phi=23$ degree	$\Phi=25$ degree

Table B.3: Data of Two Converters for 30-bus system

Bus 2 (Rectifier)	Bus 5 (Inverter)
$X_c=0.054831$	$X_c=0.054831$
$T=1.00$	$T=1.16$
$\alpha=5$ degree	$\gamma=25$ degree
$V_{dc}=1.00$ (p.u.)	$V_{dc}=0.98$ (p.u.)
$I_{dc}=0.068$ (p.u.)	$I_{dc}=1.00$ (p.u.)
$P_{dc}=0.066$ (p.u.)	$P_{dc}=-1.00$ (p.u.)
$\Phi=25$ degree	$\Phi=25$ degree

Table B.4: Data of Three Converters for 30-bus system

Bus 2 (Rectifier)	Bus 5 (Inverter)	Bus 7 (Rectifier)
$X_c = 0.054831$	$X_c = 0.054831$	$X_c = 0.054831$
$T = 1.00$	$T = 0.99$	$T = 1.00$
$\alpha = 5$ degree	$\gamma = 25$ degree	$\alpha = 5$ degree
$V_{dc} = 1.00$ (p.u.)	$V_{dc} = 1$ (p.u.)	$V_{dc} = 0.99$ (p.u.)
$I_{dc} = 1.00$ (p.u.)	$I_{dc} = 1.00$ (p.u.)	$I_{dc} = 0.69$ (p.u.)
$P_{dc} = 0.066$ (p.u.)	$P_{dc} = -1.00$ (p.u.)	$P_{dc} = 1.00$ (p.u.)
$\Phi = 25$ degree	$\Phi = 23$ degree	$\Phi = 25$ degree